Alma Mater Studiorum · Università di Bologna

DOTTORATO DI RICERCA IN

Informatica

Ciclo XXIV

Settore Concorsuale di afferenza: 01/B1 - Informatica
Settore Scientifico Disciplinare: INF/01 - Informatica

Fingerprint Recognition: Enhancement, Feature Extraction and Automatic Evaluation of Algorithms

Presentata da: Francesco Turroni

Coordinatore Dottorato:
Prof. Maurizio Gabbrielli

Tutore:
Prof. Luciano Margara

Relatore:
Prof. Davide Maltoni

Esame finale anno 2012

Abstract

The identification of people by measuring some traits of individual anatomy, physiology or other behavioral characteristics has led to a specific research area called *biometric recognition*. Several biometric technologies have been developed and successfully deployed: fingerprints, face, iris, palmprints, signature. Fingerprints are the biometric trait discussed in this Thesis because of their individuality and persistence properties, as well as cost and maturity of products.

This Thesis is focused on improving fingerprint recognition systems considering three important problems: fingerprint enhancement, fingerprint orientation extraction and automatic evaluation of fingerprint algorithms. Fingerprint enhancement and fingerprint orientation extraction can be considered as pre-processing steps to the main goal in fingerprint recognition: the automatic comparison with other fingerprints (*matching*).

An effective extraction of salient fingerprint features depends on the quality of the input fingerprint. If the quality is good, the fingerprint flow is well evident and a reliable set of features can be extracted. If the fingerprint is very noisy, we are not able to detect robust information: a large number of spurious features are extracted and we miss several genuine features. Therefore, to achieve high recognition performance it is essential to incorporate in the system a fingerprint enhancement module able to improve the quality of noisy fingerprints, thus making the subsequent processing steps more reliable.

The goal of fingerprint orientation extraction is to compute one of the most critical information in fingerprints, the local orientation: a feature denoting the direction of the ridge flow at discrete positions. A precise estimation of the orientation field would greatly simplify the estimation of other fingerprint features (singular points, minutiae) and improve the performance of a fingerprint recognition system.

Although new developments and improvements in fingerprint recognition are continuously reported, it is often difficult to understand, from the scientific literature, which are the most effective and promising methods. In fact, scientific papers typically pro-

pose recognition systems that integrate many modules (enhancement, feature extraction, matching, post-processing, etc.) and therefore an automatic evaluation of fingerprint algorithms is needed to isolate the contributions that determine an actual progress in the state-of-the-art.

After a summary of state-of-the-art in fingerprint recognition, a new fingerprint enhancement method, which is both iterative and contextual, is proposed. This approach detects high-quality regions in fingerprints, selectively applies contextual filtering and iteratively expands like wildfire toward low-quality ones. The method does not require any prior information on local orientations or frequencies. We assess the improvements given by this algorithm over both real and synthetic fingerprints using a state-of-the-art matcher.

The fingerprint orientation extraction is improved following two directions. First, after the introduction of a new taxonomy of fingerprint orientation extraction methods, several variants of baseline methods (local and global) are implemented and, pointing out the role of pre- and post- processing, we show how to improve the extraction. Second, the introduction of a new hybrid orientation extraction method, which follows an adaptive scheme, allows to improve significantly the orientation extraction in noisy fingerprints. It exploits both the local information and the experience, represented by the knowledge of plausible fingerprint orientation structures, to compute the best orientation at discrete points.

The lack of a publicly available framework to compare fingerprint orientation extraction algorithms, motivates the introduction of a new benchmark called FOE (constituted of fingerprint images, manually-marked orientation ground-truth and a metric) along with fingerprint matching benchmarks in the FVC-onGoing framework. The success of such online framework for the automatic evaluation of fingerprint algorithms, is discussed by providing relevant statistics: more than 1450 algorithms submitted and two international competitions.

Acknowledgements

This Ph.D. Thesis summarizes the work carried out with the Biometric Systems Laboratory (BioLab) since 2009. The BioLab is active at the University of Bologna since 1993 and is supported by Computer Science and Information Technology degree course (Cesena) and DEIS (Department of Electronics, Computer Sciences and Systems). The main research efforts are devoted to fingerprint/face recognition and performance evaluation of biometric systems. Collaborations with industrial partners ensure that the research activities in the BioLab are linked to real applications.

Foremost, I would like to thank my two advisors Prof. Davide Maltoni and Prof. Dario Maio for their support and guidance during the last three years I have spent at BioLab. During these years I really benefited of their experience and advices.

During my experience at the BioLab I had the fortune to work with a great team of researchers whose help, discussions and competence in the biometric field have contributed to my scientific growth. My sincere thanks to Raffaele Cappelli, Annalisa Franco and Matteo Ferrara.

I would like to thank my tutor Prof. Luciano Margara, director of the Computer Science and Information Technology degree course (Cesena), for his help and for giving me the opportunity to work in cooperation with the BioLab.

During my Ph.D. studies I had the great opportunity to meet a large number of researchers worldwide and visit for a four month period the Prof. Anil K. Jain's laboratory at Michigan State University, USA. It was an honor to work with him and his extraordinary group.

Last, but absolutely not least, a deep thanks goes to my parents Giovanna and Roberto, my brother Marco and my sweet love Chiara for their continuous support.

Francesco Turroni
Cesena, December 2011

Contents

Chapter 1

Introduction

The identification of people by measuring some traits of individual anatomy, physiology or other behavioral characteristics has led to a specific research area called *biometric recognition* [68]. Biometric technologies provide a strong mechanism for authentication and are still under continuous development. Their diffusion is mainly supported by governments, forensics and law enforcement agencies with the aim of improving the public security or in general a sense of security; in fact, the biometric identification does not directly improve the security but acts as deterrent to illegal activities.

The application of biometrics in forensics has a long history and can be considered as the big bang of the biometric recognition world. Alphonse Bertillon, chief of the criminal identification division of the police department in Paris, developed and then practiced the idea of using a number of body measurements to identify criminals in the mid-19th century. In the twentieth century law enforcement agencies have extensively used biometrics for security purposes. In the last years, the adoption of biometrics has met a large increase even in general purpose applications, due mainly to a combination of the falling cost of biometric devices, increasing sophistication of the technology and development of biometrics as a peripheral to common computer platforms. Several biometrics have been successfully developed and deployed: fingerprints, face, iris, voice and palmprints are the most currently used.

Fingerprints are the main biometric trait discussed in this Thesis; they have been subject of study of more than a century and besides, archaeological fingerprint carvings and impressions (from Neolithic [94], stones [78], clay seals [78]) were founds worldwide.

This PhD Thesis is focused on three important fingerprint recognition problems:

fingerprint orientation extraction, fingerprint enhancement and automatic evaluation of fingerprint algorithms.

Fingerprint orientation extraction and fingerprint enhancement can be considered as pre-processing steps to the main goal of the fingerprint recognition problem: the comparison with other fingerprints. More clear are the characteristics we can extract from a fingerprint, more reliable is the output of a comparison between fingerprints (*matching*).

The automatic evaluation of fingerprint recognition algorithms over common databases is very important in order to assess the performance of various algorithms and understand the most effective and promising building block technologies.

In this introductory chapter we present the basics of biometric systems describing the characteristics of the most common biometric traits. Fingerprints, that are the core of this Thesis, are described in detail in the next chapter. This chapter is finished providing the motivations and goals of this Thesis, the novel contributions to the fingerprint recognition field and describing the organization of the Thesis such that a reader can easily navigate among chapters.

1.1 Biometric Systems

Biometric Systems are systems that use anatomical and behavioral characteristics, called biometrics traits, to automatically recognize individuals [81] [133].

The use of such a characteristics is becoming essential in person identification solutions because they represent the individual's bodily identity and can neither be shared nor misplaced.

The word *biometrics* is derived from the Greek words *bios* (meaning life) and *metron* (meaning measurement), so biometrics traits are measurements from the living human body.

With the word *enrollment* we define the act of capture the biometric characteristic with a biometric sensor (for example a fingerprint scanner), the generation of a compact but expressive representation of the information (*feature set*) and finally, the organization of one or more feature sets into an *enrollment template* that will be saved in some persistent storage.

A biometric system may be a *verification system* or an *identification system.*

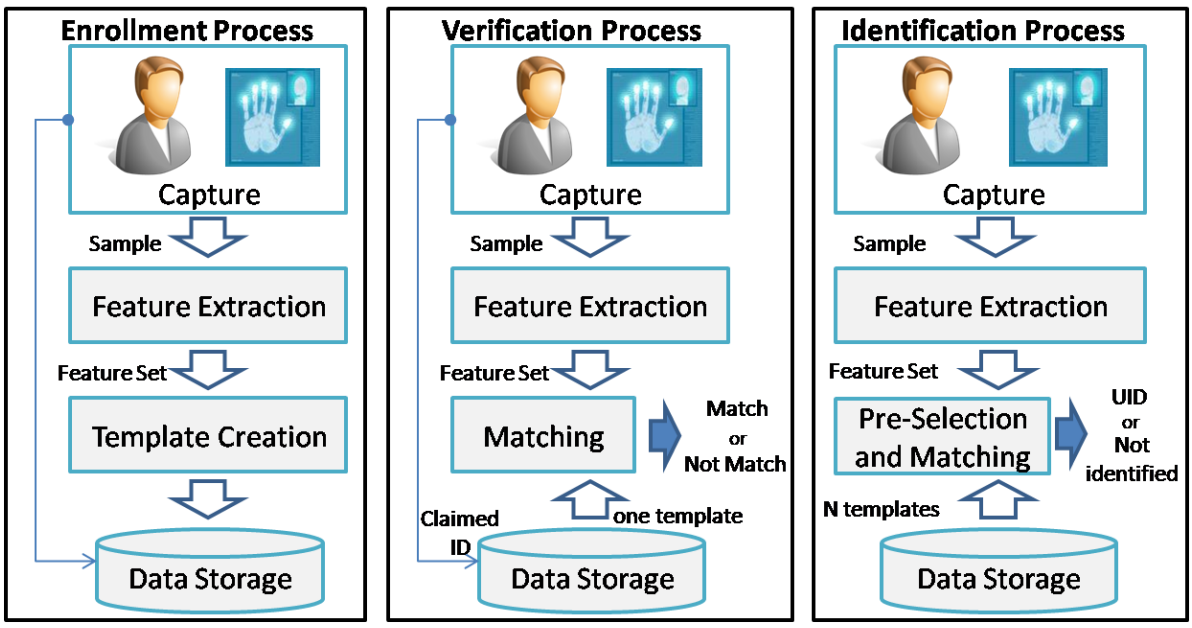

Figure 1.1: Enrollment, Verification and Identification processes.

- A verification system authenticates a person's identity comparing the acquired biometric trait with an enrolled one. It conducts a one-to-one comparison to confirm if the individual is who he claims to be. This system accepts or rejects the submitted claim of identity.

- An identification system recognizes an individual by searching in a database a match with a previously captured (enrolled) biometric reference template. It conducts one-to-many comparisons to establish if the individual is present or not in the database and if so, it returns the identifier of the enrollment reference that matched.

In Figure 1.1 the verification and identification systems are depicted; user enrollment which is common to both tasks is also graphically illustrated.

Depending on the application domain, a biometric system could operate either as an *on-line* system or an *off-line* system. An on-line system requires the recognition to be performed quickly, an immediate response is imposed and is usually *fully automatic*. An off-line system does not have this requirement, a relatively longer response delay is allowed and is usually *semi-automatic*.

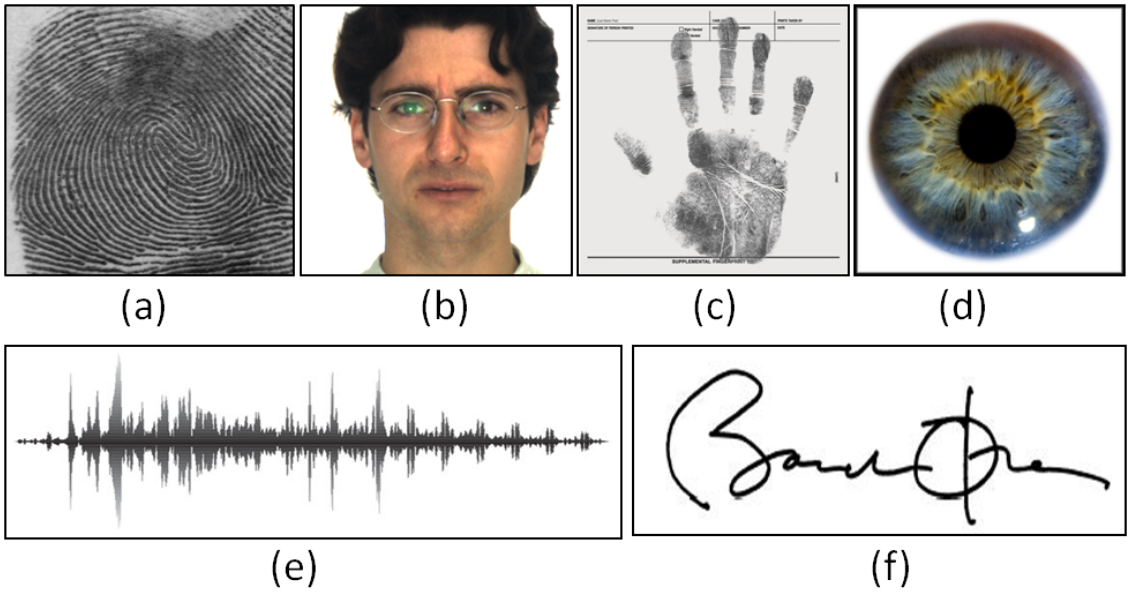

Figure 1.2: Classification of most common biometric traits. Fingerprint (a), Face (b), Hand (c), Iris (d), Voice (e), Signature (f).

1.2 Biometric Characteristics

A brief introduction to the most common biometric traits is provided below.

- *Fingerprint.* It is the biometric trait with the most desirable properties. In fact, every human being possesses fingers and hence fingerprints. They are very distinctive and permanent; even if they temporarily change slightly due to cuts and bruises on the skin, the fingerprint reappears after the finger heals. Live-scan fingerprint scanners can easily capture high quality fingerprint images simply putting a finger on the sensor. Fingerprints have a long history of use in forensic divisions for criminal investigations and associated systems are difficult to circumvent. Fingerprint recognition is one of the most mature biometric technologies and is suitable for a large number of recognition applications [90].

- *Face.* Face is one of the most acceptable biometrics traits because it is one of the most common methods of recognition that humans use in their daily visual interactions. The acquisition is easy and non-intrusive. It is very challenging to develop face recognition algorithms that are invariant to variations of age, expression, pose and environment [134].

- *Iris*. Iris recognition is the process of recognizing a person by analyzing the pattern of the iris. The image is typically acquired using a non-contact imaging process. The recognition is not to be confused with another ocular-based technology, the retina scanning. Breakthrough work to create the iris recognition algorithms required for image acquisition and one-to-many matching was pioneered by John G. Daugman [36]. The iris recognition efficacy is rarely impeded by glasses or contact lenses and has been shown to be extremely accurate at high resolution images.

- *Hand*. Some features related to the human hand are relatively invariant and peculiar to an individual [62]. The acquisition requires the cooperation of the subject to capture frontal and side view images of the palm. With appropriate devices (near-infrared imaging) is it possible recognize also the hand or finger vein structure.

- *Voice*. Voice acquisition is not intrusive and as biometric trait is not expected to be sufficiently distinctive to permit identification of a subject from a large database of identities. The voice signal depends on the quality of the acquisition device and is affect by factors such as a person's health, stress and emotional state.

- *Signature*. The signature of a person is said to be a characteristic of an individual, but it changes over time and is influenced by physical and emotional conditions. Signature has been acceptable in government, legal and commercial transactions as a method of verification for a long time.

In this Thesis we consider fingerprints because of their desiderable properties. In the last years the need of high accuracy has motivated also the interest in *multimodal biometrics*, in which several biometric traits are simultaneously used (see [68] [106] [52] [73]), for example:

- face and fingerprint ([50] [63]);

- face, fingerprint and speech ([64]);

- face, fingerprint and hand geometry ([103] [102]);

- signature and fingerprint ([41] [42]).

1.3 Motivation and goals

Thanks to their well-known distinctiveness and persistence, fingerprints are the most widely used biometric characteristic. Fingerprint recognition is a complex pattern recognition problem; designing algorithms capable of extracting salient features and matching them in a robust way is quite hard.

It is a common thinking that *automatic fingerprint recognition* is a fully solved problem since it was one of the first applications of machine pattern recognition almost fifty years ago. On the contrary, fingerprint recognition is still a challenging and important pattern recognition problem. Some of the challenges are described below.

- A reliable extraction of salient fingerprint features (*minutiae*) depends on the quality of the input fingerprint. If the quality is good, the fingerprint flow is well evident and a robust set of features can be extracted. If the fingerprint is very noisy, we are not able to detect such features reliably: a large number of spurious features are extracted and we miss several genuine features. Therefore, to achieve high recognition performance it is essential to incorporate in the automatic system a *fingerprint enhancement* module able to improve the quality of noisy fingerprints, thus making the subsequent processing steps more reliable.

- One of the most used fingerprint features is called *local fingerprint orientation* and represents the ridge flow direction at discrete positions. This feature helps to understand the global fingerprint flow and has a critical impact on subsequent processing steps. The orientation extraction in good quality images is an easy problem where simple methods from the image processing literature (gradient-based) are exploited. Reliable orientation extraction in low-quality regions is still an open problem. Some methods have been proposed to solve this problem but they do not allow to encode a prior knowledge about the admissible fingerprint structures in the orientation estimation process. Only algorithms with such a prior knowledge (i.e., encoding natural fingerprint variability), combined with the local fingerprint quality and local orientation estimations, may achieve significant higher accuracy on very low quality fingerprints.

- Although new developments and improvements in fingerprint recognition are continuously reported, it is often difficult to understand, from the scientific literature, which are the most effective and promising methods. In fact, scientific papers

typically propose recognition systems that integrate many modules (enhancement, feature extraction, matching, post-processing, etc.) and therefore it is hard to isolate the contributions that determine an actual progress in the state-of-the-art. FVC is a competition organized by the Biometric System Laboratory of University of Bologna with such an aim. After four off-line competitions, the FVC-onGoing (on-line) has been developed only for fingerprint matching (ISO templates) and verification (proprietary templates) algorithms. An extension to other fingerprint problems (orientation extraction, indexing, etc.) and eventually other biometric traits could be very useful for the community.

1.4 Novel contributions

The problem of automatic fingerprint matching has been extensively studied, but it is still not a fully solved problem. Reliable fingerprint enhancement and feature extraction, which are addressed in this work, are fundamental pre-requisites to all fingerprint recognition systems. The major contributions are listed below.

1. A novel fingerprint enhancement algorithm that improves the fingerprint matching on both synthetic and real fingerprints has been developed. The algorithm selectively applies contextual filtering starting from automatically-detected high-quality regions and then iteratively expands like wildfire toward low-quality ones.

2. A new taxonomy of fingerprint orientation extraction methods has been proposed. With a large number of experiments we show that a learning-based approach is needed in order to deal with noisy fingerprints.

3. In very noisy fingerprints the orientation extraction is a difficult task. After a deep analysis of the problem we show that parameter optimizations, pre- and post-processing stages can markedly improve accuracy of the baseline methods on bad quality fingerprints. Several algorithms (and a high number of their variations) have been implemented and tested on a specifically designed benchmark.

4. A new hybrid fingerprint orientation extraction method has been developed to enhance the performance of automatic fingerprint recognition systems. It follows an adaptive scheme using both the local and learnt information.

5. The automatic evaluation of fingerprint algorithms is fundamental to isolate the contributions that determine an actual progress in the state-of-the-art. The FVC-onGoing framework, a web-based automatic evaluation system of fingerprint algorithms, has been extended with the introduction of a new specifically designed benchmark area for fingerprint orientation extraction algorithms. We have created two benchmarks containing i) good and bad quality images, 2) the manually marked ground-truth, and 3) a metric to compare the estimated orientations with the ground-truth.

6. The FVC-onGoing is "on going" in the sense that a participant can submit algorithms at any time and outputs recognition results using standard metrics. In conjunction with two important international conferences on biometrics (International Joint Conference on Biometrics IJCB 2011 [1] held in Washington DC (USA) and the International Conference on Biometrics ICB 2012 [4] held in New Delhi (India)), we have organized two international competitions based on the FVC-onGoing framework. The first competition is about the fingerprint verification problem and the second is about the fingerprint orientation extraction. Results and conclusions are reported in this Thesis.

The research activities carried out during the Ph.D., lead to the publication of the following scientific papers: [23], [122], [19] and [24].

1.5 Thesis organization

After an introduction on biometrics and fingerprint recognition, this work is organized in three main parts. The first part is devoted to the fingerprint enhancement problem. We propose a new iterative contextual method for noisy fingerprint able to enhance the image and improve the matching. The second part describes a new classification of orientation extraction algorithms and shows how to improve the estimation with novel approaches. The third part is devoted to the automatic evaluation of fingerprint algorithms through the FVC-onGoing framework and some new competitions based on it that we organized. All these three parts include several experimental results.

This Thesis is organized according to the following chapters.

- Chapter 1 describes a general biometric recognition system analyzing and comparing the most common biometric traits. It also gives the motivations, the novel

contributions and the organization of this Thesis.

- Chapter 2 introduces at high level the fingerprint recognition problem. Starting from an historical overview we move toward a structural analysis of fingerprints describing the most common features (local ridge orientations, local ridge frequencies, minutiae) and databases (NIST and FVC). Finally, the chapter presents some standard performance measures adopted in fingerprint recognition systems and for this reason used in this Thesis. The state-of-the-art of various methods is always provided to the reader.

- Chapter 3 initially introduces the reader to the fingerprint enhancement problem. A minutiae extraction algorithm heavily relies on the quality of the input fingerprint. If the quality is good, the ridges-valley flow is well evident and a robust set of minutiae can be extracted. If the fingerprint is very noisy, the minutiae extraction algorithm may detect a large number of spurious minutiae and miss several genuine minutiae. Therefore, to achieve high recognition performance it is essential to incorporate a fingerprint enhancement module able to improve the quality of noisy fingerprints. After the problem description a new method based on iterative contextual filtering is proposed and its performance is assessed through experiments on synthetic (SFinGe) and real (FVC) fingerprints.

- Chapter 4 introduces the fingerprint orientation extraction problem. A new taxonomy for orientation extraction algorithm is provided and, according to some experiments, we show the need of learning-based orientation extraction methods, that is methods that exploit a prior knowledge of plausible fingerprint structures to improve the estimation.

- Chapter 5 frames the baseline orientation extraction algorithms according to the proposed taxonomy and describes new techniques able to improve the orientation extraction in fingerprints. We implemented and tested several well know methods and a plethora of their variants over a novel, specifically designed, benchmark, made available in the FVC-onGoing framework (see chapter 6). Through an experimental analysis we proved that parameter optimizations, pre- and post- processing stages can markedly improve accuracy of the baseline methods on bad quality fingerprints. A new hybrid orientation extraction method relying on local and learnt information is proposed and compared with baseline methods.

- Chapter 6 describes the FVC-onGoing framework, a web-based automatic evaluation system of fingerprint algorithms. The proposed system is automatic (does not require the human intervention), "on going" (a participant can submit algorithms at any time) and outputs recognition results using standard metrics. The system is expanded through the introduction of a new benchmark area for orientation extraction algorithms (FOE).

- Chapter 7 presents the results of two fingerprint recognition competitions organized by the Biometric System Laboratory of the University of Bologna [2] in conjunction with the International Joint Conference on Biometrics IJCB 2011 [1] held in Washington DC (USA) and the International Conference on Biometrics ICB 2012 [4] held in New Delhi (India).

- Chapter 8 concludes the Thesis summarizing the main results obtained and outlining future research directions.

The relationship among the chapters is illustrated in Figure 1.3. The three main parts of this Thesis are highlighted with dashed lines. Chapter 1 is recommended for all readers in order to understand the main research contributions and to have an introduction on biometrics. A reader without a background in fingerprint recognition should absolutely read the chapter 2 or a for a more detailed discussion the text [90]. Novel contributions and experimental results can be found in all remaining chapters.

Some of the methods developed in this Thesis require also a background knowledge in image processing and machine learning. A standard text on image processing is the Gonzalez and Woods, 2002 [47]. Machine learning literature is well introduced by the texts Duda et al. [38], C. Bishop [14], Theodoridis and Koutroumbas, 2008 [120].

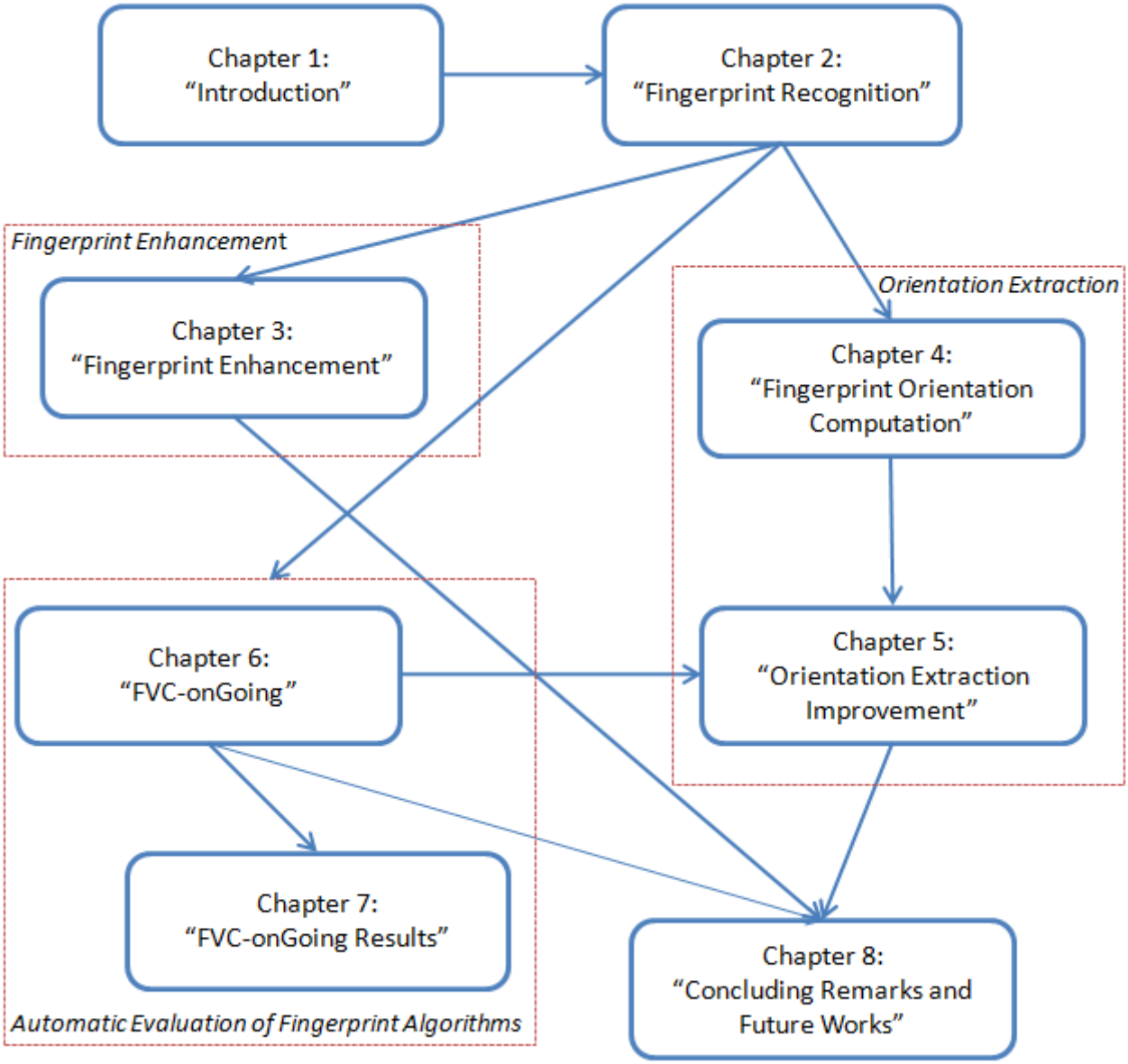

Figure 1.3: Thesis Organization.

Chapter 2

Fingerprint Recognition

The application of fingerprint based authentication systems is becoming very popular in last years, not only at industrial or defense level but also in general purpose devices like laptops, mouses, smart phones, pen drives. The word "fingerprint" is usually associated with the term "individuality", but the uniqueness is not formally established, it is just an empirical observation over millions of acquired ones.

In this chapter we present a description of the fingerprint recognition problem. Starting from an historical overview we move toward a structural analysis of fingerprints describing the most common features and databases. Finally, we present some standard performance measures adopted for fingerprint recognition systems and for this reason used in this Thesis.

2.1 Historical Overview

Despite human fingerprints have been discovered on a large number of archeological artifacts [94][78], the milestones in fingerprint science can be summarized in the following works:

- **1809**. Thomas Bewick started using fingerprint as his trademark [78].
- **1823**. Purkinje proposed the first fingerprint classification scheme based on nine categories [94].
- **1859**. William Herschel was the first european to recognize the value of fingerprints for identification purposes. He collected fingerprints and in 1977 his fingerprinting

ideas were implemented.

- **1880**. Henry Fauld suggested the individuality of fingerprints based on empirical observations [78] [94].

- **1888-1892**. Sir Francis Galton conducted an extensive study on fingerprints. In his works, he divided the fingerprints in three major classes and introduced the concept of minutiae features for comparing fingerprints. This approach is the most utilized in modern fingerprint recognition algorithms [45].

- **1899-1900**. Edward Henry established the "Henry-system" of fingerprint classification. According to this system, five classes have been introduced. This scheme was adopted in several countries. Most of the classification schemes currently used by law enforcement agencies are variants of this scheme [39].

- **20th century**. Fingerprint recognition became a standard routine in forensics. Various techniques were developed. The FBI fingerprint division was set up in 1924 with a database of 810,000 cards. Currently, the FBI IAFIS is the largest biometric database in the world, housing the fingerprints and criminal histories for more than 70 million subjects, along with more than 31 million civil prints.

2.2 Formation and Individuality

Fingerprints are fully formed at about seven months of fetus development and will remain the same throughout the person's life (*persistence property*). If superficial damage occurs, the skin will grow back in exactly the same arrangement as at birth. This is why fingerprints are a reliable means of identification at all stages of a person's life. They are even one of the last features to decompose after death. Babler in [7] described the embryologic development of epidermal ridges. A mathematical explanation for the development of epidermal ridges on fingers can be found in [77].

The details of a person's fingerprints are unique to them and only them (*uniqueness property*). Even identical twins do not have identical fingerprints. According to the assumption of uniqueness, different individuals have different salient features: if two fingerprints share many common features then an expert concludes that the fingerprints belong to the same person. The assumption of uniqueness allows forensic experts to

Figure 2.1: Examples of fingerprint scanners.

offer a strong proof towards the defendant's guilt. The fingerprint individuality is still extensively studied [90].

2.3 Acquisition of Fingerprints

The acquisition of a fingerprint can be done off-line or on-line. In the off-line acquisition the image is typically obtained by smearing ink on the fingertip and creating an inked impression of the fingertip on the paper. After this procedure, the fingerprint is digitized by an optical scanner or a high resolution camera. This kind of fingerprint is often called *rolled fingerprint*. A very important kind of off-line fingerprint image is the *latent fingerprint*: a partial fingerprint image lifted from a crime scene by a forensic expert. Compared to a rolled fingerprint, the latent is most of the times of bad quality and hard to process. In the on-line acquisition, the fingerprint is acquired by using a fingerprint scanner without any kind of ink (see some examples in Figure 2.1). A typical fingerprint scanner comprises:

- a *sensor* to read the ridge pattern on the finger surface;
- an *A/D* (Analog to Digital) converter to convert the signal;
- an *interface* module responsible for communicating with external devices.

Almost of all existing sensors belong to one of the following families: optical, solid-state and ultrasound. These sensors are also called touch sensors. With the aim of reducing the cost, recently another sensing method has been proposed: the sweep sensor, where the finger is swept over the sensor (see the fourth image in Figure 2.1). This is very common in mobile devices. A detailed description of such acquisition methods can be found in [90].

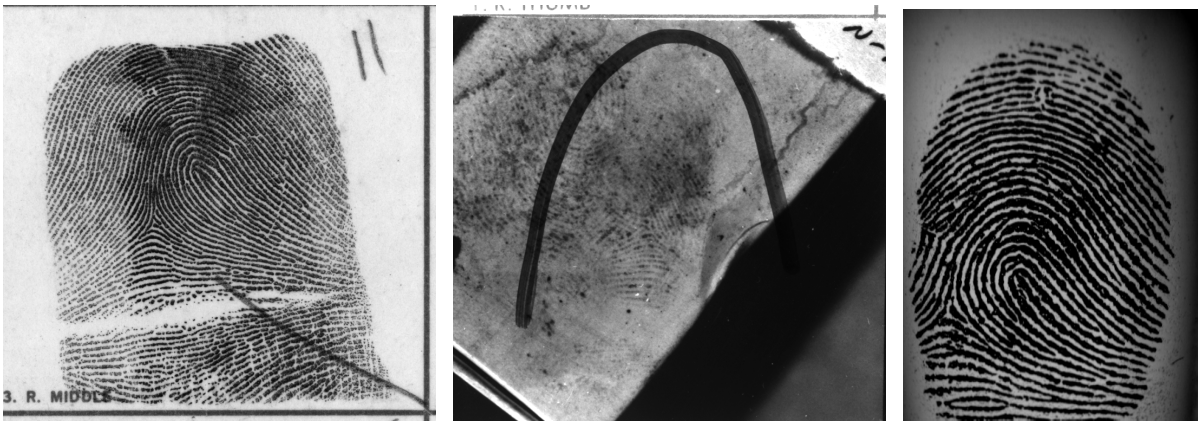

(a) (b) (c)

Figure 2.2: Examples of fingerprints acquired with different techniques. A rolled fingerprint (a), a latent fingerprint (b) and a fingerprint acquired with an optical scanner (c).

The FBI - CJIS Division has defined in [113] the main parameters characterizing the acquisition of a digital fingerprint image. In this Thesis we will consider three of them: resolution, area and number of pixels (the rest can be found in [113] and [90]).

- *Resolution*: denotes the number of pixels per inch (dpi). 500dpi is the minimum resolution for FBI-compliant scanners.
- *Area*: is the size of the rectangular area sensed by a fingerprint scanner and expressed in inch^2.
- *Number of pixels*: is the number of pixels in a fingerprint image. If Res is the resolution, h is the height of the sensing area and w the weight of the sensing area, the number of pixels is given by $Res \cdot h \times Res \cdot w$.

2.4 Fingerprint Features

The problem of representation of a fingerprint is determinant for a good recognition system and there is a need to find efficient methods to determine salient features. After the sensing phase with a fingerprint device, we have an image based representation, constituted by pixel intensity information, which is not invariant to distortions, brightness

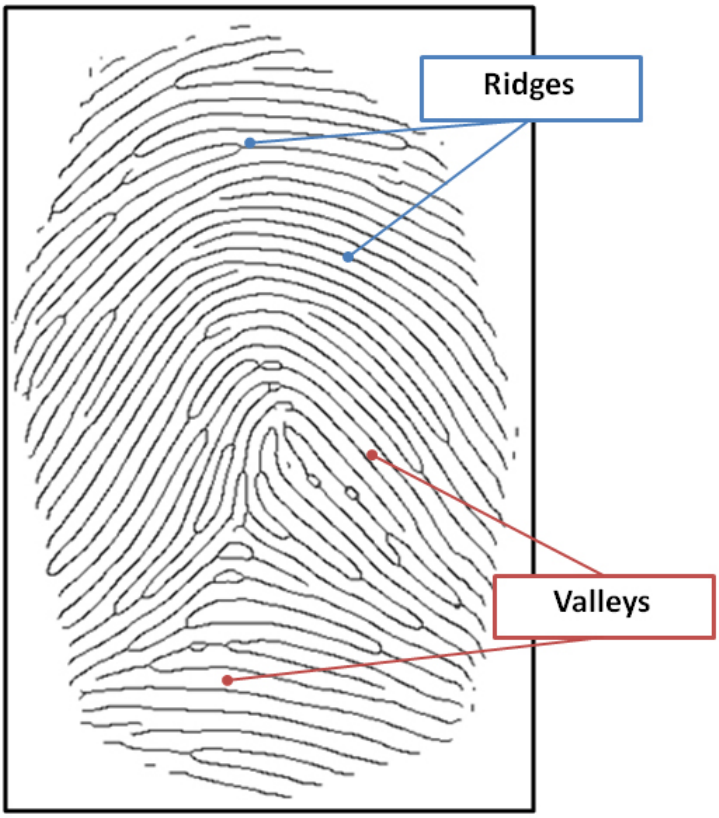

Figure 2.3: Ridges and valleys in a fingerprint image.

variations, affine transformations and requires a large amount of storage.

The available fingerprint features are organized in levels and depend particularly on the acquisition resolution. As we can see in Figure 2.3 the most evident structural characteristic of a fingerprint is a "pattern" of interleaved *ridges* (the darker areas) and *valleys* (bright areas).

At the global level a fingerprint shows a smoothed structure except in one or more regions containing distinctive characteristics called *singularities* (see Figure 2.4) which can be:

- *delta* (represented with the symbol Δ);
- *loop* (represented with the symbol $\cap$);
- *whorl* (represented with the symbol O).

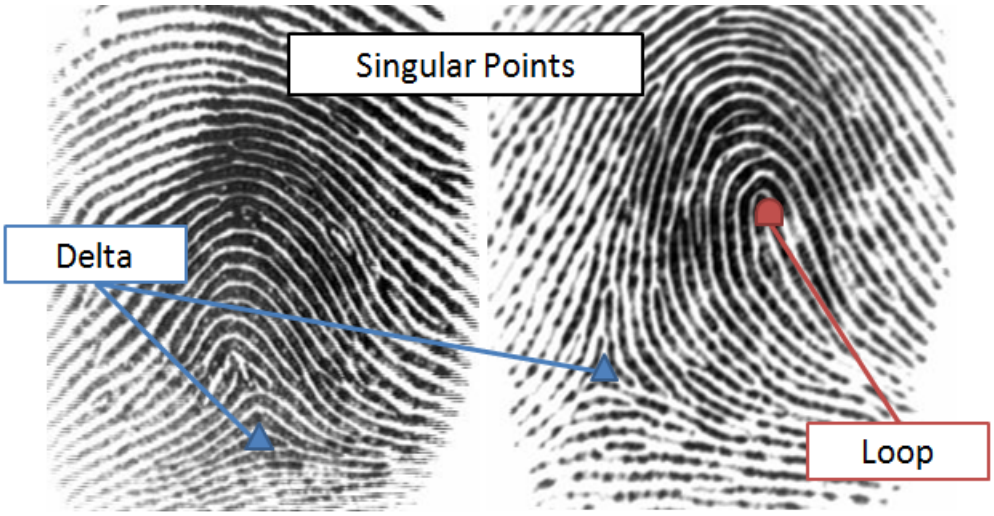

Figure 2.4: Singular Points.

With respect to these basic structures, in 1900 E. Henry [39] organized fingerprints in the five main categories (or classes) showed in Figure 2.5. The "center point" of a fingerprint is called *core* and can be defined as the north most point of the innermost ridge line. If a fingerprint does not contain loop or whorl singularities (i.e. arch category) the core is usually defined as the point of maximum ridge curvature. With the Henry fingerprints organization system it is possible speed up the search, especially in the case where the available database is very large.

At the local level, the fingerprint shows local high distinctive details called *minutiae* (or Galton details [45], in honor of the first observer). The American National Standards Institute (ANSI/NIST-ITL 1, [6]) considers four minutiae classes: *ridge endings*, *bifurcations*, *compound* and *type undetermined*; the FBI minutiae model [92] considers only ridge endings and bifurcations. The most common minutiae types are depicted in Figure 2.6 (left).

Increasing the acquisition resolution (at least 1000 dpi), it is possible detect small geometric details such as *ridge width*, *breaks*, *creases*, *scars*. The most important low level details are small points over the ridge lines called *sweat pores* (see Figure 2.6 right). 20-40 pores are sufficient to recognize a person, for this reason they are very coveted by latent fingerprint examiners but, as drawback, the image quality and the acquisition resolution have to be very high.

(a) Left Loop (b) Right Loop (c) Whorl (d) Arch (e) Tented Arch

Figure 2.5: Henry Fingerprint Classification.

2.4.1 Local Ridge Orientation

The local ridge orientation is one of the most important characteristics of a fingerprint image. The orientation extraction represents a mandatory step for the most effective fingerprint recognition algorithms. It is simple to compute if the image quality is good. In bad images, a reliable extraction is still an open problem.

Given a fingerprint $\mathbf{I}$, where the element $I_{x,y}$ represents the gray-level of pixel at $[x, y]$, the orientation image (or directional image) is a $h \times w$ matrix $\mathbf{D}$ whose elements encode the local orientation of the fingerprint ridges. Each element $\theta_{i,j} \in [0, \pi[$, corresponding to node $[i, j]$ of a squared-meshed grid, is located over pixel $[x_i, y_j]$ and denotes the average orientation of the fingerprint ridges estimated in a window centered in $[x_i, y_j]$.

Most of this Thesis, describes how to improve the fingerprint orientation extraction, so a detailed description of this problem can be found in Part II, Part III and indirectly in Part I.

2.4.2 Local Ridge Frequency

The local ridge frequency, denotes the number of ridges per unit length along a hypothetical segment centered at $[x, y]$ and orthogonal to the local ridge orientation $\theta_{i,j}$. As for the local ridge orientation, the frequency image $\mathbf{F}$ is estimated at discrete positions and it varies considerably across different regions.

Hong et al. [53] estimate the frequency counting the average number of pixels between consecutive pixels along the direction orthogonal to the local ridge orientation. Maio and Maltoni in [85] exploit the variation theorem to estimate the unknown fre-

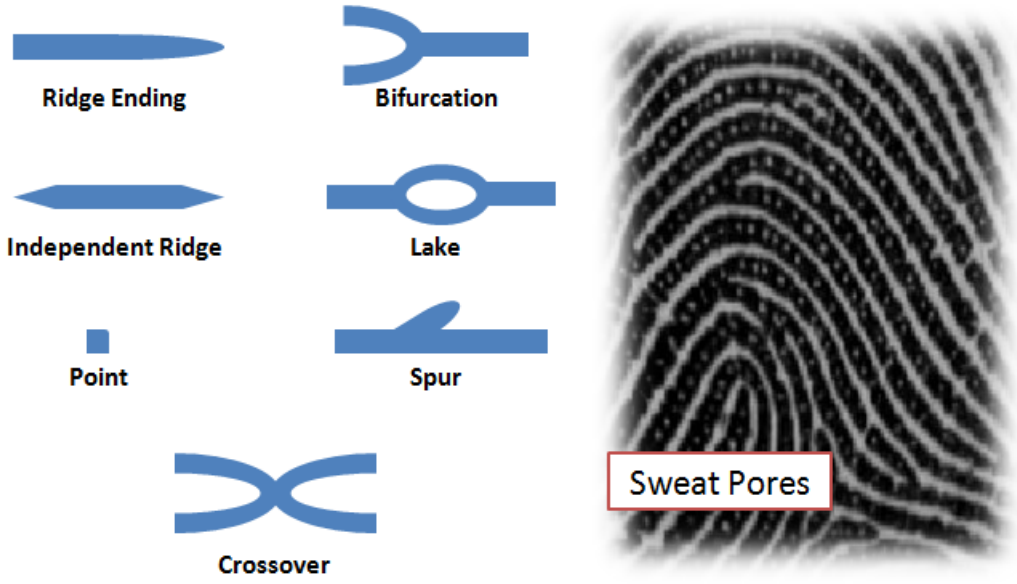

Figure 2.6: The most common minutiae (left) and a fingerprint portion where sweat pores are well evident (right).

quency and Chikkerur et. al in [32] use an approach based on the short-time Fourier transform analysis.

2.4.3 Minutiae

The extraction of fingerprint minutiae is a very important task especially because most of automatic systems are based on minutiae matching. The simpler method to extract minutiae converts the input fingerprint image in a binary image (binarization), applies a thinning to reduce the ridges size to one pixel and then, the resulting skeleton image is scanned to detect the pixels corresponding to minutiae. Some examples of binarization-based methods are [114] [93] [33] [100]. Another approach to minutiae detection, that avoid the image binarization and thinning, is the direct gray-scale extraction. The method of Maio and Maltoni [86] is one of the most representative algorithms belonging to this family.
After the minutia detection, a minutiae filtering step is often necessary in order to remove spurious minutiae in very noise fingerprint regions.

2.5 Fingerprint Matching

Given a couple of fingerprints, automatic fingerprint matching is the process of automatically verify if the two fingerprints belong or not to the same individual. In the first case we have a *match* otherwise we have a *non-match*.

Large intra-class variability in different acquisitions of the same finger (due for example to displacement, rotation, overlap, variable pressure, noise non-linear distortion), makes the fingerprint matching a difficult problem. The difficulty is even higher in case we deal with latent fingerprints. Another type of variability that makes the problem difficult, is the intra-class variability: fingerprints of different fingers may sometimes appear quite similar.

Hereafter, we denote the representation of the fingerprint acquired during the enrollment as the template (**T**) and the representation of the fingerprint to be matched as the input (**I**). The template is a representation of a fingerprint in terms of salient features (minutiae type, minutiae positions, local ridge orientations, local ridge frequencies, quality) obtained after a feature extraction phase. When we talk of input image, we talk about the pixel-based image obtained after the acquisition with a fingerprint scanner.

Fingerprint matching methods can be classified in three main families:

- *Correlation-based matching.* Methods belonging to this family, superimpose two fingerprints and compute the correlation between the corresponding pixels for different alignments. Usually a cross-correlation measure, representing the image similarity, is maximized between two images [90]. Due to displacements and rotations the simple cross-correlation is not enough, it should be measured considering different positions and angles.

  In general the correlation is not a robust matching method because of i) non-linear distortions that make the global structure in impressions of the same finger very different; ii) the skin condition may significantly vary the image characteristics (brightness, contrast, ridge thickness); iii) the computation of the cross-correlation for different positions and angles is computationally inefficient. Correlation-based matching computing local correlation has been proposed by [8] while, in [59] [60] and [112], has been proposed to use a symmetric phase only filter with restricted domain to reduce the effect of the noise. Correlation using neural networks has been proposed in [135] while more sophisticated correlation techniques based on advanced correlation filters can be found in [123].

- *Minutiae-based matching.* Minutia matching is the most widely used method for fingerprint matching. The minutiae are extracted from two fingerprints and stored in feature vectors as points in the two-dimensional plane. The idea behind minutiae-based matching consists of find the correct alignment between a template and the features extracted from an input image.
  A couple of minutiae are considered "matching" is the spatial distance between them is smaller than a spatial threshold and the direction difference between them is smaller than an angular threshold. The fingerprint alignment is mandatory in order to maximize the number of matching minutiae.
  Automatic matchers must convert the number of matching minutiae in a similarity score. This can be performed using a matching minutiae normalization approach or exploiting more information like quality.
  The minutia-based matching problem is extensively studied and a large number of works have been published on this topic [101] [56]. In [90] can be found a detailed description of the problem and references to the most recent methods.
  For our matching experiments, we will use the Minutia Cylinder-Code (MCC) proposed by Cappelli et al. in [17] and [18]. MCC is a novel minutiae-only representation and matching technique for fingerprint recognition. MCC relies on a robust discretization of the neighborhood of each minutia into a 3D cell-based structure named cylinder and provides simple but effective techniques for the computation and consolidation of cylinder similarities to determine the global similarity between two fingerprints. MCC is very fast and suitable to be simply coded in hardware, due to the bit-wise nature of the matching technique; this allows its porting on inexpensive secure platforms such as a smart-card or a system-on-a-chip.

- *Non-Minutiae feature-based matching.* Approaches belonging to this family do not use the minutiae to perform matching but use some other features of the fingerprint ridge pattern (e.g. local ridge orientation and frequency, texture, shape). The main motivation of not using the minutiae is that their extraction is difficulty in extremely low-quality fingerprint images; the comparison is done in term of features extracted by the ridge pattern. The most popular technique belonging to this family is represented by the FingerCode [66] [67] [105] [104].

Database	Description
NIST DB 4 [130] NIST DB 9 [131] NIST DB 10 [128] NIST DB 14 [129]	Thousands of images scanned from rolled inked impressions on cards.
NIST DB 24 [132]	100 live video sequences from 10 individuals to study the effect of finger rotation and plastic distortion.
NIST DB 27 [46]	Latent fingerprint images of good, bad and ugly quality.

Table 2.1: NIST Databases.

Competition	Num. of Databases	Size of each DB A:evaluation B:training	Difficulty		
			Low	Medium	High
FVC2000 [87]	4	A: 100x8 B:10x8	DB 1 2 4		DB 3
FVC2002 [88]	4	A: 100x8 B:10x8	DB 1 2 3 4		
FVC2004 [89]	4	A: 100x8 B:10x8		DB 1 2 3 4	
FVC2006 [25]	4	A: 140x12 B:10x12	DB 2 4	DB 3	DB 1

Table 2.2: FVC Databases. Each database (DB1, DB2, DB3, DB4) is partitioned in two disjoint subsets A and B: A is used for the algorithm performance evaluation, B is made available to the participants as a development set to allow parameter tuning (training). The notation SxT in the database size denotes S fingers and T samples per finger.

2.6 Fingerprint Databases

In the following section, we describe the fingerprint recognition databases that we use to assess the performance of the algorithms proposed in this Thesis. Before the organization of the first fingerprint verification competition FVC2000 [87], the only public domain fingerprint databases were the National Institute of Standard and Technology (NIST, [58]) databases. They constitute a good starting point for the development of automatic fingerprint recognition systems, but are not well suited for the evaluation of algorithms operating on live-scan mode. With the FVC campaigns ([87], [88] [89] [25]) it was possible to track performance of state-of-the-art fingerprint matching algorithms through a fair comparison with a common protocol.

Table 2.1 describes the main features of NIST databases while Table 2.2 describes the main features of FVC databases.

2.7 Synthetic Fingerprint Generation

The performance of new fingerprint recognition algorithms is usually evaluated on relatively small databases. A dataset of a huge number of real fingerprints is hard to obtain and most of the time hard to share because of privacy legislations that often protect such personal data. These limitations make the recognition accuracy estimates highly data dependent with poor generalization abilities on fingerprints acquired in different environments. To overcome this problem in [22] and [90] has been proposed a synthetic fingerprint generator able to derive datasets of arbitrary size of realistic fingerprint images.

2.8 Accuracy Measurements

A general biometric system, no matter what type of biometric trait we consider, can be view as a pattern recognition system that offers a (usually) binary decision to a given input. Let us consider for example the matcher module in a fingerprint verification system: when a fingerprint is presented to the system we expect, after an internal processing, a decision of the type match/non-match with a template already stored in a database. However, due to imperfect sensing conditions (e.g., noisy fingerprint due to sensor malfunction), alterations in the user's biometric characteristic (e.g., cuts, scars, wet or dry fingerprint), changes in ambient conditions and variations in the user's interaction with the sensor, the system may output the wrong answer.

As pattern recognition system, a biometric system inevitably makes incorrect decisions, so we need a framework through which measure the system errors. The bayesian decision theory [38] offers all we need to measure errors in biometric systems.

The response of a matcher in a generic biometric recognition system is usually a similarity score s that measures the similarity between two biometric feature sets. The system decision is regulated by a *threshold* t: pairs of feature sets generating similarity score higher than or equal to t are called *matching pairs*; whereas pairs producing scores lower than t are called *non-matching pairs*. A similarity score is known as a *genuine score* if it is a result of matching two biometric samples of the same user; it is known as an *impostor score* if it involves comparing two biometric samples originating from different users.

A generic biometric verification system makes two types of errors:

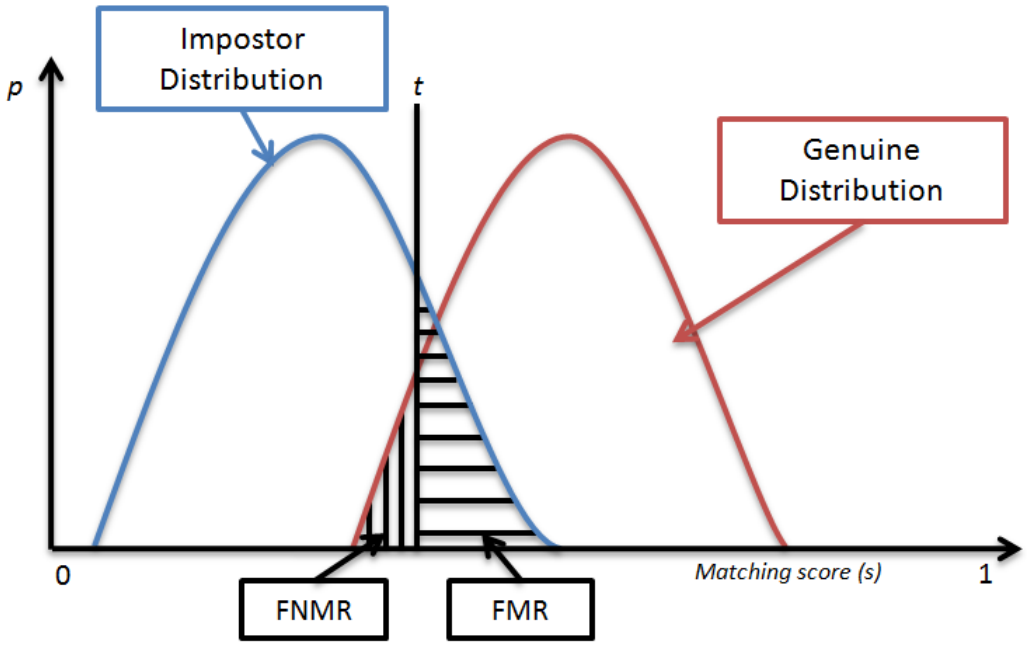

Figure 2.7: False Non-Match Rate and False Match Rate for a given threshold (t) value.

- it can decide that biometric measurements from two different individuals belong to the same one (called *false match* or *false acceptance*);
- or decide that two biometric measurements from the same person belong to two different persons (called *false non-match* or *false rejection*).

In a biometric system, the *False Match Rate* (FMR) can be defined as the probability that an impostor score exceeding the threshold t; in the same way, the *False Non-Match Rate* (FNMR) may be defined as the probability that a genuine score falling below the threshold t. Generally to evaluate the accuracy of a generic biometric system one must collect scores produced from a number of genuine matching (called *genuine distribution*), and scores generated from a number of impostor matching (called *impostor distribution*). Figure 2.7 reports FMR and FNMR over genuine and impostors distributions.

It is worth noting from Figure 2.7 that FMR and FNMR are functions of the system threshold t. If t is decreased to make the system more tolerant, the FMR increases and FNMR decreases; vice versa, if t is raised to make the system more secure, then FMR decreases and FNMR increases.

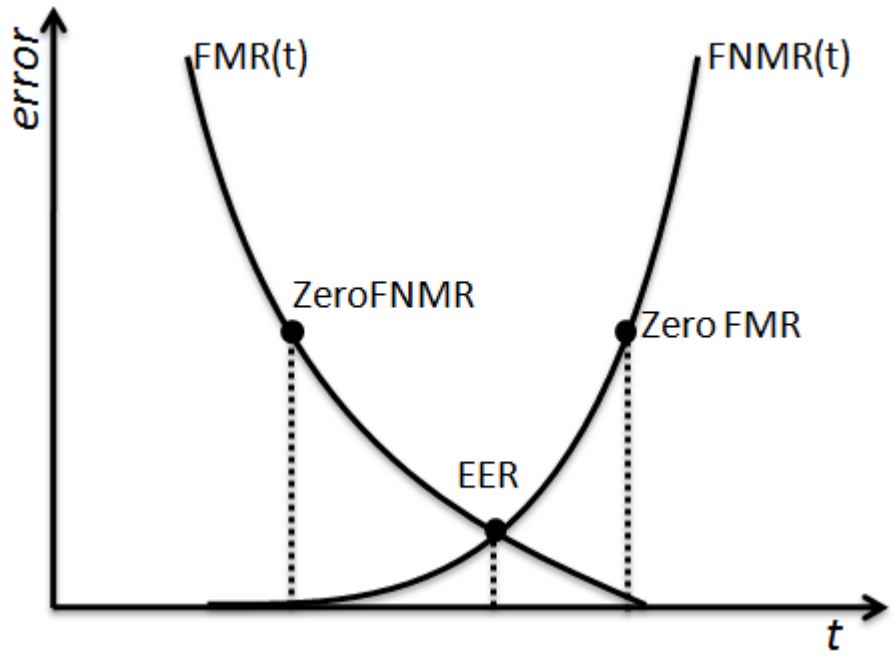

Figure 2.8: False Non-Match Rate and False Match Rate curves for a given threshold t. The Equal Error Rate, the ZeroFNMR and ZeroFMR are highlighted.

A system designer may not know in advance the particular application for which the system may be used. So it is advisable to report system performance at all operating points (threshold, t). The FMR and FNMR at various values of t can be summarized using a *Detection-Error Tradeoff* (DET) curve that plots the FNMR against the FMR at various threshold and provides a more direct view of the error-vs-error tradeoff (see [90]). If we plot the FMR against 1-FNMR we obtain an other important curve called *receiver operating characteristic* (ROC).

Additionally to the above distributions and curves, some "compact" indices are also used to summarize the accuracy of a generic biometric verification system [90]:

- *Equal-Error Rate* (EER) denotes the error rate at the threshold t for which FMR and FNMR are identical (see Figure 2.8);
- *ZeroFNMR* is the lowest FMR at which no FNMR occur (see Figure 2.8);
- *ZeroFMR* is the lowest FNMR at which FMR occur (see Figure 2.8);
- *FMRx* is the lowest FNMR for FMR$\leq \frac{1}{x}$;

- *FNMRx* is the lowest FMR for FNMR$\leq \frac{1}{x}$.

The real performance requirements of a biometric system are very much application related. For example, in some forensic applications such as criminal identification, it is the FNMR that is a major attention and not the FMR: that is, we do not want to ignore a criminal even at the risk of manually examining a large number of potential matches identified by the biometric system. At the other extreme, a very low FMR may be the most important factor in a highly secure access control application, where the primary objective is not to let in any impostors although we are concerned with the possible inconvenience to legitimate users due to a high FNMR[90]. In the same way, the performance estimation of a generic biometric identification system can be derived by the error estimates in the verification mode.

Part I

Novel Enhancement Method for Fingerprints

Chapter 3

Fingerprint Enhancement

A minutiae extraction algorithm heavily relies on the quality of the input fingerprint. If the quality is good, the ridges-valley flow is well evident and a reliable set of minutiae can be extracted. If the fingerprint is very noisy, the minutiae extraction algorithm may detect a large number of spurious minutiae and miss several genuine minutiae. Therefore, to achieve high recognition performance it is essential to incorporate a fingerprint enhancement module able to improve the quality of noisy fingerprints, thus making the subsequent processing steps more reliable.

A fingerprint image enhancement algorithm receives an input fingerprint image, applies a set of intermediate steps on the input image, and finally outputs the enhanced image.

A fingerprint region can be assigned to one of the following three categories:

- well-defined region, where the ridge-valley flow is well defined;
- recoverable region, where ridges are corrupted by some kind of noise but the neighboring regions provide some information about the underlying structure;
- unrecoverable region, where the noise is so high that the ridge-valley flow cannot be reconstructed.

Figure 3.1 shows an example of such regions.

The goal of a fingerprint enhancement algorithm is to retain the information in well-defined regions, improve the quality in recoverable regions and mark as unrecoverable the remaining regions. Since the objective of a fingerprint enhancement algorithm is

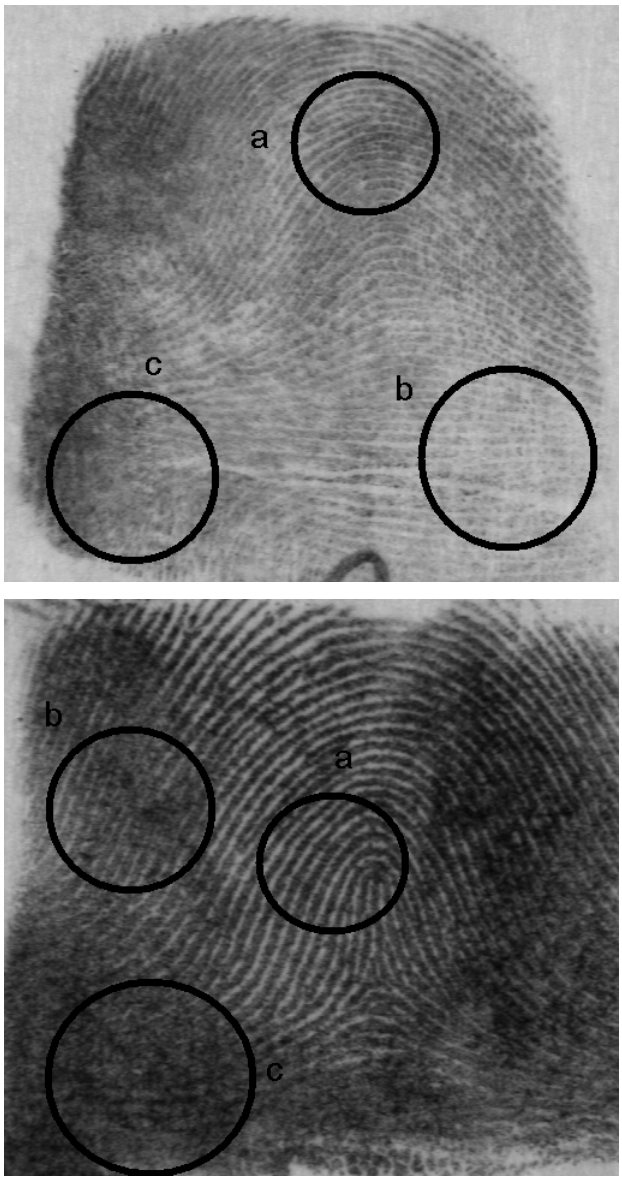

Figure 3.1: Fingerprint Regions. Well-defined region (a), recoverable region (b) and unrecoverable region (c).

to improve the clarity of ridge structures of input fingerprint images to facilitate the subsequent processing steps (ridges and minutiae extraction), a fingerprint enhancement algorithm should not result in any spurious ridge structures. This is very important because spurious ridges or unwanted artifacts may change the structure of input fingerprints; as a result, the individuality may change.

An automatic detection and classification of fingerprint regions is not an easy task; in general, the available information like local ridge orientation, local ridge frequency, image contrast and other local features are combined to compute a quality index: a number that expresses the local or global fingerprint quality.

In this chapter we describe the state-of-the-art in fingerprint enhancement and provide novel solutions to this important problem. We describe a new fingerprint enhancement algorithm that selectively applies contextual filtering starting from automatically-detected high-quality regions and then iteratively expands toward low-quality ones. The proposed algorithm does not require any prior information like local orientations or frequencies. Experimental results over both real (FVC2004 and FVC2006 (see section 2.6)) and synthetic (generated by the SFinGe software (see section 2.7)) fingerprints demonstrate the effectiveness of the proposed method.

3.1 State-of-the-art

Fingerprint enhancement methods can be divided in three groups:

- *Pixel-wise.* Methods exploiting pixel-wise image processing operations are the most simpler enhancement techniques, where the pixel intensity in a given point depends on its previous value and global parameters. Common operations include normalization [53], intensity transformations, histogram processing, image subtraction, image averaging [47]. In general, pixel-wise methods do not change the ridge-valley flow and do not produce good fingerprint enhancement results without further processing steps, in particular for noisy images. Good enhancement results can be achieved exploiting pixel-wise methods as pre-processing in advanced fingerprint recognition algorithms. Recent works on image normalization include [76] and [111].

- *Contextual-filtering.* Methods exploiting contextual information are the most common approaches to fingerprint enhancement [90]. The context is usually represented by local orientation, local frequency and local quality and is utilized to adapt the filter characteristics to each specific foreground region.
  The first contextual-filtering based method for enhance fingerprints was proposed in [95] and [96]. Contextual filtering in Fourier domain was proposed by Sherlock, Monro and Millard in [108] and [109]. One of the most used contextual filtering

method is based on Gabor filters, as proposed by Hong et al. in [53]. Gabor filters have both frequency-selective and orientation-selective properties and have optimal joint resolution in both spatial and frequency domains. Filtering approaches in the frequency domain or in a mixture of spatial and frequency domain have been proposed by various authors [110] [32] [71] [54].

- *Multi-resolution.* This analysis has been proposed to remove noise from fingerprint images through a decomposition and compensation technique. The image is firstly decomposed into different frequency bands and then
  - at low and intermediate frequencies bands the ridge-valley flow is cleaned and gaps are closed;
  - at high frequencies the details are preserved.

  The state of the art in multi-resolution analysis is represented by [5] [55], [29], [43] and [44].

3.2 Enhancement with Contextual Iterative Filtering

The enhancement abilities with contextual methods heavily rely on a good context extraction represented by the local ridge orientation, local ridge frequency and local image quality. In noisy fingerprints it is not possible to extract a reliable context because of poor quality regions that may introduce unwanted artifacts.

In the following sections we propose a new enhancement algorithm where contextual filtering is applied according to an iterative scheme. To the best of our knowledge, just a few works exist in literature on fingerprint enhancement based on iterative filtering.

Zhu and Zhang [138] proposed a top-down Fourier method that initially filters the whole image and then divides the filtered image in smaller sub-images. Each sub-image is similarly filtered and sub-divided until the image size is smaller than a threshold. This approach does not provide good results if the fingerprint has fragmentary ridges with high curvature.

Sutthiwichaiporn et al. [116] proposed an iterative filtering approach for fingerprint enhancement using matched filters. After a preprocessing and a Signal-to-Noise-Ratio

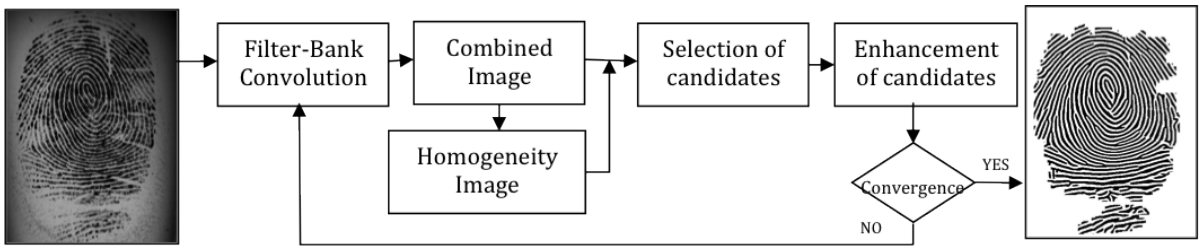

Figure 3.2: Flow-chart of the proposed iterative enhancement algorithm.

analysis in the spatial-frequency domain, matched filters are applied to all image blocks. An iterative restoration process diffuses high-quality spectrum of the enhanced fingerprint into low-quality regions. The algorithm is not effective if the quality is not properly estimated.

The basic idea of our proposed approach is to selectively apply contextual filtering starting from high-quality region and then iteratively expanding like wildfire to low-quality regions. If low-quality regions were aggressively enhanced at the first iterations, wrong local contextual information would lead to a bad recovery of the ridge line structure; our strategy tries to make the contextual information more reliable at the border of low-quality regions so that when they will be considered for enhancement, better results can be achieved.

3.3 Iterative Fingerprint Enhancement

The flow-chart of the proposed approach, shown in figure 3.2, is composed of five main steps: i) filter-bank convolution, ii) combined image computation, iii) homogeneity image computation, iv) selection of the candidates and v) enhancement of the candidates. The input of the proposed approach is a gray-scale noisy fingerprint where the ridge flow has been segmented from the background. The output consists in a binary image. Each step of the computation is explained in the following sections.

3.3.1 Convolution with a Gabor filter-bank

A Gabor filter is defined by a sinusoidal plane wave (the second term in Equation 3.1) tapered by a Gaussian (the first term in Equation 3.1). The even symmetric two-

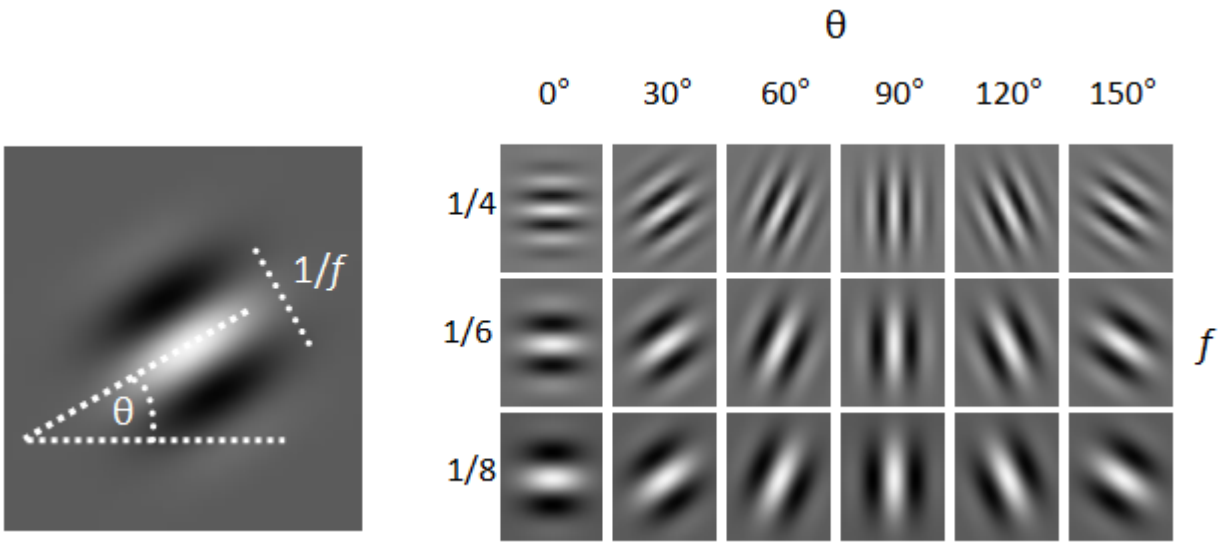

Figure 3.3: A Gabor filter-bank with six orientations θ (columns) and three frequencies f (rows).

dimensional Gabor filter has the following form:

$$g(x, y : \theta, f) = exp\Big\{ -\frac{1}{2}\Big[\frac{x_\theta^2}{\sigma_x^2} + \frac{y_\theta^2}{\sigma_y^2}\Big]\Big\} \cdot cos(2\pi f \cdot x_\theta) \tag{3.1}$$

where θ is the orientation of the filter and $[x_\theta, y_\theta]$ are the coordinates of $[x, y]$ after a clockwise rotation of the Cartesian axes by an angle of $(90° - \theta)$. Such filter depends on four parameters $(\theta, f, \sigma_x, \sigma_y)$ even if often it is used with $\sigma_x = \sigma_y$.

A Gabor filter-bank is defined as a set $G = \{g_{i,j}(x, y)|i = 1..n_o, j = 1..n_f\}$ of Gabor filters, where n_o is the number of discrete orientations $\{\theta_i|i = 1..n_o\}$ and n_f the number of discrete frequencies $\{\theta_j|j = 1..n_f\}$.

Let $\mathbf{I}$ a $h \times w$ fingerprint image, the output of the convolution between $\mathbf{I}$ and the filter-bank G is a set V of $n_o \cdot n_f$ images where $\mathbf{V^{i,j}} = [v_{x,y}^{i,j}], x = 1..w, y = 1..h$ denotes the response image to a filter $g_{i,j}$ with orientation θ_i and frequency f_j.

Typically n_o is set to 8 or 16 and n_f in the range [1,4] (see Figure 3.3). To save computation time in low-cost and computation-limited fingerprint systems, the filter-bank can be pre-computed.

3.3.2 Combined Image

The set of responses V, obtained after the convolution, is used to compute a single combined image $\mathbf{C} = [c_{x,y}], x = 1..w, y = 1..h$, where the combination is performed according to the max filter response:

$$c_{x,y} = v_{x,y}^{l,t} \tag{3.2}$$

where $l, t = argmax_{i,j}|v_{x,y}^{i,j}|$ and $i = 1..n_o, j = 1..n_f$.

Figures 3.5a and 3.5b show a fingerprint image and the combined image (obtained after four iterations of the proposed algorithm), respectively. It is worth noting that good quality regions in the combined image 3.5b are more visible than bad quality ones and represents a point from which expand the fingerprint enhancement.

As side effect of the combination we obtain a pixel-level orientation image $\mathbf{O} = \{o_{x,y}|x = 1..w, y = 1..h\}$ and frequency image $\mathbf{F} = \{f_{x,y}|x = 1..w, y = 1..h\}$:

$$o_{x,y} = \theta_l, \;\; f_{x,y} = f_t \tag{3.3}$$

The pixel-level orientation image is shown in Figure 3.5d. The orientations are mapped in the range [0, 255] so similar colors represent similar orientations. From this representation we can obtain a meshed-grid representation simply centering a window each s elements in the pixel-level orientation image and then averaging (considering the double angle representation) the orientations in the window.

A first possible alternative for the computation of 3.2 is based on the average value. Instead of compute the combination according to the max filter response, we can compute $c_{x,y}$ as

$$c_{x,y} = \frac{1}{n_f \cdot n_o} \sum_{i=0}^{n_o} \sum_{j=0}^{n_f} v_{x,y}^{i,j}. \tag{3.4}$$

The advantage of 3.4 is that the computation time is reduced. The disadvantage is that we cannot keep track of the filter with best response, the homogeneity image (see next section) cannot be computed and the final quality of the enhancement is consequently lower.

A second possible alternative for the computation of the combined image is first to process each image $\mathbf{V^{i,j}}$ with a gaussian mask and then apply the 3.2. Following this approach, the response $v_{x,y}^{i,j}$ is modified as

$$v_{x,y}^{i,j} = \frac{\sum_{s=0}^{n_o} \sum_{t=0}^{n_f} v_{x,y}^{s,t} \cdot G_{mask}^{i,j}[s,t]}{\sum_{s=0}^{n_o} \sum_{t=0}^{n_f} G_{mask}^{i,j}[s,t]} \tag{3.5}$$

where $i = 1..n_o, j = 1..n_f$ and $G^{i,j}_{mask}$ is a $n_f \cdot n_o$ image such that

$$G^{i,j}_{mask}[s,t] = exp\Big(-\frac{d\phi(o_{i,j}, o_{s,t})^2}{2\sigma_o^2}\Big) \cdot exp\Big(-\frac{(f_j - f_t)^2}{2\sigma_f^2}\Big) \tag{3.6}$$

where $d\phi(o_{i,j}, o_{s,t})$ denotes a difference between angles (see next section) and σ_o^2, σ_f^2 are the variances of the two gaussian functions. After the application of this gaussian filter, the combination is obtained as in 3.2. The advantage of this approach is that each response $v^{i,j}_{x,y}$ is weighted by a gaussian function centered in $[i,j]$. The disadvantage of

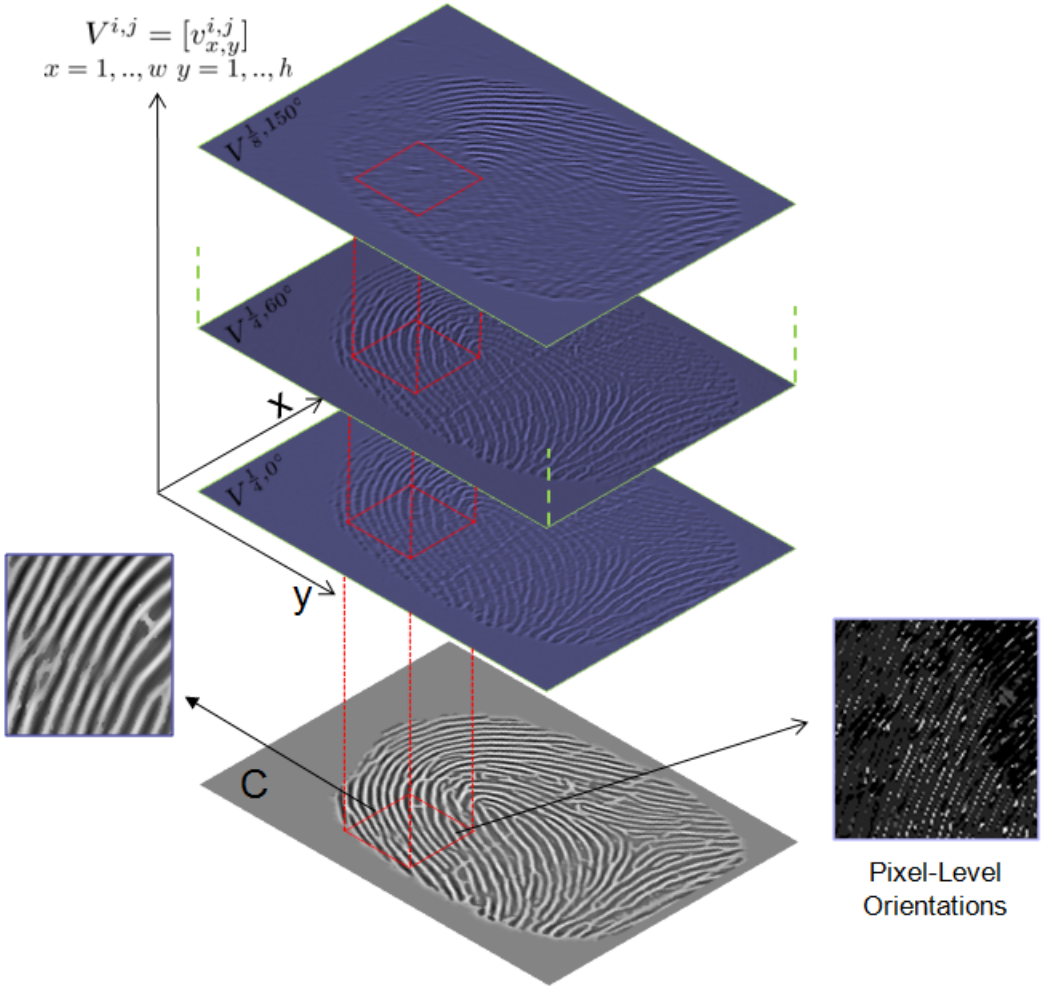

Figure 3.4: Combination **C** of a set of response images **V** with the maximum absolute value method. As side effect of the combination we obtain a pixel-level orientation image **O**.

this approach is that it is computationally expensive.

3.3.3 Homogeneity Image

The homogeneity image $\mathbf{H} = \{h_{x,y} | x = 1..w, y = 1..h\}$ encodes the local ridge flow homogeneity. In principle, except for singularity regions, ridges run smoothly across the fingerprint pattern, and sudden changes in the orientation and frequency should not exist. In practice, such discontinuities are determined by noise or ridge alteration such as creases or scratches.

The homogeneity at location [x,y] is defined as:

$$h_{x,y} = \frac{\sum_{p,k} c_{p,k} \cdot s_{p,k}}{\sum_{p,k} c_{p,k}} \tag{3.7}$$

where $p, k = -\frac{m}{2}, .., +\frac{m}{2}$ and $s_{p,k}$ is an orientation homogeneity measure computed as:

$$s_{p,k} = \frac{\pi}{2} - |d\phi(o_{x,y}, o_{p,k})| \tag{3.8}$$

where

$$d\phi(\theta_1, \theta_2) = \begin{cases} \theta_1 - \theta_2, & \text{if } -\frac{\pi}{2} \leq \theta_1 - \theta_2 < \frac{\pi}{2} \\ \pi + \theta_1 - \theta_2, & \text{if } \theta_1 - \theta_2 < -\frac{\pi}{2} \\ \pi - \theta_1 + \theta_2, & \text{if } \theta_1 - \theta_2 \geq \frac{\pi}{2} \end{cases} . \tag{3.9}$$

Finally, $\mathbf{H}$ is normalized to fit its values in the range [0,1]. As shown in Figure 3.5c, darker regions denote a low homogeneity: the ridge pattern in the combined image is fragmentary.

The homogeneity image varies during the iterative process. At the first iterations, in particular if the quality of the input image is low, the homogeneity image has many dark regions, while at the end of the process most regions are bright.

3.3.4 Selection of the Candidates

Both $\mathbf{C}$ and $\mathbf{H}$ are used to select the set of candidate pixels, according to a *top-ranking* criterion. The idea is to select a percentage of good quality pixels, that is pixels with strong (positive or negative) responses to the filtering and possibly belonging to highly-homogeneous regions.

Let $\mathbf{P} = \{p_{x,y} | x = 1..w, y = 1..h\}$ be a matrix whose elements are computed as:

$$p_{x,y} = c_{x,y} \cdot h_{x,y} \cdot r_{x,y} \tag{3.10}$$

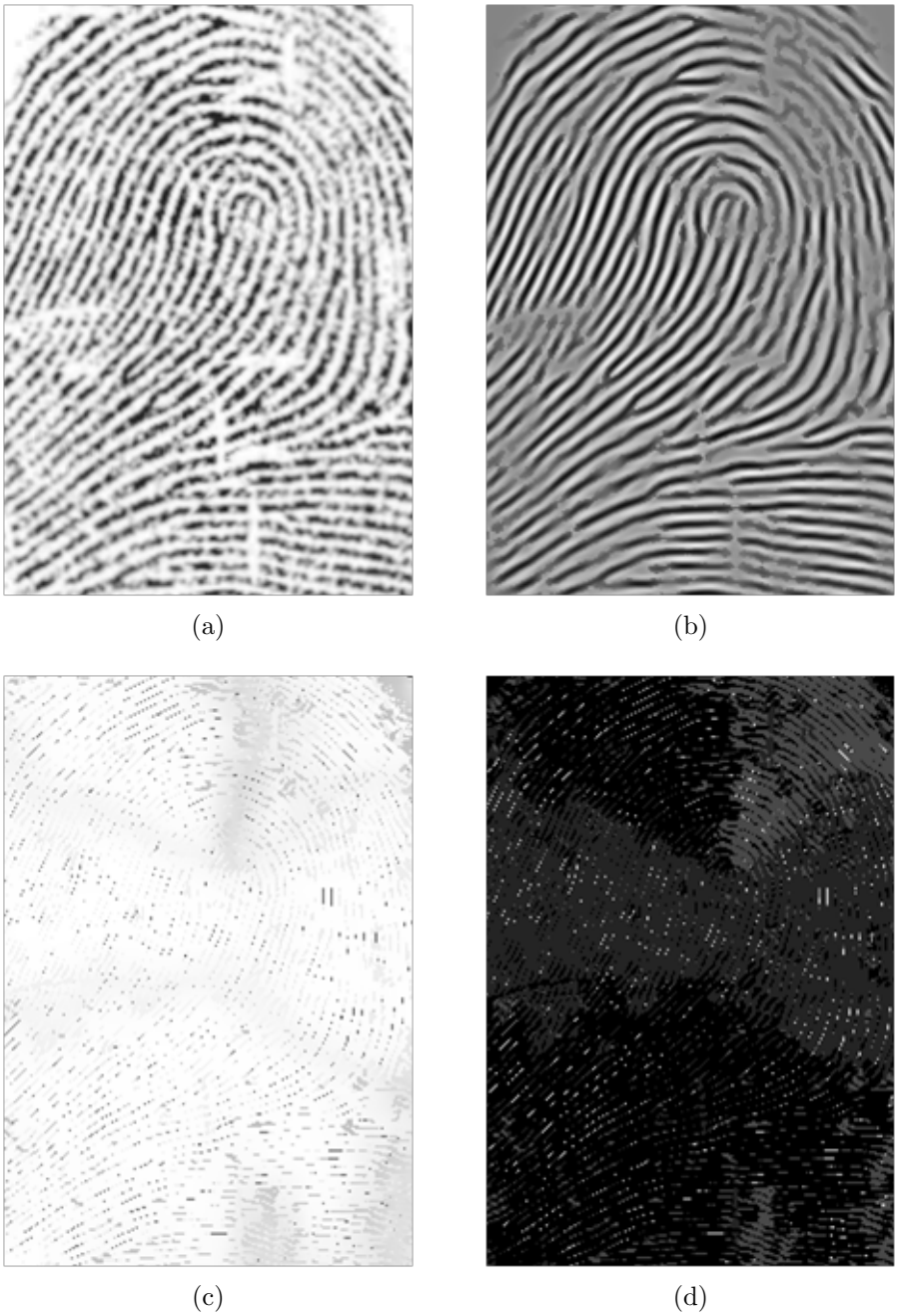

(a) (b)

(c) (d)

Figure 3.5: Original fingerprint image (a), combined image (b), homogeneity image (c) and pixel-level orientation image (d) at the fourth iteration of the proposed algorithm.

where $\mathbf{R} = \{r_{x,y}|x = 1..w, y = 1..h\}$ is a selection matrix such that $0 < r_{x,y} \leq 1$. $\mathbf{R}$ controls the selection of candidate pixels in successive iterations; all $r_{x,y}$ values are initialized to 1, but when a pixel $I_{x,y}$ is selected then the corresponding $r_{x,y}$ is multiplied by a decay constant $0 \leq \rho < 1$, in order to inhibit its selection in the successive iterations.

Elements in $\mathbf{P}$ are then sorted and two sets $\mathcal{A}$ and $\mathcal{B}$, corresponding to ridges and valleys, respectively, are determined by taking the first and last percentile γ:

$$\mathcal{A} = \{I_{x,y}|rank(p_{x,y}) \leq \gamma \cdot |\mathbf{P}|\} \tag{3.11}$$

$$\mathcal{B} = \{I_{x,y}|rank(p_{x,y}) \geq (1 - \gamma) \cdot |\mathbf{P}|\} \tag{3.12}$$

where the function $rank(\cdot)$ outputs the position in the ranking of a given element $p_{x,y}$ and $|\mathbf{P}|$ represents the number of matrix items in $\mathbf{P}$.

3.3.5 Enhancement of the Candidates

The enhancement is carried out with the following scheme:

$$\Delta_{x,y} = \begin{cases} 0, & \text{if } I_{x,y} \in \mathcal{A} \\ 255, & \text{if } I_{x,y} \in \mathcal{B} \end{cases} \tag{3.13}$$

$$I_{x,y} = I_{x,y} \cdot (1 - \epsilon) + \Delta_{x,y} \cdot \epsilon, \qquad \forall I_{x,y} \in A \cup B \tag{3.14}$$

where $0 < \epsilon \leq 1$ controls the amount of enhancement. Figure 3.6 shows an example of selection/enhancement at a given iteration.

The algorithm continues iterating until a convergence criterion is satisfied: the maximum number of iterations is reached or no more low-quality regions exist in the image. Figure 3.7 and Figure 3.8 show how a noisy fingerprint evolves with the proposed iterative algorithm. Good quality regions are well detected during the first iterations. From such regions the enhancement is propagated toward bad quality regions.

3.4 Experimental Results

To evaluate the performance of the proposed iterative fingerprint enhancement method, we apply it on synthetic and real fingerprints. In the first case we measure the performance according to a difference between the enhanced image and a master binary image, in the second case using the statistics reported in section 2.8.

(a) (b) (c)

Figure 3.6: Enhancement of the candidates and resulting image at the fourth iteration of the proposed algorithm. The enhancement of pixels belonging to set $\mathcal{A}$ (a) and $\mathcal{B}$ (b) is reported. The application of these masks to the fingerprint is shown in (c).

Figure 3.7: Evolution of a noisy fingerprint during the iterative enhancement process.

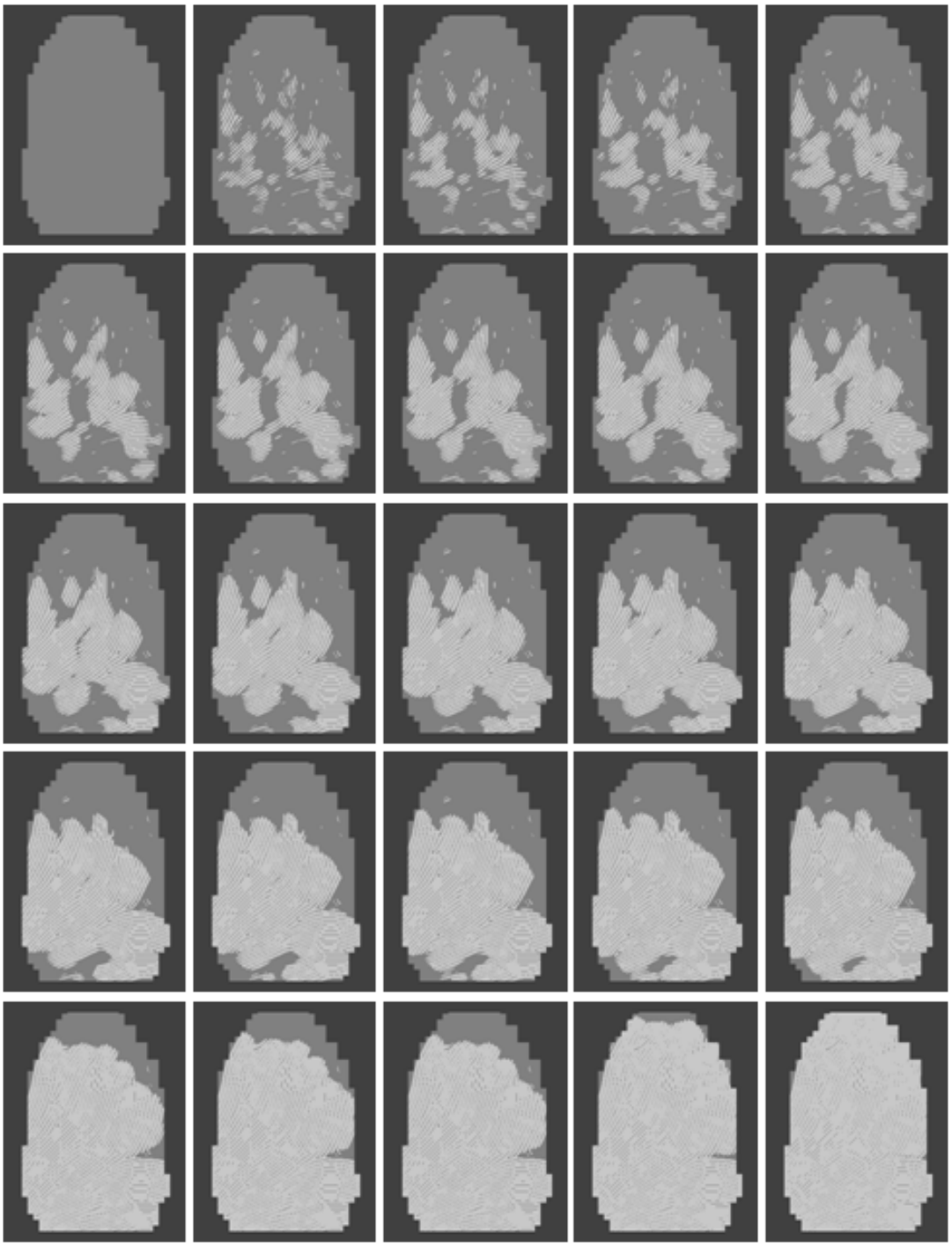

Figure 3.8: Selection of candidate pixels during the enhancement of the fingerprint in Figure 3.7. The enhancement starts from high-quality region and then iteratively expands like wildfire toward low-quality regions.

3.4.1 Enhancement of Synthetic Fingerprints

For a sound assessment of the effectiveness of a fingerprint enhancement approach, a dataset including both a noisy and a clean version of each fingerprint would be needed. Unfortunately it is not possible to collect such a dataset, hence has been used a synthetic fingerprint generation to produce a surrogate database that suit our needs.

As mentioned in section 2.7 there exists an important tool able to generate synthetic fingerprints called SFinGe suitable to our needs. By using SFinGe [22] [90], it is possible to generate datasets of arbitrary difficulty and, for each fingerprint, we can generate a ground-truth consisting of:

- Foreground map (binary image that defines the external silhouette of the fingerprint).
- Local orientation image.
- Local frequency image.
- Binary image (master fingerprint without noise).
- Minutiae position and directions.

For the experiments here reported it is particularly useful the knowledge of the ground-truth binary image, since in principle the ideal output of an effective enhancement approach is a (noisy free) binary or near binary image. So the pixel-level mean absolute difference between the enhanced image and the corresponding ground-truth binary image is an effective metric for assessing fingerprint enhancement.

A synthetic dataset of 50 medium/high noisy fingerprint with corresponding ground-truth has been generated. Some examples of such synthetic images are shown in Figure 3.9 (first column). The images in the synthetic dataset have been enhanced with three algorithms:

- baseline Gabor where the local orientation and frequencies are automatically estimated;
- baseline Gabor with the ground-truth orientation and frequency;
- the proposed iterative method.

Figure 3.9: Enhancement of synthetic fingerprints (first column) with the Gabor method (third column) and the proposed iterative method (fourth column). The second column shows the foreground regions.

The pixel-level mean absolute difference between the enhanced image and the master fingerprint has been evaluated and the results are reported in Table 3.1.

Results show that the proposed iterative approach perform better than classical Gabor enhancement and its error is not far from the Gabor + Ground-truth (orientation and frequency) that can be considered a sort of "oracle" method. Figure 3.9 shows the enhancement of two synthetic fingerprints with the baseline Gabor (third column) and the proposed method (fourth column).

3.4.2 Influence on Fingerprint Matching

The ultimate goal of fingerprint enhancement is the improvement of matching accuracy. To assess the enhancement performance of the proposed algorithm, has been conducted

Baseline Gabor	Gabor + Ground-truth	Proposed Iterative Method
33.85	28.88	30.99

Table 3.1: Mean absolute difference between the enhanced image and the master fingerprint over the synthetic DB.

Algorithm	EER(%)		
	FVC2004 DB2	FVC2004 DB3	FVC2006 DB2
Gabor [53]	6.569	3.640	2.325
Matched Filters [116]	7.320	3.570	-
Proposed Iterative	5.678	3.175	0.659

Table 3.2: Fingerprint verification accuracy. The proposed method is compared with the baseline Gabor approach and the method proposed in [116] over the FVC databases (reported in 2.6).

a quantitative analysis on the FVC2004 (DB2, DB3) and FVC2006 (DB2) databases (see section 2.6). Three different algorithms were compared in our experiments: the proposed method, the baseline Gabor [53] and the Sutthiwichaiporn's iterative method based on matched filters [116]. The Gabor approach has been used with the default parameters as proposed by the authors in [53]. Matching experiments were conducted following the FVC protocol [3] and using a state-of-the-art minutiae extractor and matcher (MCC, [17] [18]).

Table 3.2 compares the Equal Error Rate (EER, see section 2.8 and [90]) of the above algorithms over the benchmark datasets. Results of the iterative method based on matched filters are those reported in [116].

It is worth noting that the proposed enhancement method improves the matching accuracy with respect to the baseline Gabor and the Sutthiwichaiporn's iterative method. Figure 3.10 (first three columns) shows the enhancement of three fingerprints that belong to the FVC2006 database using the baseline Gabor (second column) and the proposed algorithm (third column). The restoration capabilities are very high over fingerprints with various degradations: too dry (first fingerprint), too wet (second fingerprint) and with a large amount of scratches and ridge breaks (third fingerprint). The fourth column of Figure 3.10, shows the enhancement of the fingerprint 32_7 from FVC2004 DB2A (the same example reported in [116]). This fingerprint is characterized by a wide unrecover-

able region in the central part, but since our approach currently tries to recover the whole fingerprint foreground area, the reconstruction in this region is bad. However, a visual comparison with the enhanced image in [116] reveals that, outside the unrecoverable region, our processing algorithm leads to a smaller number of false and miss minutiae.

Figure 3.10: Enhancement of fingerprints with various degradations. Three fingerprints (11_2, 21_11, 47_3) that belong to the FVC2006 DB2 database (first column) have been enhanced using the baseline Gabor [53] (column two) and the proposed iterative method (column three). The fourth column shows the enhancement of the 32_7 image (FVC2004 DB3) with the proposed method.

Part II

Improving the Fingerprint Orientation Extraction

Chapter 4

Fingerprint Ridge Orientation Computation

4.1 Introduction

It is well known that to develop a reliable fingerprint recognition system a robust image enhancement and image features extraction are needed.

The fingerprint matching is defined as the recognition step where given two fingerprints, the degree of similarity or a decision (match/not-match) is returned. A reliable minutiae-based matching, is based on a robust fingerprint preprocessing that allows to extract from a gray-scale image the corresponding minutiae.

The most important steps, prior the minutiae extraction process, are the local ridges orientation estimation, local ridges frequency analysis, fingerprint segmentation and singularities extraction. Practical analysis shows that poor image quality severely affects the recognition performance. Reliable orientation extraction in low-quality regions is still an open problem and new approaches are often proposed in the literature. A good orientation estimation can simplify and improve the subsequent features extraction steps.

4.2 Problem Formulation

Given a fingerprint $\mathbf{I}$, where the elements $I_{x,y}$ represent the gray-level of pixel at $[x, y]$, a fingerprint orientation image (or directional image), is a $h \times w$ matrix $\mathbf{D}$ whose elements

encode the local orientation of the fingerprint ridges.

Each element $\theta_{i,j} \in [0, \pi[$, corresponding to node $[i, j]$ of a squared-meshed grid (see Figure 4.1), is located over pixel $[x_i, y_j]$ and denotes the average orientation of the fingerprint ridges estimated in a window centered in $[x_i, y_j]$. The subdivision of the input fingerprint in a squared-mesh structure is mainly motivated by a drastic reduction of computational efforts in the estimation of the local orientations.

Let s be the step of the squared-meshed grid: the coordinates of each pixel are

$$[x_i, y_j] = [b + s \cdot i, b + s \cdot j] \tag{4.1}$$

where b is a border offset expressed in pixels.

Usually an additional value $r_{i,j}$ is associated with each element $\theta_{i,j}$ to denote the reliability (or consistency) of the orientation. Low values for $r_{i,j}$ correspond to an high degree of uncertainty in the local orientation knowledge.

4.3 Ground Truth Markup

In a fingerprint image, the ground truth orientation image represents the true orientation image that we would compute.

Given a fingerprint image the knowledge of the associated true orientation image is useful for several tasks such as:

- segmentation;
- evaluation (i.e. comparisons between the ground truth image and the estimated orientation image).

Let G be the *ground truth information*, which is defined as a pair $(\mathbf{D}^g, F)$, where:

- $\mathbf{D}^g$ is the ground truth orientation image, whose elements $\theta^g_{i,j} \in [0, \pi[$ denote the true ridge orientation at pixel $[x_i, y_j]$;
- $F = \{(i, j)_k\}$ defines the grid nodes of the orientation elements belonging to the fingerprint foreground.

An example of fingerprint image with the associated ground truth is reported in Figure 4.2.

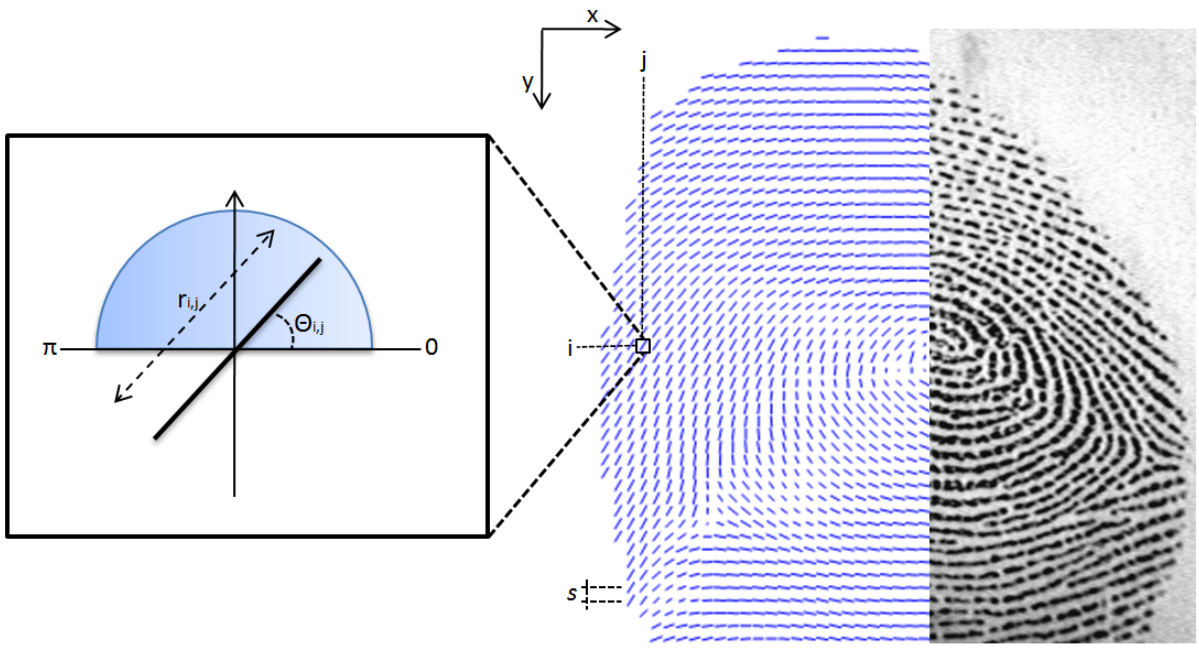

Figure 4.1: A fingerprint image and the corresponding orientation image computed over a squared-meshed grid ($s = 8$). Each orientation element $\theta_{i,j}$ belongs to the open interval $[0, 180[$. The length of each grid element is proportional to its reliability r.

Let $\mathbf{D}$ be the estimated orientation image of a given fingerprint, the comparison with its ground-truth $G = (\mathbf{D}^g, F)$ may be performed by means of the *Root Mean Square Deviation*:

$$RMSD(\mathbf{D}, G) = \sqrt{\frac{\sum_{(i,j)\in F} d\phi(\theta_{i,j}, \theta^g_{i,j})^2}{|F|}} \tag{4.2}$$

where $|F|$ is the cardinality of set F and the difference between angles is given by

$$d\phi(\theta_1, \theta_2) = \begin{cases} \theta_1 - \theta_2, & \text{if } -\frac{\pi}{2} \leq \theta_1 - \theta_2 < \frac{\pi}{2} \\ \pi + \theta_1 - \theta_2, & \text{if } \theta_1 - \theta_2 < -\frac{\pi}{2} \\ \pi - \theta_1 + \theta_2, & \text{if } \theta_1 - \theta_2 \geq \frac{\pi}{2} \end{cases} \tag{4.3}$$

Given a dataset $\mathbf{X}$ of n fingerprints with the corresponding ground-truth orientation images, the accuracy over the whole dataset $\mathbf{X}$ can be denoted by the Average RMSD:

$$AvgErr(\mathbf{X}) = \frac{1}{n} \sum_{(\mathbf{D},G)\in\mathbf{X}} (RMSD(\mathbf{D}, G)) \tag{4.4}$$

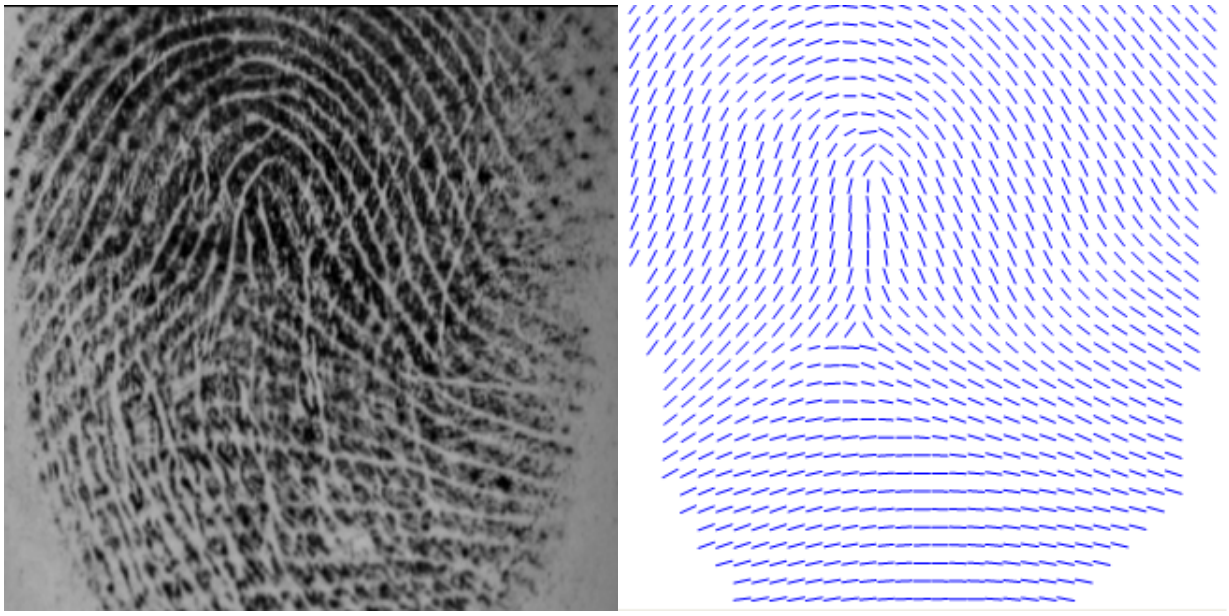

Figure 4.2: A fingerprint image and the manually marked ground-truth.

Note that 4.4 equally weights extraction errors across the whole foreground; this choice is well suited in most of the feature extraction tasks where orientations are needed (e.g. minutiae detection). Other metrics may be more appropriate for specific tasks, such as singularity detection, where errors close to singularities should have higher weights.

The manual markup by a human expert of the entire fingerprint is a very long task and for a large dataset it could be impractical. In [21] has been introduced a software tool that allows a semi-automatic markup of the local orientation through the following procedure:

- the user selects the positions where he wants manually set the orientations;
- the tool inserts a local orientation element which is initially automatically calculated according to the Gradient based approach [9] [90];
- the user can adjust the orientation element, to visually match the true ridge orientation;
- the system automatically interpolates all the other local orientations through a Delaunay triangulation (see Figure 4.3).

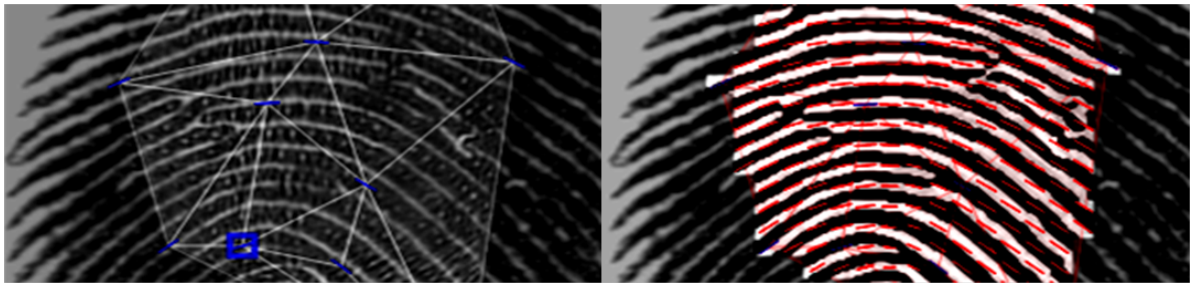

Figure 4.3: Ground-truth markup. Some local orientations are marked up by the user (vertices of triangles on the left image); others are interpolated by the software (right image).

Usually just few manual estimations are necessary in regions far from singular points, where the pattern exhibits low curvature, while more inputs are needed in regions of high curvature. Note that the markup procedure does not require the user to provide quality estimates; however regions where the ridge pattern is totally corrupted can be excluded from the foreground.

From now on, when we will talk about ground truth orientation image, we will refer to the orientation image computed semi-automatically with this tool.

4.4 A New Taxonomy

Section 3.2 of [90] provides a classification of the local orientation extraction techniques and proposes the following families:

- gradient-based approaches;
- slit- and projection- based approaches;
- estimation in the frequency domain;
- other approaches.

In [90], orientation image regularization and orientation image global modeling are discussed apart, because of their cross-applicability. Here, in order to better frame the existing approaches, we try to isolate the basic steps involved in the whole local orientation estimation process; in particular we identify four sequential stages:

- *Preprocessing*: this stage typically consists in an isotropic enhancement of the fingerprint image (e.g., contrast stretching, low pass filtering, etc.). Being the orientations still not available, this step cannot rely on orientation-based contextual filtering. As we will see, this step is very important for low quality fingerprints. It is worth noting that a preprocessing which is optimal for the orientation estimation is not necessarily optimal as well for other fingerprint feature extraction steps and therefore, after orientation extraction, it could be necessary to roll back to the original image before further processing.

- *Local analysis*: each orientation $\theta_{i,j}$ is estimated, by using image information (i.e., pixel intensities) from a local window centered in $[x_i, y_j]$. Several different techniques can be used to perform such a local analysis and to derive the orientation. Section 4.4.1 provides more details.

- *Global analysis*: by arguing that orientations cannot be reliably extracted in very noisy areas, and that a local smoothing is not effective where the signal is dominated by the noise, some researchers proposed to perform a global estimation of the orientations. The idea is to exploit information extracted from good quality regions to recover bad quality regions. In fact, because of the limited variability of fingerprint orientation patterns in nature, good quality orientations, even if far from noisy regions, can help to put constraints in the estimations at problematic places. Most of the global analysis approaches (more details are provided in the following sections) require an initial orientation estimation, which can be performed through a local analysis step.

- *Postprocessing*: in this final stage some regularization (e.g., local smoothing, relaxation, etc.) can be applied to the local orientation estimates, to reduce noise and improve results in low quality regions.

The implementation of all the above stages is not necessary, and in general only a minority of the existing approaches run across the whole sequence of steps.

4.4.1 Local Analysis

- **Gradient**: this is the simplest and most widely used approach for extracting local ridge orientations [90] [100] [9] in a fingerprint image **I**. The gradient in a given

point $[x, y] \in \mathbf{I}$ is a two dimensional vector

$$[\nabla_x(x, y), \nabla_y(x, y)] \tag{4.5}$$

where ∇_x and ∇_y represent the derivatives of $\mathbf{I}$ in $[x, y]$ with respect to the x and y directions. The gradient phase angle denotes the direction of the maximum intensity change; the direction of an hypothetical edge that crosses the region centered in $[x, y]$ is orthogonal to the gradient phase angle at $[x, y]$. Pixelwise orientation estimations are typically obtained through convolution with derivative operators (e.g., Sobel or Prewitt masks [47]).
This method is simple, efficient, works well for many good quality fingerprint images but has some drawbacks:

1. computing the gradient using the classical convolution masks (Sobel or Prewitt) and consequently the angle θ as the arctangent of the ∇_y/∇_x ratio, presents problems due to the non-linearity and discontinuity around 90 °;
2. the gradient is very sensitive to noise;
3. we have problems in averaging gradient estimates due to the circularity of angles.

To solve these problems Kass and Witkin [75] proposed an elegant solution. Their idea is to double the angles and encode an orientation estimate as a two dimensional vector:

$$\mathbf{d} = [r \cdot cos(2\theta), r \cdot sin(2\theta)] \tag{4.6}$$

where r denotes the strength of the estimate and 2θ allows the gradient estimates to be averaged.
Many orientation extraction methods have been proposed based on the above idea. Ratha, Chen and Jain in [100] compute the dominant ridge orientation $\theta_{i,j}$ combining multiple gradient estimates within a $n \times n$ window centered in $[x_i, y_j]$. Bazen and Gerez in [9] proposed a method based on Principal Component Analysis (PCA, [38] [13] [14]) that computes the direction and the strength in any pixel location. They also prove that their method provides exactly the same results as the averaged square-gradient method. Donahue and Rokhlin in [37] explore the use of level curves in image analysis. They compute curvatures by fitting concentric circles to the tangent directions via least-squares minimization. Wang et al. in [125] and

[127] proposed an enhanced gradient-based algorithm introducing a voting scheme based on the reliability measure of the estimated orientations in four overlapping blocks. A discussion on noise and orientation bias caused by the discrete operators that approximate to the differentiation can be found in [69], where an operator that better approximates the integration process is proposed. Finally, the use of complex gradients was proposed by Bigün et al. in [11] and [12].

- **Slit-based**: the idea is to define a fixed number of reference orientations (slits) and to select the best orientation computing a statistic over pixel gray-values along the slits. The first slit based method was proposed in 1969 by Stock and Swonger [114]. A recent implementation was provided by Oliveira and Leite [97]: the standard deviation of the gray-scale of the pixels corresponding to each slit is computed and the optimal slit is determined according to the maximum standard deviation difference between a given slit and the orthogonal one. Filterbank-based approaches in the image domain [51], that select the orientation according to the largest filter response, can be enclosed in this family: in fact, each filter in the bank can be conceived as a specific slit-detector.

- **Frequency domain**: a local analysis in the frequency domain is performed to extract the dominant orientation in each local window of the image. The approach proposed in [32] is based on Short Time Fourier Transform (STFT) analysis. The image is divided into partially overlapped blocks whose intensity values are cosine tapered moving from the center toward the borders. For each block, the Fourier Transform is computed and its spectrum is mapped to polar coordinates. The probability of a given orientation (within the block) is then computed as the marginal density function by factoring out the radial components related to the frequency of the signal.

- **Tracing-based**: the approach proposed in [48] traces ridge and valley lines and builds a coherent structure of locally parallel line segments from which the local orientation estimation is derived.

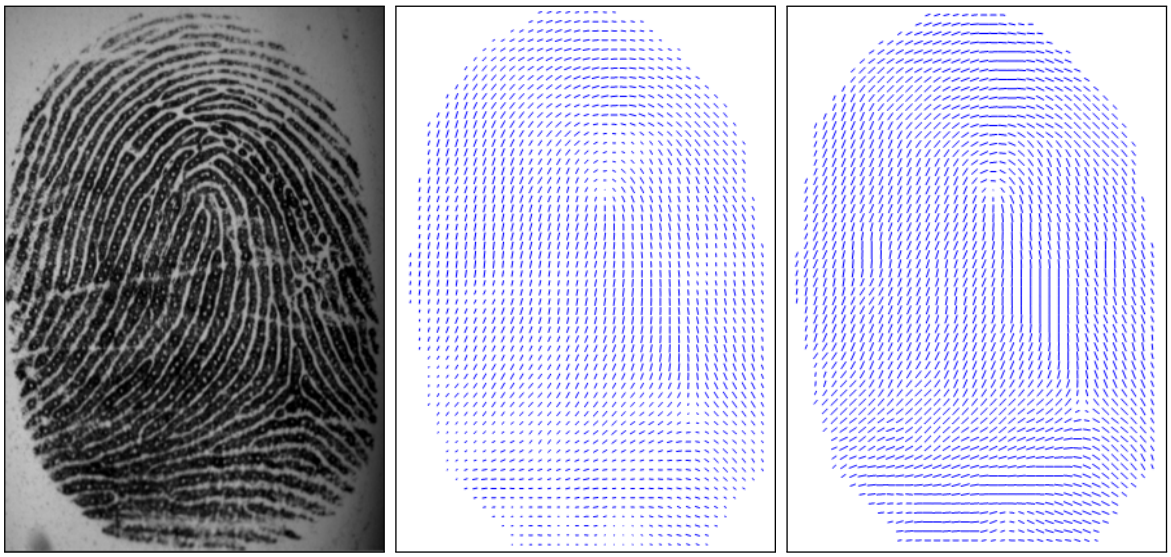

Figure 4.4: Ridges orientation extraction with the gradient method [100] (center) and the slit method (right, using [97])

4.4.2 Global Analysis

In low quality fingerprints the computation of local ridge orientations is a very hard task. If the fingerprint contains creases, local scratches or cluttered noise all the previously local-analysis-based methods output an imprecise and not-smoothed orientation image that can lead to hard subsequent fingerprint processing steps. Methods based on global analysis, suppose a global mathematical model for ridge orientation and can output a smoothed orientation image. In general, these methods

1. start with the so called *coarse orientation field*, which is the starting noisy orientation image computed with a (usually) local simple method (i.e., gradient);
2. adopt a global model to describe the fingerprint structure;
3. compute the parameters corresponding to the best-fitting model to the given coarse orientation field (using the singular point positions and number if available);
4. reconstruct a smoothed orientation image with the computed parameters.

- **Geometric models**: the fingerprint global orientation is modeled through a geometric function (usually defined in the complex plane). The function relies on the

number and position of singularities and is controlled by a set of other parameters [107] [124] [137] [136] [57]. Model fitting requires the a-priori knowledge of singularities (this can be very problematic for low quality fingerprints) and proceeds through an optimization process.

In [107] Sherlock and Monro described a mathematical model (called Zero-Pole Model) to synthesize a fingerprint orientation image from the position of loops and delta alone. This method takes a loop as zero and a delta as pole in the complex plane. In this work the authors admit that the proposed model is more suitable to describe the ideal topology pattern rather than real cases. In fact, it does not cover all possible fingerprints structures. This model supposes known the position of cores z_c and deltas z_d. The orientation θ_z in a point z of the complex plane is the sum of their influences:

$$\theta_z = \frac{1}{2}\left[\sum_{i=1}^{deltas} arg(z - z_{d_i}) - \sum_{j=1}^{cores} arg(z - z_{c_j})\right] \tag{4.7}$$

where $arg(\cdot)$ returns the phase angle of the complex number.

Vizcaya and Gerhardt in [124] improved the zero-pole model using a piecewise linear approximation around singularities to adjust the zero and pole's behavior:

$$\theta_z = \frac{1}{2}\left[\sum_{i=1}^{deltas} g_{d_i}\Big(arg(z - z_{d_i})\Big) - \sum_{j=1}^{cores} g_{c_j}\Big(arg(z - z_{c_j})\Big)\right] \tag{4.8}$$

where $g(\cdot)$ are nonlinear functions that preserve the singularity at the given point. The problem is reformulated as finding the parameters of the nonlinear functions minimizing some measure of orientation error. The authors also proposed an optimization technique to determine the model parameters starting from an estimation of the orientation image.

These two models have some drawbacks. They are effective near the singular points, lack of accuracy far from singular points and they are not able to deal with arch type fingerprints (without singular points). Zhou and Gu in [137] proposed an improved model for the orientation estimation using a rational complex function. The idea is to represent the image plane as a complex space. The orientation in a given point z is computed as half the argument of a complex number, output of a rational complex function:

$$\theta_z = \frac{1}{2} arg\left[f(z) \cdot \frac{P(z)}{Q(z)}\right] \tag{4.9}$$

where $P(z)$ and $Q(z)$ are polynomial functions which respectively depend on known cores and deltas. The idea is to find the parameters of the function $f(z)$ chosen from a set of functions (i.e. polynomials with a given degree) and minimize the difference between θ_z and the coarse orientation in z. The authors in [136] improved their model in regions of high curvature and discontinuity.
Huckermann et al. in [57] proposed to model orientation fields of fingerprints with quadratic differentials, parameterized by a few geometrically interpretable parameters invariant under euclidean motions. In [35] Dass proposed an interesting approach where singularities and orientations are updated in an interleaved way during the optimization process, but the computational complexity of his method is too high for many practical applications. Li and Yau in [74] observed that in fingerprints the regions far from singular points have common properties that can be exploited to develop a model able to predict the fingerprint orientation. First they compute the coarse orientation field and its reliability, than compute a coarse prediction model using the first order phase portrait and finally construct a polynomial model to form the final predicted orientation model. An improvement of this method was proposed in [79] and [80].

- **Global approximation**: the fingerprint global orientation is modeled through a parametric function (typically a set of smoothed basis functions) independently of the singularities. Optimal parameter values are determined by minimizing the differences between the model orientations and corresponding estimates obtained through local analysis. Model fitting can be limited to reasonable quality areas, to limit the effects of unreliable local estimations. FOMFE approach [126] is based on 2D Fourier series expansion of two nonlinear differential equations in the phase plane. The method consider a vector $\mathbf{V}_{2\theta} = [\mathbf{V}_c, \mathbf{V}_s]$, where the entries are pairs $\mathbf{v}= (v_c, v_s)$ and v_c and v_s are the phase functions of $cos(2\theta)$ and $\sin(2\theta)$ (double angle 4.6). The idea is to find the parameters of a mapping function $\mathbf{f}$ such that $\dot{\mathbf{v}} = \mathbf{f}(\mathbf{v})$ with $\mathbf{f}$ represented by a 2D Fourier expansion. The fingerprint orientation model can be write:

$$\mathbf{V}_c = \mathbf{P}(\mathbf{x}) \cdot \mathbf{B}_c \cdot \mathbf{Q}^T(\mathbf{y}) \tag{4.10}$$

$$\mathbf{V}_s = \mathbf{P}(\mathbf{x}) \cdot \mathbf{B}_s \cdot \mathbf{Q}^T(\mathbf{y}) \tag{4.11}$$

where $\mathbf{V}_c$ and $\mathbf{V}_s$ are the input data, $\mathbf{B}_c$ and $\mathbf{B}_s$ are Fourier expansion coefficients

and $\mathbf{P}(\mathbf{x})$ and $\mathbf{Q}(\mathbf{y})$ correspond to the coordinate points in the phase portrait. The parameters $\boldsymbol{\alpha}$ of the Fourier expansion are computed starting from the coarse orientation field and minimizing

$$min_{\alpha} \quad \|\boldsymbol{\Phi}\boldsymbol{\alpha} - \mathbf{b}\|^2 \tag{4.12}$$

where $\boldsymbol{\Phi}$ contains the basis expansions evaluated in each point and $\mathbf{b}$ is the observation vector with v_c or v_s. The solution of this optimization problem is obtained in closed form. This method has a low-computational cost and can seamlessly summarize global features, including high curvature regions around singularities. Ram et al. technique [99] uses Legendre polynomials and a minimization approach. They proceed by estimating the parameter vectors $\mathbf{a}$ and $\mathbf{b}$ of the Legendre expansion matrix Φ through the minimization of a nonlinear functional. The computation is performed in two steps: in the first, it roughly approximates the model's parameters using a closed form solution for the least squares approximation obtaining $\mathbf{a}_0$ and $\mathbf{b}_0$, the initial solutions; in the second, the nonlinear problem

$$min_{\mathbf{a},\mathbf{b}} \quad \sum_{i=1}^{n} w_i \left[sin\left(\frac{1}{2} arctan \frac{\Phi(\mathbf{p}_i)\mathbf{a}^T}{\Phi(\mathbf{p}_i)\mathbf{b}^T} - O(\mathbf{p}_i) \right) \right]^2 \tag{4.13}$$

is solved in order to deliver the accurate parameters. In the functional $\mathbf{p}_i = (x, y)$ are the plane coordinates, w_i are weights and $O(\mathbf{p}_i)$ are the elements of the coarse orientation field. The nonlinear optimization procedure can be performed using the standard Line Search or the Levenberg-Marquard algorithm [83]. A global method based on a two steps refinement technique has been recently proposed in [72].

4.4.3 Limitations of classical methods

The classical orientation extraction methods previously described have some limitations. For a very noisy image the orientation extraction with methods based on local analysis is often unsatisfactory and only the superimposition of a method based on global analysis may provide a more effective improvement. With global analysis methods

- we often find a good smoothed solution, even if sometimes the solution can significantly deviate from the underlying orientation;

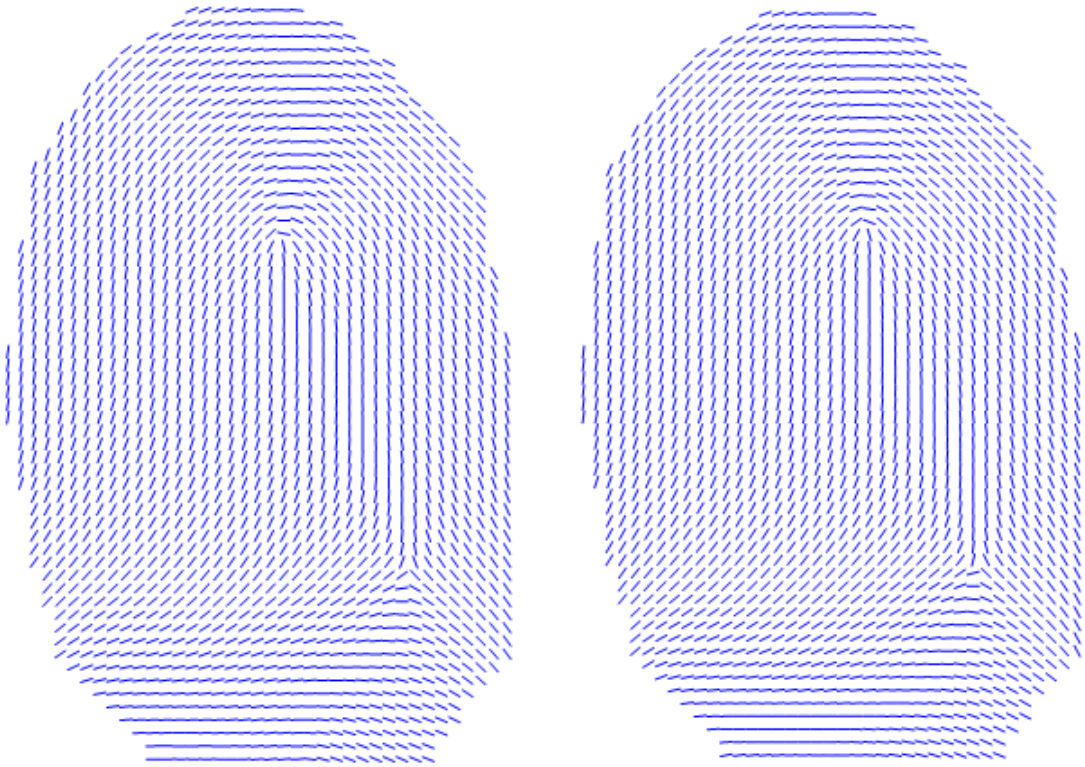

Figure 4.5: Ridges orientation extraction for the same fingerprint in Figure 4.4 with the FOMFE method [126] (left) and the Legendre Polynomials based method [99] (right).

- the coarse orientation field is always an orientation image computed with local analysis methods; as result, the noise in some regions may be amplified by the chosen approximating global model.

In order to better understand the problem we have built a new benchmark for local orientation extraction approaches with associated orientation ground-truth and we have implemented some of the best-known techniques in literature, including both methods based on local windows and methods based on a global modeling of the orientation image: gradient [100], slit-based (using the Oliveira and Leite approach [97]), FOMFE [126] and Legendre-Polynomials-based [99]. In our analysis we do not consider geometric models because of the dependency of these methods on the singularity position (which in our opinion makes them less attractive).

The proposed benchmark [23] is motivated by the fact that no other benchmarks to directly and quantitatively measure the orientation extraction accuracy are publicly

available. The benchmark, which contain just 50 fingerprints, will be additionally extended in chapter 6 and made available to the community. So far, it consists of the following datasets:

- *Good Quality Dataset*: 11 fingerprints of good quality with the corresponding orientation ground truth.
- *Bad Quality Dataset*: 40 fingerprints of low and very-low quality with the corresponding orientation ground truth.

The rationale behind the choice of these two datasets is that a good orientation extraction algorithm should be able to deal with very low quality images without losing accuracy on good quality ones.

Given a dataset $\mathbf{X}$ of n fingerprint images with the corresponding ground-truth orientation images, the comparison between each estimated orientation image $\mathbf{D}$ and the ground truth $G = (\mathbf{D}^g, F)$ is performed by means of the root mean square deviation (Equation 4.2) and the average error over the whole dataset is given by the Equation 4.4.

During the experimentation, in order to find the optimal configuration for each algorithm, the key parameters have been tested in following ranges:

- window size (gradient and slit-based): [15-20] pixels;
- number of smoothing cycles (gradient and slit-based): [0-4];
- slit window size (slit Based): [5-10] pixels;
- trigonometric polynomial order (FOMFE): [2-5] (see [126]);
- Legendre Polynomial order (Legendre-Polynomials-Based): [5-8] (see [99]).

Note that the first two parameters (window size and number of smoothing cycles) have effect on all the four algorithms since the implementation of FOMFE and Legendre-Polynomials-Based relies on the gradient algorithm for a coarse orientation estimation.

By taking all the possible combinations of the above parameters, a total of 300 algorithms instances have been tested. Each algorithm instance has been evaluated on the two datasets. Table 4.1 reports, for each algorithm, the set of parameter values that allow optimal results on the Bad Quality Dataset without degrading the performance

on the Good Quality Dataset. Table 4.2 reports the results on both datasets using such optimal parameters.

From the results reported in Table 4.2, the following observation may be made. The gradient based approach performs better than more complex methods on good quality fingerprint images. In fact, the average deviation from the ground-truth on the whole Good Quality Dataset is less than 6°. On the other hand, on the Bad Quality Dataset the gradient algorithm exhibits the worst accuracy, while the best result is achieved by the slit-based approach.

In these experiments, the FOMFE and Legendre algorithms, despite their superior approximation ability and higher complexity, do not seem able to clearly outperform the much simpler gradient approach. In fact, while FOMFE and Legendre can satisfactorily recover small-medium corrupted regions surrounded by reliable orientation estimations, they often fail to recover large noisy areas especially in proximity of the foreground-background transition.

Figure 4.6 shows an example of estimation over a portion of an image of low quality, where the noise is not so high to make ridge lines unrecognizable. While a trained human can quite accurately detect the true ridge line orientation over the whole image, all the tested algorithms fail to extract the correct orientations in the bottom-left part of the fingerprint, resulting in a RMSD higher than 30°.

Algorithm	**Window Size**	**Smooth Cycles**	**Poly. Order**	**Slit Size**
Gradient	16	2		
Slit-Based	17	2		8
FOMFE	15	2	4	
Legendre	15	2	8	

Table 4.1: Optimal Algorithm Parameters.

Algorithm	**Good Dataset**	**Bad Dataset**
Gradient	5.90°	22.79°
Slit-Based	6.07°	18.84°
FOMFE	5.97°	22.00°
Legendre	7.16°	21.99°

Table 4.2: Average errors on the two datasets using the optimal parameters.

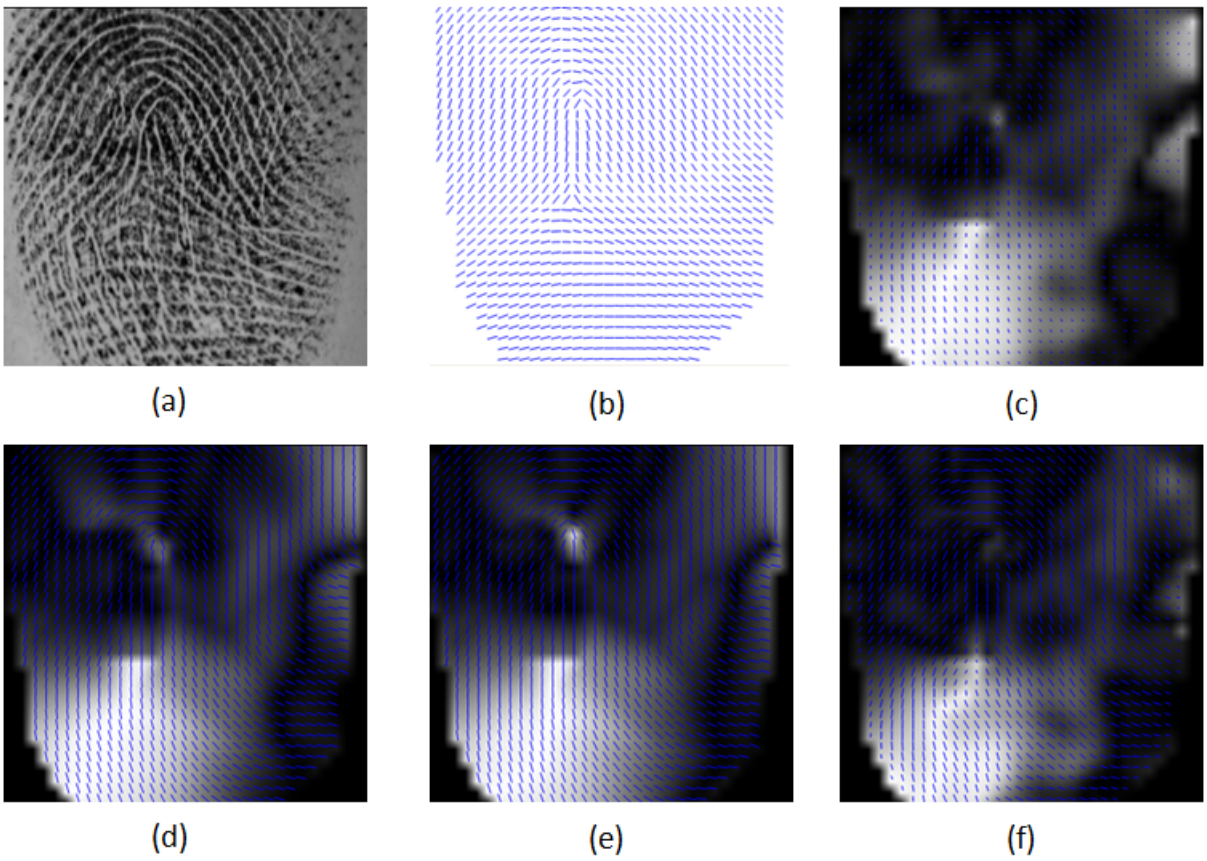

Figure 4.6: (a) Fingerprint image; (b) Ground truth; (c) Gradient (RMSD=32,11°); (d) Slit-Based (RMSD=30.42°); (e) FOMFE (RMSD=32.00°); (f) Legendre (RMSD=31.91°). For (c), (d), (e) and (f), the background shows local orientation errors (dark areas are those in which the orientation is closest to the ground truth; light areas are those where the error is larger).

4.4.4 Learning Based Models

According to the results reported in Table 4.2 all considered methods do not allow to encode a prior knowledge about the admissible fingerprint structures in the orientation estimation process. Only algorithms with such a prior knowledge (i.e., encoding natural fingerprint variability) may achieve significant higher accuracy on very low quality fingerprints. This kind of knowledge can be encoded with *learning based methods*.

Methods falling in this category attempt to learn, from a dataset of fingerprint images, the natural variability of global orientation patterns, independently of the singularities. Active shape models [34] have been successfully used in this context by [98]. The resulting method is called Active Fingerprint Ridge Orientation Model (AFROM). Given a dataset $\mathbf{X}$ of n fingerprints, the learning step of the AFROM method is:

- for each fingerprint computes the coarse orientation field with a standard method (i.e. gradient) and then computes the m coefficients of a model based method (i.e. Legendre Polynomials Based): these parameters are organized in a $n \times m$ matrix $\mathbf{P}$;
- the Principal Components Analysis (PCA, [38]) is applied to the set of parameters $\mathbf{P}$ in order to find a linear subspace where realistic fingerprints "reside". According to PCA the projection matrix $\mathbf{U}$ with eigenvectors and the mean vector $\boldsymbol{\mu}$ are computed;
- a vector of parameters $\mathbf{p}_i$ can be projected in the reduced space of dimensionality $k < m$ and back-projected using the standard equations

$$\mathbf{d}_i = \mathbf{U}^T(\mathbf{p}_i - \boldsymbol{\mu}) \qquad projection \tag{4.14}$$

$$\mathbf{p}_i = \boldsymbol{\mu} + \mathbf{U}\mathbf{d}_i \qquad backprojection \tag{4.15}$$

After the learning step, the directional image for a test fingerprint is computed finding the best parameter vector $\mathbf{d}$ that allows to generate plausible structures (see Figure 4.7). The search is performed in the subspace minimizing the following regularized empirical risk:

$$min_{\mathbf{d}} \quad \sum_{i=1}^{n} w_i \left[sin\left(\frac{1}{2} arctan \frac{\Phi(\mathbf{p}_i)\mathbf{a}^T}{\Phi(\mathbf{p}_i)\mathbf{b}^T} - O(\mathbf{p}_i) \right) \right]^2 + \lambda \left[\frac{1}{P(\mathbf{p}_i)} + P(\mathbf{p}_i) \right]^2 \tag{4.16}$$

This problem is similar to 4.13 but $\mathbf{d}$ is initialized to the null vector (the origin in the original space) and $\mathbf{a}$,$\mathbf{b}$ are computed with the projection formula. The second term represents the squared regularizer that constraints the orientation vector to length one. $P(\cdot)$ is defined as

$$P(\mathbf{p}_i) = \Phi(\mathbf{p}_i)\mathbf{a}^T + \Phi(\mathbf{p}_i)\mathbf{b}^T \tag{4.17}$$

This learning model represents a first tentative to introduce the prior knowledge in the fingerprint orientation estimation. The greatest drawback is due to:

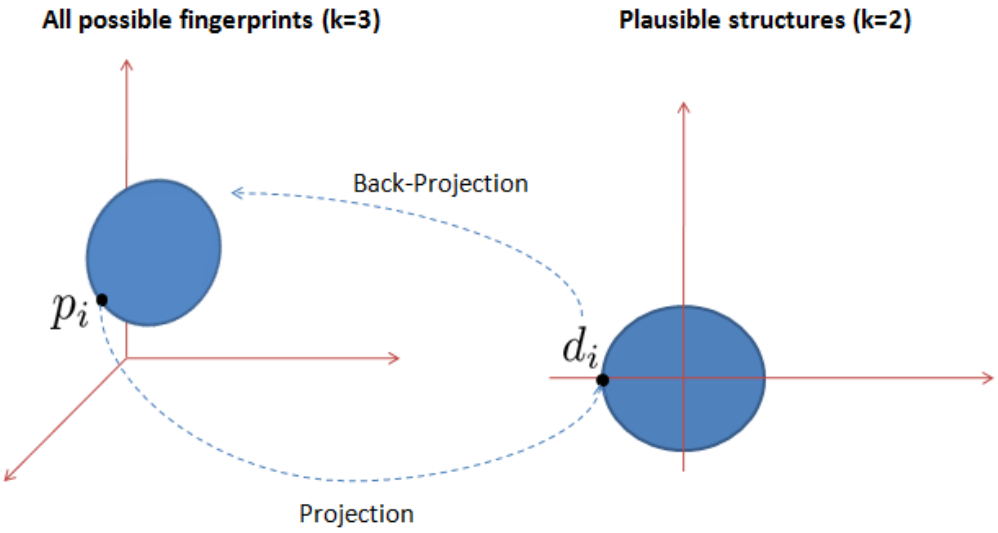

Figure 4.7: The original fingerprints space (left) and the PCA reduced subspace (right). A parameter vector $\mathbf{p}_i$ is projected in $\mathbf{d}_i$, a vector lying the reduced space, in order to find the nearest plausible fingerprint structure minimizing the penalized objective function 4.16

- the application of PCA as a training algorithm. The assumptions of linearity may not hold, it does not account for fingerprint labels as additional knowledge and if a fingerprint structure is not seen during the training, may not be possible converge to the true pattern;
- good quality fingerprints are over-smoothed because of the application of a global analysis model in the optimization.

Other attempts have been recently done by [30] using graphical models and proximity rules.

Chapter 5

Orientation Extraction Improvement

5.1 Introduction

In this chapter we frame the baseline orientation extraction algorithms according to the proposed taxonomy and describe techniques able to improve the orientation extraction in fingerprints. We implemented and tested several well know methods and a plethora of their variants over a novel, specifically designed, benchmark, made available in the FVC-onGoing framework (see Part III). We proved that parameter optimizations, pre- and post- processing stages can markedly improve accuracy of the baseline methods on bad quality fingerprints.

5.2 Baseline Methods

In section 4.4 we defined pre-processing, local analysis, global analysis and post-processing as the basics steps involved in the whole local orientation estimation process. Table 5.1 includes some of the best-known orientation estimation approaches and highlights their decomposition in terms of the processing stages and method categories. It is worth noting that the implementation of all the processing stages is not necessary, and only a minority of the existing approaches run across the whole sequence of steps. To better identify an algorithm, in the following sections we use a unique "code" as shown in first column of Table 5.1.

In this Thesis we have considered and implemented methods from each category, except for: (i) the "geometric models" category because of the dependency of these methods

Method	Category	Pre-Proc.	Loc. Analysis	Glob. Analysis	Post-Proc.
J95 [100]	Gradient	-	Gradient	-	Smoothing
O07 [97]	Slit-based	-	Slit	-	Smoothing
G06 [32]	Frequency Domain	Removed DC	STFT	-	Smoothing
W07 [126]	Global Approximation	-	Gradient	2D Fourier Exp.	-
R10 [99]	Global Approximation	-	Gradient	Polynomial Approx.	-
R09 [98]	Learning-based	-	Gradient	Polynomial Approx. ASM	-

Table 5.1: Baseline Fingerprint Orientation Extraction Methods.

on the singularity position (which in our opinion makes them less attractive); (ii) the tracing-based approach [48] which is, however, considered in section 5.6 for comparison purposes. In choosing the methods to implement we focused on baseline methods with a simple implementation, and/or methods made available by their authors in source code. In this Thesis, we denote Table 5.1 algorithms as *baseline algorithms*.

5.3 The Benchmark

The evaluation of the improvements in orientation extraction algorithms is made possible by the FVC-onGoing framework. In Part III, we describe a web-based automated evaluation system for fingerprint recognition algorithms where tests are carried out on a set of sequestered datasets and results are reported on-line by using well known performance indicators and metrics.

The aim of the system is to track the advances in fingerprint recognition technologies, through continuously updated independent testing and reporting of performances on given benchmarks.

Recently, we added a new benchmark area in the FVC-onGoing framework (FOE) in order to assess the accuracy of fingerprint orientation extraction algorithms. This new area contains two benchmarks (FOE-TEST and FOE-STD-1.0) and a metric (*AvgErr*, see Equation 4.4) to evaluate the difference between an extracted orientation image and the ground-truth.

For practical purposes, in the following sections we call FOE-TEST as *Set A* and the FOE-STD-1.0 as *Set B*. More details about the benchmarks can be found in Part III. Here we just remind that each dataset can be divided into:

- *Good Quality Dataset*: 10 fingerprints of good quality acquired using optical scan-

ners with the corresponding orientation ground truth.

- *Bad Quality Dataset*: 50 fingerprints of low and very-low quality acquired using optical scanners with the corresponding orientation ground truth.

Even if each set (A and B) currently contains just 50 bad quality images and 10 good quality images, the total number of orientation estimations is 94,758 for *Set A* and 108,822 for *Set B*.

5.4 Improving the Orientation Extraction

Tables 5.3 and 5.4 show the accuracy of our implementation of baseline algorithms. Symbols and abbreviations used in this table (and in the following ones) are listed in Table 5.2. Each algorithm in Tables 5.3 and 5.4 has two entries (i.e., rows):

- the "without-star" row corresponds to the default implementation of the algorithm (i.e., where the parameter values suggested by the authors are used);
- the "with-star" row corresponds to an optimized version of the baseline algorithm whose parameter values have been tuned (by trial and error) on *Set A* (training set).

The parameter optimization was carried out by minimizing *AvgErr* on the bad quality dataset, but with the constraint $AvgErr < 7°$ on the good quality dataset. In both default and optimized versions of each algorithm, pre- and post- processing stages (if any) are those suggested by the authors, with no further optimizations.

All the global modeling methods implemented require an initial orientation image: in this work we usually use the gradient-based local technique [100], often followed by some amount of smoothing. Note that in the tables reporting results on global methods, this kind of "initial" post-processing is not reported in the "Post-processing" column (which always refers to the final post-processing), but in the column "Local Analysis - Type", after the local technique name.

Approach R09 requires a separate dataset to learn an internal model of fingerprint orientation distribution in nature. To this purpose, a large dataset of good quality fingerprints is needed (corrupted fingerprints should be excluded from the training set to avoid that inadmissible patterns are learnt). For this reason we selected, from NIST

Abbreviation	Meaning
Method XXX-Y	XXX=method identifier Y=index of variant
s:X dir:Y	Slit width (X) and number of directions (Y) in the slit-based method
Sm:AxBxC	A smoothing rounds over a BxC window
RDC	The DC Components are removed
Ov:X Blk:Y	Overlap(X) and Block Size (Y) in the STFT method
Polyn. XX:YY	XX=polynomial type (FO =Fourier, LE = Legendre, C1 = Chebyshev type 1, C2 = Chebyshev type 2) YY=polynomial degree
ASM	Active Shape Modeling
μ	Regularization parameter in learning based models
weighted:X	X= Weighting scheme (S = strength, R = regularity)
IS:X	Image smoothing over a squared window of size X
MF:X	Median Filtering over a squared window of size X
τ:X	Replacement threshold

Table 5.2: Symbols and abbreviations used in the following tables.

special database 14 [129], the 6164 (23% of the database) fingerprints with NFIQ = 1 (see [117]).

Algorithm R09 and R10 require to solve a nonlinear optimization problem with no closed form solution. As suggested in the corresponding papers, the underlying iterative minimization has been performed using the Levenberg-Marquardt algorithm [83], a widely used choice for nonlinear least squares problems.

From Table 5.4 (last two columns) we note that:

- Slit-based and Frequency domain approaches outperform the gradient-based one (especially on bad-quality fingerprints);
- unlike one could expect, the gain given by global-approximation and learning-based approaches over gradient is just marginal and limited to bad quality fingerprints;
- parameter optimization over a training set (*Set A*) results in a performance improvement also on the separate test set (*Set B*).

Figure 5.1 shows two examples of local orientation extraction using the optimized algorithms reported in Tables 5.3 and 5.4: the good-quality pattern (top image) is accurately dealt with by local approaches (c, d, e), but not by global ones (f, g, h); on

Method	Pre-Proc.	Loc. Analysis		Glob. Analysis		Post-Proc.
		Type	Win. Size	Type	Poly.	
J95	-	Gradient	16	-	-	Sm:1x3x3
J95-2 *	-	Gradient	41	-	-	Sm:1x3x3
O07	-	Slit s:09 dir:16	15	-	-	Sm:1x3x3
O07-2 *	-	Slit s:10 dir:16	35	-	-	Sm:1x3x3
G06	RDC	STFT Ov:6 Blk:12	24	-	-	Sm:1x3x3
G06-2 *	RDC	STFT Ov:1 Blk:25	27	-	-	Sm:1x3x3
W07	-	Gradient Sm:1x3x3	16	FOMFE	FO:04	-
W07-2 *	-	Gradient Sm:2x3x3	16	FOMFE	FO:05	-
R10	-	Gradient Sm:1x3x3	17	Polyn. Approx.	LE:08	-
R10-2 *	-	Gradient Sm:2x5x5	18	Polyn. Approx.	LE:09	-
R09	-	Gradient Sm:1x3x3	17	Polyn. Approx. ASM μ:3e-9	LE:12	-
R09-2 *	-	Gradient Sm:1x5x5	16	Polyn. Approx. ASM μ:3e-10	LE:09	-

Table 5.3: Baseline algorithms with default ("without-star" rows) and optimized ("with-star" rows) parameters. The accuracy of each algorithm is reported in Table 5.4.

Method	AvgErr Set A (degrees)		AvgErr Set B (degrees)	
	Good	Bad	Good	Bad
J95	5.41	22.18	6.08	22.77
J95-2 *	5.54	20.04	6.03	20.99
O07	5.24	20.50	5.74	19.67
O07-2 *	5.20	18.08	5.83	17.75
G06	4.86	19.86	5.46	18.43
G06-2 *	5.03	18.65	5.40	17.19
W07	6.03	19.60	6.15	20.63
W07-2 *	6.11	19.24	6.25	20.34
R10	5.73	20.28	6.32	20.80
R10-2 *	6.27	19.23	6.55	20.38
R09	6.85	19.64	7.73	20.51
R09-2 *	6.84	19.39	6.93	20.32

Table 5.4: Results of the algorithms described in Table 5.3.

the other hand, the bad quality pattern (bottom image) is better modeled by global approaches.

In the following sections we show how these results can be improved by optimizing pre- and post- processing steps and by implementing variants of existing techniques.

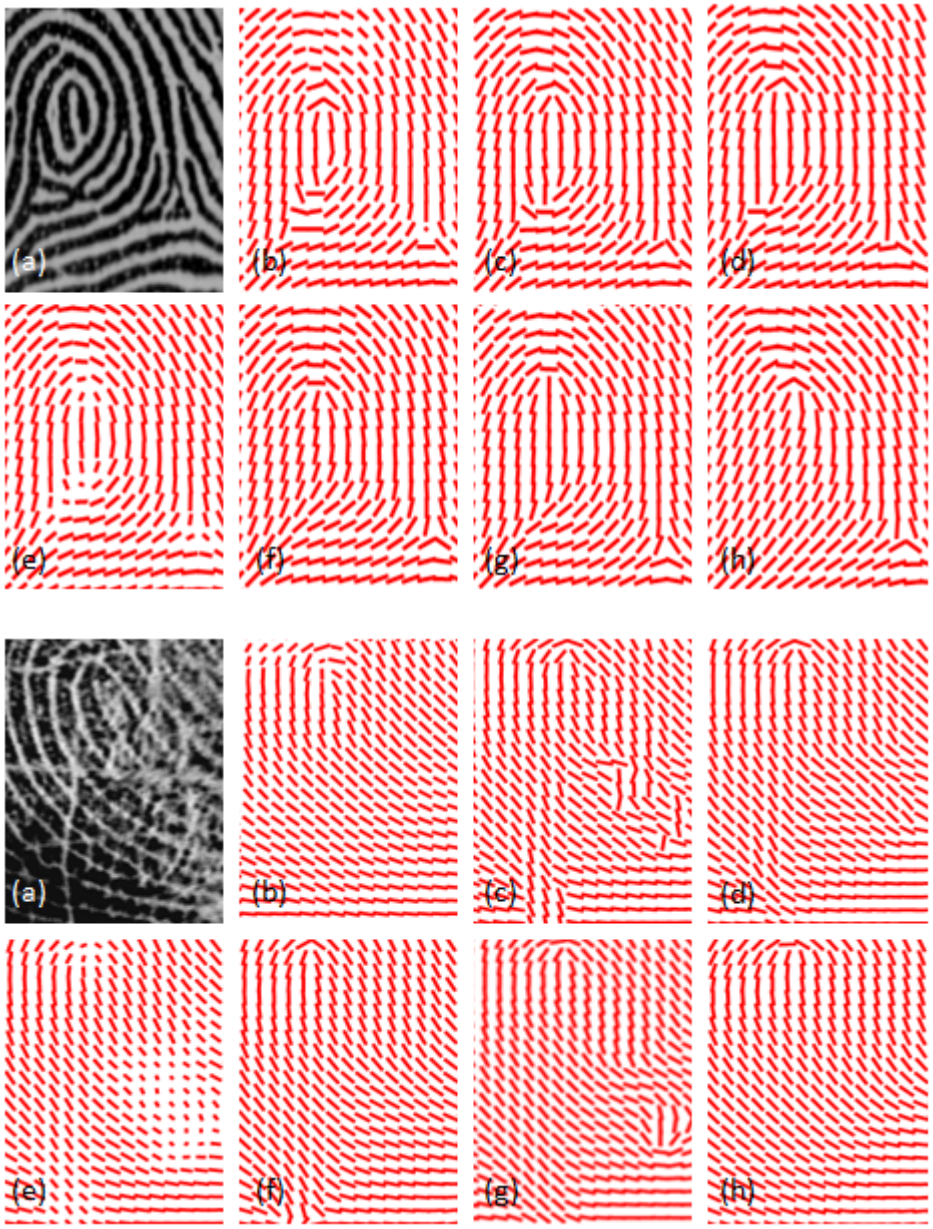

Figure 5.1: Orientation extraction with baseline methods on a portion of a good and a bad quality image. Original fingerprint image (a), ground-truth (b), gradient (c), slit-based (d), frequency domain (e), global approximation (Legendre) (f), global approximation (FOMFE) (g), learning-based (h).

5.4.1 Post-Processing

One or more iterations of arithmetic average over a $m \times m$ (3×3 or 5×5) square windows $W_{i,j}$ centered at $[i, j]$ is implemented as post-processing step for each element.

As proposed by [11] and [75], an orientation estimate $\theta_{i,j}$ at $[i, j]$ can be encoded in the double angle representation by the vector $\mathbf{d}$ where $\mathbf{d}_{i,j} = r_{i,j} \cdot [cos(2\theta_{i,j}), sin(2\theta_{i,j})]$ and $r_{i,j}$ is a coherence value denoting the confidence in the orientation estimation (whose computation is approach-dependent). The arithmetic average of orientations over $W_{i,j}$ is performed as follows:

$$\mathbf{d}_{i,j} = \frac{1}{m^2}\Big[\sum_{p,q \in W_{i,j}} r_{p,q} \cdot cos(2\theta_{p,q}), \sum_{p,q \in W_{i,j}} r_{p,q} \cdot sin(2\theta_{p,q})\Big] \tag{5.1}$$

The benefit of orientation averaging was highlighted by several authors ([90] [9] [100] [16]) and its efficacy in restoring small damaged areas is well recognized. However, the extent to which post-processing can be applied (i.e., windows size, number of iterations) without excessively over smoothing the underlying signal was still unknown.

Tables 5.5 and 5.6 show the accuracy of baseline algorithms with optimized post-processing. In general, adding a pre- or post- processing stage could require a different parameter setting: all the variants of baseline algorithms reported in this work undergone a parameter optimization on *Set A*.

For global analysis approaches we found that post processing is not only useless, but often leads to a performance drop; this is not surprising since their underlying model fitting techniques already produce smoothed results. For this reason, in Tables 5.5 and 5.6 we reported results of these approaches without any post-processing.

All the local analysis approaches seem to benefit from a quite aggressive post-processing (1 or 2 iterations over 5×5 windows); comparison of J95-3, O07-3 and G06-3 with the corresponding entries in Table 5.4 (J95-2, O07-2 and G06-2) show a marked improvement on bad quality fingerprints, without noticeably affecting accuracy on good quality ones. Figure 5.2 shows the effect of both mild and aggressive post-processing on a bad quality fingerprint orientation image.

5.4.2 Pre-Processing

Two types of image pre-processing have been considered:

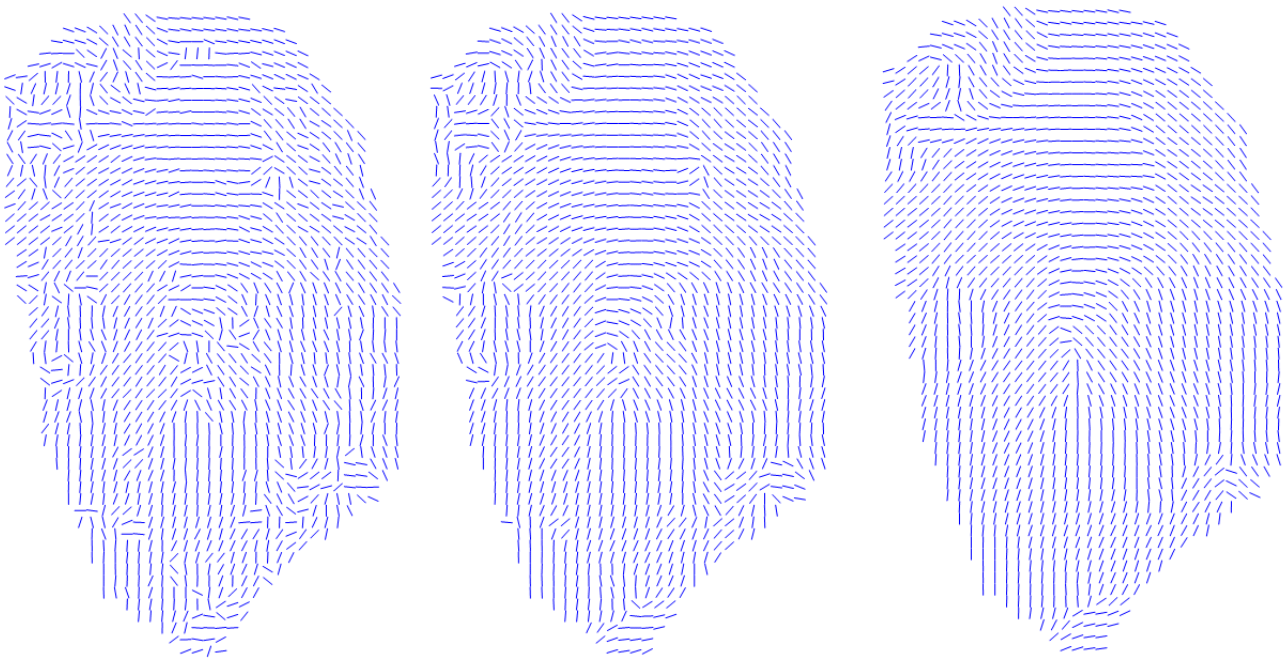

(a) original orientation image (b) 1 round 3x3 (c) 2 rounds 3x3

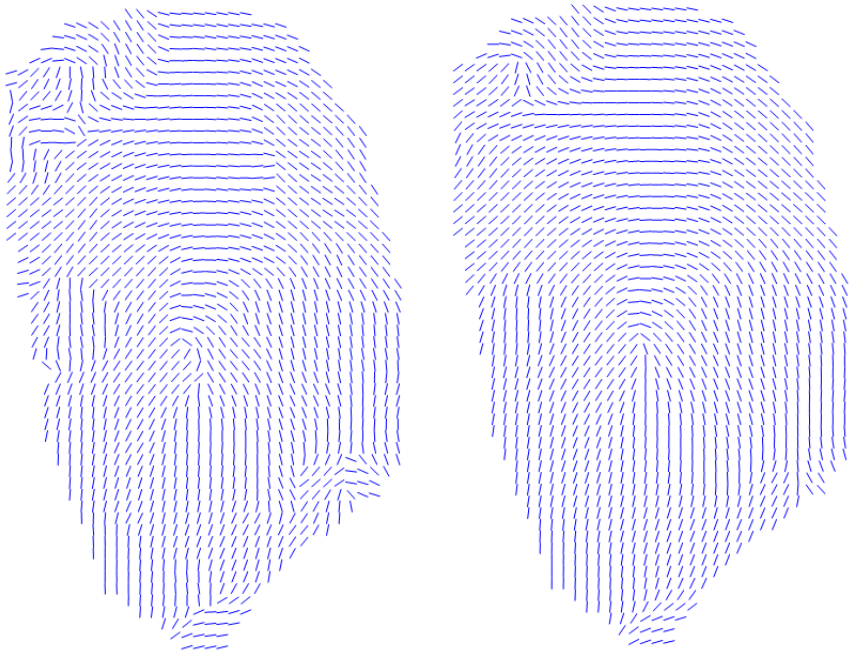

(d) 1 round 5x5 (e) 2 rounds 5x5

Figure 5.2: Effects of both mild and aggressive post-processing using 3x3 and 5x5 smoothing masks on a bad quality fingerprint.

Method	Pre-Proc.	Loc. Analysis		Glob. Analysis		Post-Proc.
		Type	Win. Size	Type	Poly.	
J95-3	-	Gradient	41	-	-	Sm:1x5x5
O07-3	-	Slit s:9 dir:16	35	-	-	Sm:2x5x5
G06-3	RDC	STFT Ov:1 Blk:25	27	-	-	Sm:2x5x5
W07-2	-	Gradient Sm:2x3x3	16	FOMFE	FO:05	-
R10-2	-	Gradient Sm:2x5x5	18	Polyn. Approx.	LE:09	-
R09-2	-	Gradient Sm:1x5x5	16	Polyn. Approx. ASM μ:3e-10	LE:09	-

Table 5.5: Post-Processing + Parameter Optimization. The accuracy of each algorithm is reported in Table 5.6.

Method	AvgErr Set A (degrees)		AvgErr Set B (degrees)	
	Good	Bad	Good	Bad
J95-3	5.79	19.59	6.03	20.60
O07-3	5.60	16.57	5.93	16.57
G06-3	5.25	15.65	5.30	14.71
W07-2	6.11	19.24	6.25	20.34
R10-2	6.27	19.23	6.55	20.38
R09-2	6.84	19.39	6.93	20.32

Table 5.6: Results of the algorithms described in Table 5.5.

- *gaussian smoothing*, which can be applied once or more times with mask of size 3×3 or 5×5;

- *median filtering* [47] over a window of size 3×3 or 5×5.

Both pre-processing steps help reducing noise and limiting the influence of fingerprint pores (appearing as bright blobs inside dark ridges), whose presence at this stage can be detrimental. The mild blurring produced as a consequence of these steps is not a problem due to the coarse nature of information (general ridge-flow orientation) we are looking for (see Figure 5.3).

Tables 5.7 and 5.8 highlight the effects of pre-processing. Gaussian smoothing combined with median filtering allows to markedly increase accuracy of most methods, including global-analysis-based ones. It is worth noting that, with optimal parameter tuning and both pre- and post- processing, methods of all the categories achieve quite close accuracy, with an error lying in the range 14-16 degrees over bad quality finger-

Method	Pre-Proc.	Loc. Analysis		Glob. Analysis		Post-Proc.
		Type	Win. Size	Type	Poly.	
J95-4	IS:3	Gradient	45	-	-	Sm:1x5x5
J95-5	IS:3 MF:3	Gradient	45	-	-	Sm:1x5x5
O07-4	IS:3	Slit s:9 dir:16	41	-	-	Sm:2x5x5
O07-5	IS:3 MF:3	Slit s:9 dir:16	41	-	-	Sm:2x5x5
G06-4	RDC IS:3	STFT Ov:1 Blk:25	27	-	-	Sm:2x5x5
G06-5	RDC IS:3 MF:3	STFT Ov:1 Blk:25	27	-	-	Sm:2x5x5
W07-3	IS:3	Gradient Sm:2x5x5	16	FOMFE	FO:05	-
W07-4	IS:3 MF:5	Gradient Sm:2x5x5	15	FOMFE	FO:05	-
R10-3	IS:3	Gradient Sm:2x5x5	20	Polyn. Approx.	LE:09	-
R10-4	IS:3 MF:5	Gradient Sm:2x5x5	15	Polyn. Approx.	LE:09	-
R09-3	IS:3	Gradient Sm:2x5x5	24	Polyn. Approx. ASM μ:3e-9	LE:09	-
R09-4	IS:3 MF:5	Gradient Sm:2x5x5	17	Polyn. Approx. ASM μ:3e-9	LE:09	-

Table 5.7: Pre-Processing + Post-Processing + Parameter Optimization. The accuracy of each algorithm is reported in Table 5.8.

Method	AvgErr Set A (degrees)		AvgErr Set B (degrees)	
	Good	Bad	Good	Bad
J95-4	5.35	17.73	5.55	17.31
J95-5	5.24	17.14	5.43	16.36
O07-4	5.74	16.54	6.07	15.78
O07-5	5.71	16.65	6.06	15.52
G06-4	5.17	15.51	5.29	14.16
G06-5	5.14	15.46	5.29	14.00
W07-3	5.73	17.16	5.72	16.86
W07-4	5.55	15.84	5.55	14.49
R10-3	5.46	17.64	5.89	17.33
R10-4	5.69	16.15	5.92	14.99
R09-3	6.98	16.95	6.91	17.14
R09-4	6.84	15.46	6.97	14.70

Table 5.8: Results of the algorithms described in Table 5.7.

prints in *Set B*. The best accuracy on bad quality fingerprints is still achieved by G06-5.

Figure 5.3: The right column shows the effect of a median filter with a 3x3 window applied to the two fingerprint images on the left column.

5.4.3 Acting on Polynomials Type

In this section we focus on global approximation approaches R10 and R09 and check whether some benefits can be achieved or not by changing the polynomial type. We propose variants of both R10 and R09 by using Chebyshev polynomials instead of Legendre ones.

The adoption of Chebyshev polynomials is supported by [82] [91], whose authors argue that Chebyshev polynomials provide better estimation of a continuous function than Legendre ones; in particular, the partial sums of a first-kind Chebyshev expansion of a continuous function in [1,-1] converge faster than the partial sums of an expansion in any other orthogonal polynomial.

A variant of R10 based on Chebyshev polynomials has also been recently introduced in [119] where a rule-based approach is implemented to locally choose between two orthogonal polynomials (Legendre and Chebyshev).

Both R10 and R09 try to jointly approximate sine and cosine components of the orientations (in the double angle notation) with linear combinations of fixed nonlinear basis functions $\boldsymbol{\varphi}(x, y)$ [14]. The global modeling of an input orientation image D is obtained by solving a nonlinear optimization problem defined as:

$$min_{\boldsymbol{p_s},\boldsymbol{p_c}} \sum_{(i,j)\in F} sin\Big[\frac{1}{2}tan^{-1}\Big(\frac{\boldsymbol{p_s^T}\boldsymbol{\varphi}(x_i, y_j)}{\boldsymbol{p_c^T}\boldsymbol{\varphi}(x_i, y_j)}\Big) - \theta_{i,j}\Big]^2 \tag{5.2}$$

where parameters $\boldsymbol{p_s}$ and $\boldsymbol{p_c}$ are the unknown vectors for the sine and the cosine approximation, $\boldsymbol{\varphi}(x_i, y_j)$ is a vector containing the set of basis functions computed at pixel $[x_i, y_j]$, $\theta_{i,j}$ is the input orientation at $[i, j]$ in the squared-mesh grid and F denotes the set of foreground elements.

This problem is regularized in [98] to have vectors with unit length (i.e., by adding a positive term that penalizes solutions formed by non-unit-length vectors).

In the following we replace Legendre with Chebyshev polynomials in the definition of $\boldsymbol{\varphi}(x, y)$. Chebyshev polynomials of the first and second kind are always orthogonal in [-1,1] and differ in form and weight function [115]. The univariate Chebyshev polynomials of the first kind $\varphi^{c1}(x)$ and second kind $\varphi^{c2}(x)$, whose Rodrigues representation can be found in [91], can be efficiently computed using the recurrence relations:

Chebychev first kind	**Chebychev second kind**
$\varphi_0^{c1}(x) = 1$	$\varphi_0^{c2}(x) = 1$
$\varphi_1^{c1}(x) = x$	$\varphi_1^{c2}(x) = 2x$
$\varphi_n^{c1}(x) = 2x[\varphi_{n-1}^{c1}(x) - \varphi_{n-2}^{c1}(x)]$	$\varphi_n^{c2}(x) = 2x[\varphi_{n-1}^{c2}(x) - \varphi_{n-2}^{c2}(x)]$

For our modeling purposes, we need bivariate polynomials: let d be the degree of the Chebyshev polynomial, then:

$$\boldsymbol{\varphi}(x, y) = [\varphi_{0,0}, \varphi_{1,0}, \varphi_{1,1}, \varphi_{2,0}, \varphi_{2,1}, .., \varphi_{d,0}, .., \varphi_{d,d}] \tag{5.3}$$

where $\varphi_{i,j} = \varphi_{i-j}(x)\beta(x) \cdot \varphi_j(y)\beta(y)$ and $\beta(\cdot)$ is the weighting function ($\frac{1}{\sqrt{1-x^2}}$ for the first kind and $\sqrt{1-x^2}$ for the second kind). According to this representation, the dimensionality of $\boldsymbol{\varphi}(x, y)$, $\boldsymbol{p_s}$ and $\boldsymbol{p_c}$ is $(d + 1) + d(1 + d)/2$.

The first four rows of Tables 5.9 and 5.10 show variants of R10-4 and R09-4 where Chebyshev polynomials of first and second kind are used, respectively. For R10-5 and R10-6 we notice a slight improvement on both the good and bad dataset of Set B with respect to the Legendre-based version R10-4. The benefits of these polynomials are more evident for learning-based models R09-5 and R09-6, where, besides a moderate improvement over the bad dataset, the Chebyshev variants achieve a considerable improvement over the good dataset with respect to R09-4.

5.4.4 Weighting Schemes

In Equation 5.2 all initial orientation estimates $\theta_{i,j}$ are equally weighted during the optimization. As a consequence, orientation elements in regions which are highly corrupted by noise are trusted as orientation elements in good quality regions. A more robust global modeling should be achieved by weighting the orientation elements according to their quality $q_{i,j}$:

$$min_{\boldsymbol{p_s},\boldsymbol{p_c}} \sum_{(i,j)\in F} q_{i,j} \cdot sin\Big[\frac{1}{2}tan^{-1}\Big(\frac{\boldsymbol{p_s^T}\boldsymbol{\varphi}(x_i,y_j)}{\boldsymbol{p_c^T}\boldsymbol{\varphi}(x_i,y_j)}\Big) - \theta_{i,j}\Big]^2 \tag{5.4}$$

A similar weighting scheme applied to the FOMFE approach was recently proposed by [118]. In this Thesis, we tested two implementations:

- in the former, $q_{i,j}$ is computed as the strength in [9];
- in the latter $q_{i,j}$ is computed as the regularity of the orientation field as defined in [20].

In both cases, $q_{i,j}$ belongs to the interval [0,1] and reaches its maximum when the corresponding orientation estimate has maximum trustworthiness.

The last seven rows of Tables 5.9 and 5.10 highlight the effects of weighting. The results show that using a strength-based weighting can lead to a slight improvement on bad quality fingerprints (compare, for example, R09-7, R09-8 and R09-9 with R09-5 and R09-6). At this stage the regularity-based weighting (not reported in the table) does not seem to produce any relevant improvement.

Method	Pre-Proc.	Loc. Analysis		Glob. Analysis		Post-Proc.
		Type	Win. Size	Type	Poly.	
R10-5	IS:3 MF:5	Gradient Sm:2x5x5	15	Polyn. Approx.	C1:09	-
R10-6	IS:3 MF:5	Gradient Sm:2x5x5	16	Polyn. Approx.	C2:09	-
R09-5	IS:3 MF:5	Gradient Sm:2x5x5	15	Polyn. Approx. ASM μ:3e-7	C1:09	-
R09-6	IS:3 MF:5	Gradient Sm:2x5x5	15	Polyn. Approx. ASM μ:3e-7	C2:09	-
W07-5	IS:3 MF:5	Gradient Sm:2x5x5	15	FOMFE weighted:S	FO:05	-
R10-7	IS:3 MF:5	Gradient Sm:2x5x5	15	Polyn. Approx. weighted:S	LE:09	-
R10-8	IS:3 MF:5	Gradient Sm:2x5x5	13	Polyn. Approx. weighted:S	C1:09	-
R10-9	IS:3 MF:5	Gradient Sm:2x5x5	13	Polyn. Approx. weighted:S	C2:09	-
R09-7	IS:3 MF:5	Gradient Sm:2x5x5	15	Polyn. Approx. weighted:S ASM μ:3e-9	LE:09	-
R09-8	IS:3 MF:5	Gradient Sm:2x5x5	13	Polyn. Approx. weighted:S ASM μ:3e-7	C1:09	-
R09-9	IS:3 MF:5	Gradient Sm:2x5x5	13	Polyn. Approx. weighted:S ASM μ:3e-7	C2:09	-

Table 5.9: Improvement of global approximation methods with Pre-Processing, Polynomial variations and weighting. The accuracy of each algorithm is reported in Table 5.10.

Method	AvgErr Set A (degrees)		AvgErr Set B (degrees)	
	Good	Bad	Good	Bad
R10-5	5.19	15.93	5.48	14.47
R10-6	5.10	16.02	5.24	14.47
R09-5	6.03	15.68	5.87	14.32
R09-6	5.70	15.62	5.67	14.26
W07-5	5.49	15.78	5.59	14.37
R10-7	5.54	15.68	6.03	14.36
R10-8	5.14	15.77	5.37	14.32
R10-9	4.99	15.93	5.20	14.39
R09-7	6.66	15.48	6.60	14.10
R09-8	6.19	15.66	6.04	14.02
R09-9	5.71	15.23	5.86	14.03

Table 5.10: Results of the algorithms described in Table 5.9.

5.5 Adaptive Orientation Extraction

From Table 5.8 and Table 5.10 it can be observed that, often, an improvement on bad quality images does not imply an improvement on good quality ones. This is particularly true for learning-based models R09-7, R09-8 and R09-9, where improvement on bad

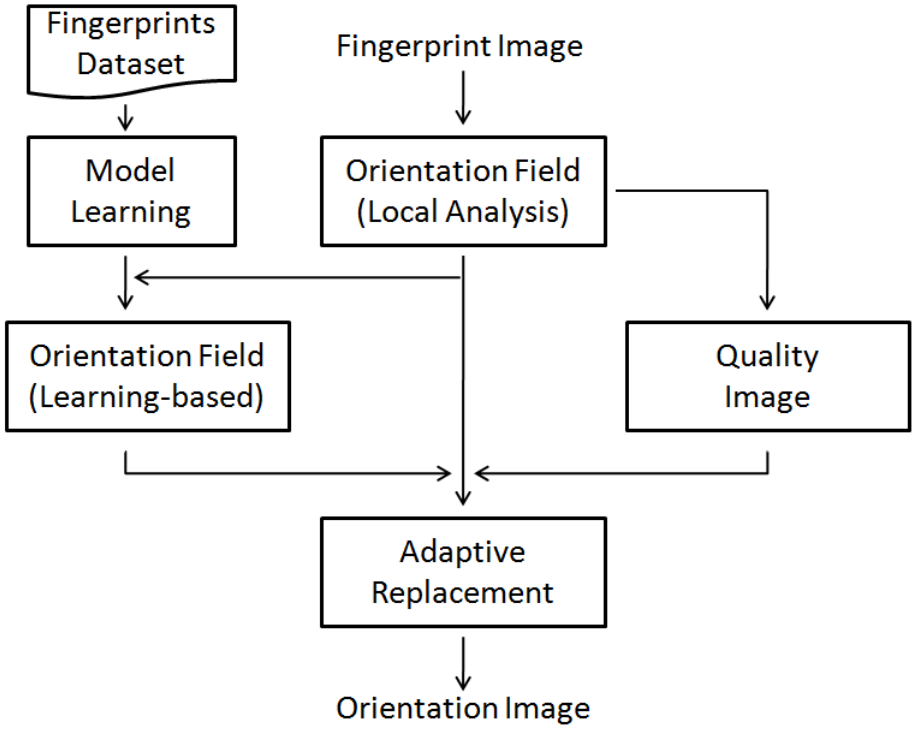

Figure 5.4: The flow chart of the proposed hybrid orientation extraction method.

quality images comes at the expense of a slight accuracy deterioration on good quality fingerprints. This happens because learning-based methods try to bring back a noisy input pattern into a smoothed, previously-learned pattern: this can be useful for bad quality images, but could lead to a too coarse approximation in good quality fingerprints (or fingerprint regions).

Based on the above considerations, in this section we propose an adaptive approach that tries to combine the advantages of both local and learning-based models.

The adaptive approach relies on a local method such as J95-5 or G06-5, but replaces orientations estimated in bad quality regions with those provided by a robust learning-based approach such as R09-8 or R09-9. A final post-processing stage (see section 5.4.1) is implemented to smooth transition regions, thus avoiding sharp changes.

More formally, let $\mathbf{D}^{Loc} = [\theta_{i,j}^{Loc}]$ be the $h \times w$ orientation image computed with a local model, and let $\mathbf{Q} = [q_{i,j}]$ be a $h \times w$ matrix denoting the element quality (e.g., strength or regularity).

Given a threshold $\tau \in [0, 1]$, let $\mathbf{Q}' = [q'_{i,j}]$ be a weighting matrix derived from $\mathbf{Q}$ as

Method	Pre-Proc.	Loc. Analysis		Glob. Analysis		Post-Proc.
		Type	Win. Size	Type	Poly.	
Adaptive-1	IS:3 MF:5	Gradient Sm:2x5x5 τ:0.67	13	Polyn. Approx. weighted:R ASM μ:3e-7	C1:09	Sm:1x3x3
Adaptive-2	IS:3 MF:5	Gradient Sm:2x5x5 τ:0.75	13	Polyn. Approx. weighted:R ASM μ:3e-7	C2:09	Sm:1x3x3
Adaptive-3	RDC IS:3 MF:3	STFT Sm:2x5x5 Ov:2 Blk:25 τ:0.67	29	Polyn. Approx. weighted:R ASM μ:3e-7	C1:09	Sm:1x3x3

Table 5.11: Replacement Based Methods. The accuracy of each algorithm is reported in Table 5.12.

Method	AvgErr Set A (degrees)		AvgErr Set B (degrees)	
	Good	Bad	Good	Bad
Adaptive-1	4.77	14.92	5.05	13.73
Adaptive-2	4.77	14.97	5.14	13.97
Adaptive-3	5.63	14.73	5.76	13.45

Table 5.12: Results of the algorithms described in Table 5.11.

follows:

$$q'_{i,j} = \begin{cases} 1 & \text{if } q_{i,j} > \tau \\ q_{i,j} & \text{otherwise} \end{cases} \tag{5.5}$$

Let $\mathbf{D}^{Glob} = [\theta_{i,j}^{Glob}]$ the orientation image (computed using $\mathbf{D}^{Loc}$ as the initial orientation field and a weighting scheme with weights $\mathbf{Q}'$, then the output orientation image $\mathbf{D} = [\theta_{i,j}]$ is computed as:

$$\theta_{i,j} = \begin{cases} \theta_{i,j}^{Loc} & \text{if } q_{i,j} > \tau \\ \theta_{i,j}^{Glob} & \text{otherwise} \end{cases} \tag{5.6}$$

A final post-processing stage with a $m \times m$ smoothing window is applied over the directional image $\mathbf{D}$.

Tables 5.11 and 5.12 show some results of such an adaptive approach. The optimal replacement threshold was determined over *Set A*. As expected, Adaptive-1, Adaptive-2 and Adaptive-3 allow to reduce the error on both bad quality and good quality fingerprints. Figures 5.5, 5.6 and 5.7 show an example of orientation extraction with the adaptive approach.

5.5.1 Learning of plausible fingerprint structures

The learning procedure in the proposed adaptive algorithm is based on Active Shape Models (ASM, [34]). An ASM is a statistical model of the shape of objects developed by Cootes and Taylor such that iteratively deform to fit to an example of the object in a new image. The statistical model of the global shape variation is built from a training set. The learnt model, called Point Distribution Model (PDM), is used to fit a template to unseen occurrences. The Point Distribution Model is estimated using the Principal Components Analysis (PCA), where the mean shape is extracted and the directions of maximal variance are determined organizing the eigenvectors according to the eigenvalues in descending order. The ASM algorithm deforms iteratively the mean shape until it finds the best shape matching within the input image.

Best-practice in machine learning methods is to perform learning in a separate dataset from that used for testing. The ASM algorithm requires a dataset to learn an internal model of fingerprint orientation distribution in nature. In our experiments, the training set is represented by a dataset of parameters of a global model computed over a set of fingerprint images. To this purpose, a large dataset of good quality fingerprints is needed (corrupted fingerprints should be excluded from the training set to avoid that inadmissible patterns are learnt). For this reason, as in previous experiments, we selected from NIST special database 14 [129], the 6164 (23% of the database) fingerprints with NFIQ index quality equal to 1 (see [117]).

The ASM algorithm is applied as described in section 4.4.4 where both the reduced dimensionality k and the regularization parameter λ are found empirically. The optimal value for k ($\leq 2n$ possible values) is chosen so as to explain a certain proportion p of the variance in the training shapes. Usually the reduced dimensionality is given by the smallest k such that $\sum_{i=1}^{k} \rho_i \geq p \sum_{i=1}^{2n} \rho_i$, where ρ_i is the ith eigenvalue. With $k = 80$,

the first eighty eigenvalues explain the 98% of the dataset. The optimal value for the regularization parameter λ belongs to the interval [3e-6,3e-7].

5.6 Results on Gottschlich et al. Benchmark

Gottschlich et al. recently proposed in [48] a benchmark for fingerprint orientation extraction (abbreviated with GOT in the following) which includes ground-truth information.

They also propose to measure the error as the number of orientation estimates deviating more than 15 degrees from the ground truth value. The main differences between our proposed benchmark FOE (see Part II) and GOT are:

- **Sampling**. FOE adopts a uniform sampling over the fingerprint foreground area; GOT provides ground truth data at sparse positions, typically in proximity of noisy regions or creases/scratches.
- **Training/Test sets**. FOE provides separate training (A) and test (B) sets; GOT provides only one set.
- **Number of fingerprints**. FOE: for each set (A, B) 10 good quality and 50 bad quality fingerprints. GOT: 60 fingerprints.
- **Number of orientation estimates**. FOE: 94,758 (*Set A*), 108,822 (*Set B*). GOT: 1,782.
- **Error metric**. FOE: *AvgErr* on bad quality dataset with the constraint $AvgErr < 7$ degrees on good quality dataset. GOT: number of estimations with error < 15 degrees.
- **Benchmark difficulty**. FOE: *AvgErr* of the baseline method J95-2 (one of the best known) over bad quality fingerprints *Set B* is 20.99°. *AvgErr* of J95-2 over GOT is 7.48°. This implies that GOT difficulty is markedly lower than FOE (bad quality dataset), and not much higher than FOE (good quality dataset), where J95-2 *AvgErr* is 6.03°.

Summarizing, we believe that FOE is more appropriate than GOT for orientation extraction benchmarking because:

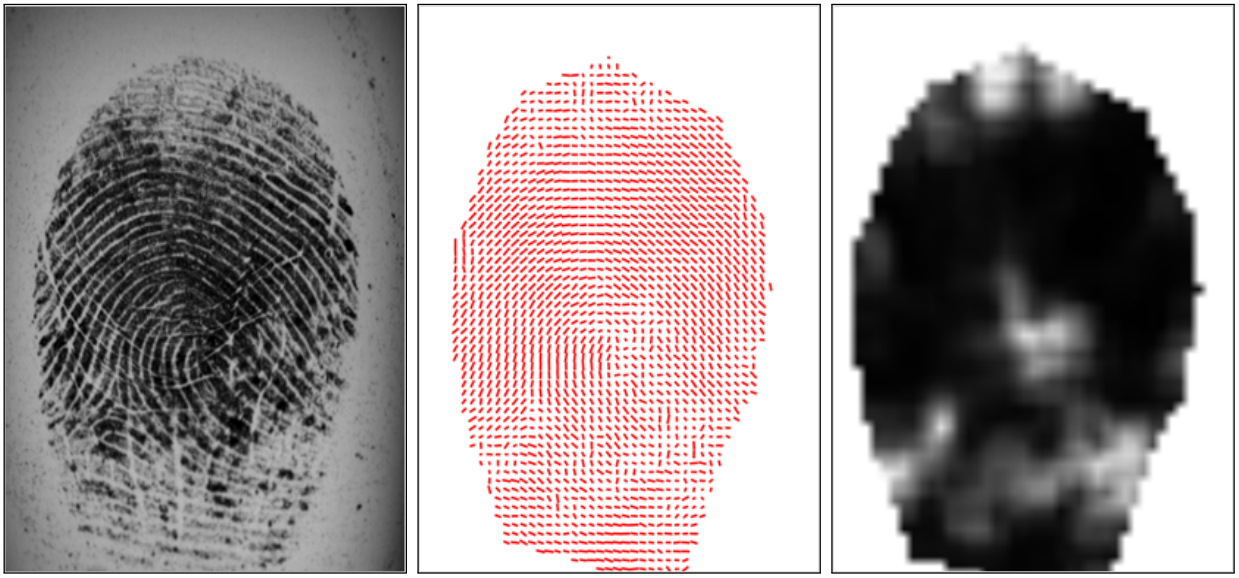

(a) Fingerprint image (b) Gradient method (c) Regularity Map

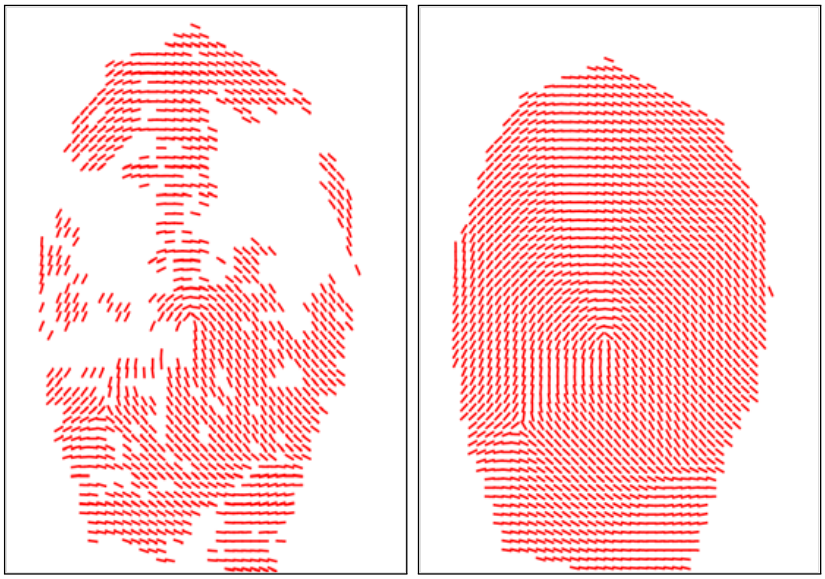

(d) Learning method (e) Final Image

Figure 5.5: Example 1 of the Adaptive-3 algorithm.

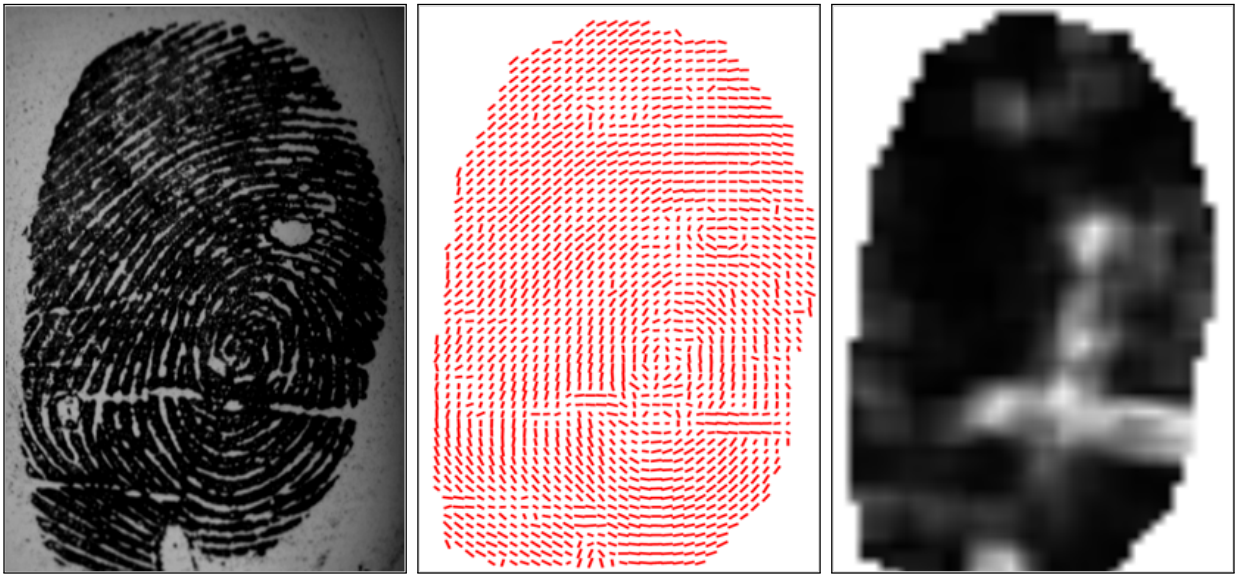

(a) Fingerprint image (b) Gradient method (c) Regularity Map

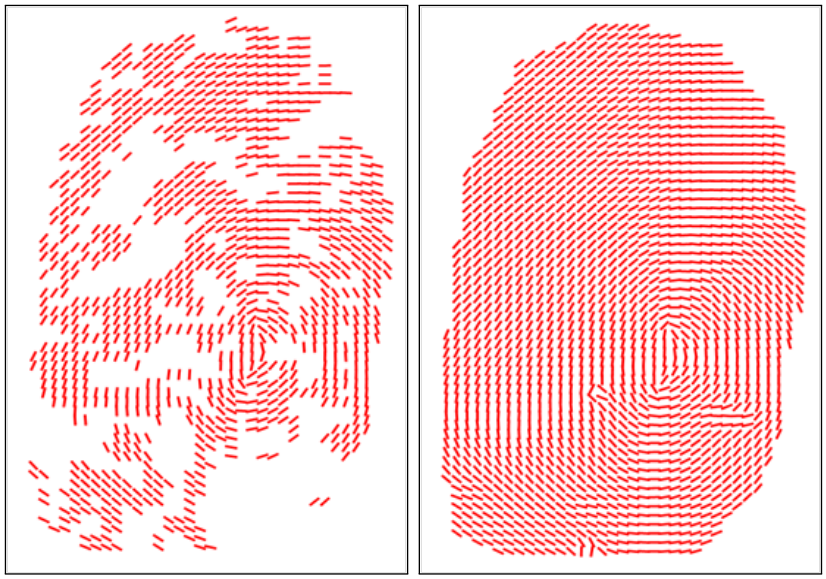

(d) Learning method (e) Final Image

Figure 5.6: Example 2 of the Adaptive-3 algorithm.

(a) Fingerprint image

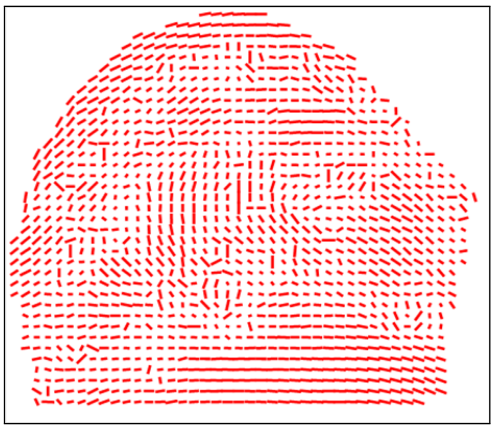

(b) Gradient method

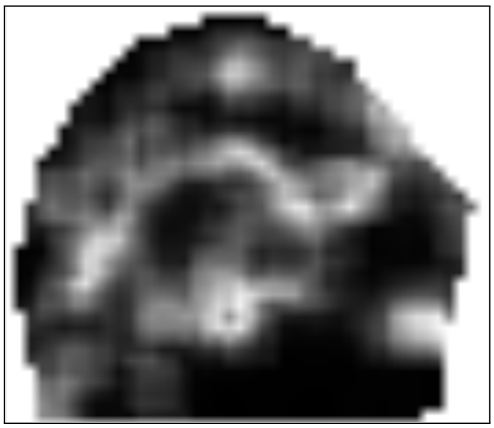

(c) Regularity Map

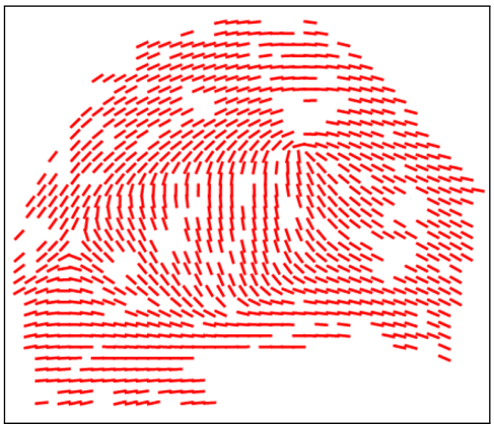

(d) Learning method

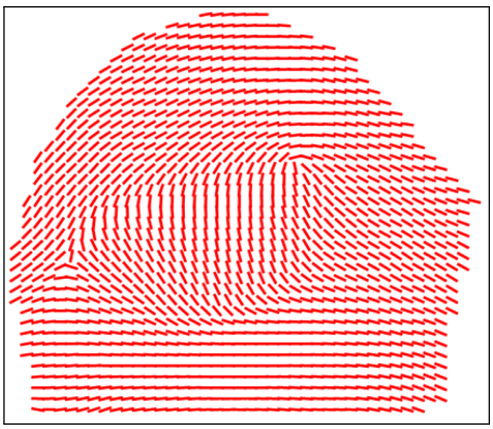

(e) Final Image

Figure 5.7: Example 3 of the Adaptive-3 algorithm.

1. it provides separate training/test datasets;
2. the total number of orientation estimates is two orders of magnitude larger;
3. the difficulty of the benchmark is much higher, thus allowing to better point out performance differences among algorithms.

However, in order to provide more support to previous sections outcomes, it is interesting to assess the performance of their algorithms also in the context of GOT.

Table 5.13 shows the performance of some considered algorithms and of the three algorithms discussed in [48]. Besides the error metric proposed in [48], in the table we also report the *AvgErr* on both FOE *Set B* and GOT.

The first seven rows of the table show results of some considered algorithms without any parameter optimization for the GOT benchmark. In fact, due to the absence of a separated training set, parameter tuning could lead to overfitting. However, since GOT is a not so hard dataset we also report the results of two algorithms where we simply "turned-off" the pre-processing stage.

Finally, the last three rows contain the results reported in [48]. It is worth noting that:

- results achieved on GOT benchmark are in line with those obtained on FOE, if we consider that GOT difficulty is closer to FOE Good dataset than FOE Bad dataset;
- the baseline implementation of the gradient achieves a performance very close to that reported in [48];
- the approach Adaptive-3 (with no parameter adjustment with respect to the training on FOE) outperforms other approaches, confirming to be both accurate (on good quality fingerprints) and robust (on bad quality ones);
- performance of G06-5 and Adaptive-3 on GOT show that if the images quality is just moderately bad, some benefits can be achieved by skipping pre-processing.

5.6.1 Statistical Significance

Through our experiments, has been proved that parameter optimizations, pre- and post-processing stages can markedly improve accuracy of baseline methods on bad quality

Category	Method	FOE Set B AvgErr (deg)		GOT Num. of Estimates
		Good	Bad	$> 15°$ and AvgErr (deg)
Gradient	J95-2	6.03	20.99	120 (7.48)
Gradient	J95-5	5.43	16.36	99 (6.74)
Slit-based	O07-5	6.06	15.52	112 (7.19)
Frequency Dom.	G06-5	5.29	14.00	99 (6.44)
Global Approx.	R10-8	5.37	14.32	120 (7.26)
Learning-based	R09-9	5.86	14.03	109 (7.25)
Adaptive-3		5.76	13.45	76 (6.06)
Frequency Dom.(no pre-proc.)	G06-5	5.30	14.71	68 (5.73)
Adaptive-3 (no pre-proc.)		5.77	14.13	63 (5.68)
Line-sensor from [48]		-	-	79
Gradient from [48]		-	-	119
Multiscale operator [48]		-	-	259

Table 5.13: Results on GOT benchmark.

fingerprints. For instance, on the bad quality dataset B, the accuracy of the gradient method improves from an average error of 22.77° to 16.36°, and the STFT method from 18.43° to 14.00°.

It is worth noting that such results are statistically significant: in fact, the 90% confidence intervals of the average errors (calculated with a nonparametric bootstrap approach as in [15]) are smaller than $\pm 0.4°$.

A novel adaptive approach combining the accuracy of local-based analysis (in good quality regions) and the robustness of learning-based global analysis (in bad quality regions) achieved the overall best performance on both FOE and GOT.

Although the FOE benchmark is the most appropriate for the evaluation of orientation extraction algorithms, an indirect assessment could be also obtained by using the different algorithms as a module of a given fingerprint verification system. Table 5.14 compares FOE accuracy with the Equal Error Rate (see section 2.8) of a baseline fingerprint verification algorithm embedding some representative orientation extraction algorithms. It is worth noting that high FOE accuracy corresponds to lower verification EER (positive correlation of 94%).

Method	AvgErr on Set B Bad Quality (degrees)	EER on FVC2006 DB2 [25] (%)
J95	22.77	0.796
J95-5	16.36	0.343
O07	19.67	0.411
O07-5	15.52	0.279
G06	18.43	0.374
G06-5	14.00	0.227
W07	20.63	0.680
W07-5	14.37	0.279
R10	20.80	0.664
R10-9	14.39	0.227
R09	20.51	0.722
R09-9	14.03	0.263
Adaptive-3	13.45	0.206

Table 5.14: FOE Accuracy vs. Fingerprint Verification Accuracy

Part III

Automatic Evaluation of Fingerprint Algorithms

Chapter 6

FVC-onGoing

Although new developments and improvements in fingerprint recognition are continuously reported [90], it is often difficult to understand, from the scientific literature, which are the most effective and promising methods. In fact, scientific papers typically propose recognition systems that integrate many modules (enhancement, feature extraction, matching, post-processing, etc.) and therefore it is hard to isolate the contributions that determine an actual progress in the state-of-the-art.

In this chapter we introduce the FVC-onGoing, a web-based automatic evaluation system of fingerprint algorithms. The proposed system is automatic (does not require the human action), "on going" (a participant can submit algorithms at any time) and outputs recognition results using standard metrics.

After a brief introduction to the Fingerprint Verification Competition (FVC), we describe the system architecture, the existing benchmarks and we propose a new benchmark for fingerprint orientation extraction (FOE) to be hosted in the FVC-onGoing framework.

6.1 The Fingerprint Verification Competition (FVC)

Performance evaluation is important for all biometric modalities and particularly so for fingerprint recognition, which is receiving widespread attention for citizen identity verification and identification in large-scale applications.

Unambiguously and reliably assessing the performance of current fingerprint recognition technology is mandatory for understanding its limitations and addressing future

research.

After the success of the first four fingerprint verification competitions (FVC2000 [87], FVC2002 [88], FVC2004 [89] and FVC2006 [25]), the Biometric System Laboratory at University of Bologna [2] has decided to organize a new online evaluation campaign for fingerprint recognition technologies: FVC-onGoing.

6.2 Aims and Architecture of FVC-onGoing

FVC-onGoing offers a web-based automatic evaluation of fingerprint recognition algorithms on a set of sequestered datasets, reporting results using well known performance indicators and metrics. The aim is to track the advances in fingerprint recognition technologies, through continuously updated independent testing and reporting of performances on given benchmarks.

The benchmark datasets does not evolve over time; in case new datasets are added in the future, they form a different benchmark or a new version of an existing one: in this way, only results obtained on the same data will be compared. The algorithms are evaluated using strongly supervised approaches (see [26]), to maximize trustworthiness of the results.

While previous FVC initiatives were organized as "competitions", with specific calls and fixed time frames, FVC-onGoing is:

1. an "on going competition" always open to new participants;

2. an evolving online repository of evaluation metrics and results.

One of the main goals of FVC-onGoing is to fully automate the main steps of the evaluation: participant registration, algorithm submission, performance evaluation, and reporting of the results. To this purpose, the Biometric System Laboratory developed a web-based evaluation framework, whose architecture and typical workflow are shown in Figure 6.1.

After a beta testing period, the FVC-onGoing web site [3] started accepting algorithm submissions on June 22, 2009. At the time this Thesis is being written, a total of 377 participants have registered, 1492 algorithms have been evaluated and the results of 68 algorithms have been published.

Currently nine benchmarks are available on FVC-onGoing, grouped into three benchmark areas:

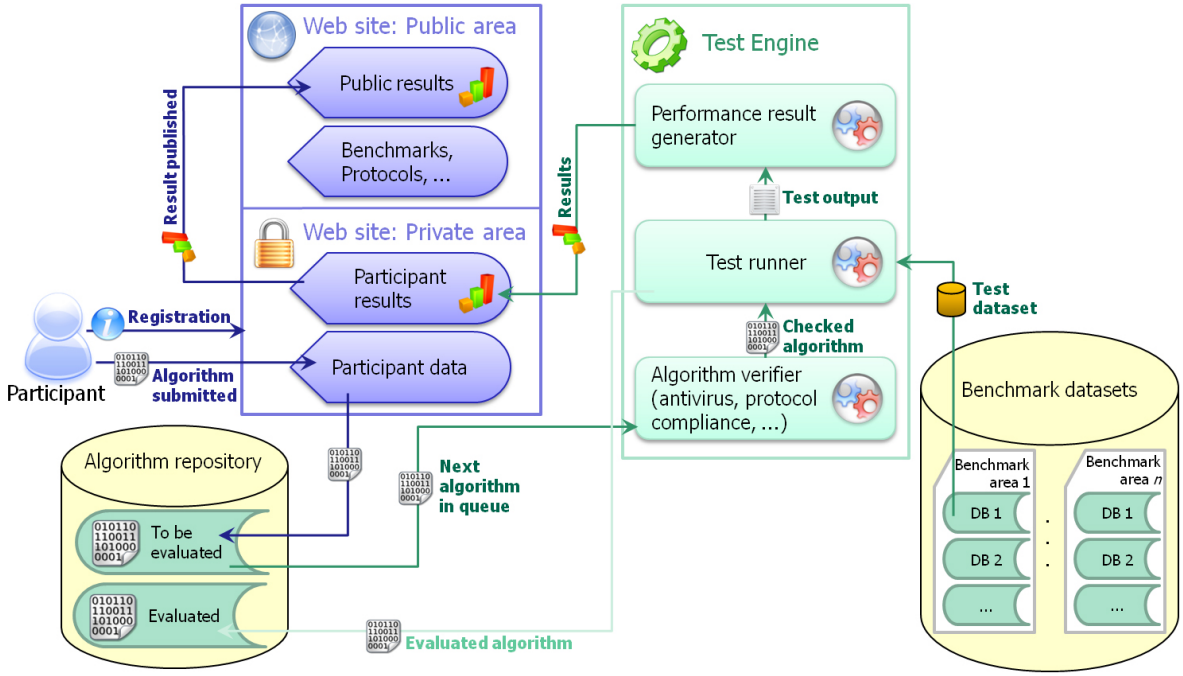

Figure 6.1: FVC-OnGoing Architecture. The diagram shows the architecture of the FVC-onGoing evaluation framework and an example of a typical workflow: a given participant, after registering to the web site, submits an algorithm to one of the available benchmarks; the algorithm (binary executable program compliant to a given protocol) is stored in a specific repository. Each algorithm is evaluated by the Test Engine that, after some preliminary checks, executes it on the dataset of the corresponding benchmark and processes its outputs (e.g. matching scores) to generate all the results (e.g. EER [90], score graphs). The participant can see the results in its "private area" and then may decide to publish the results in the public section of the FVC-onGoing web site.

- **FV**: this benchmark area contains fingerprint verification benchmarks. Fingerprint verification consists in comparing two fingerprints to determine whether they are impressions of the same finger or not (one-to-one comparisons). Algorithms submitted to these benchmarks are required to enroll fingerprints into proprietary or standard templates and to compare such templates to produce a similarity score.

  1. **FV-TEST**. A simple dataset useful to test algorithm compliancy with the evaluation protocol.

  2. **FV-STD-1.0**. Fingerprint images acquired in operational conditions using

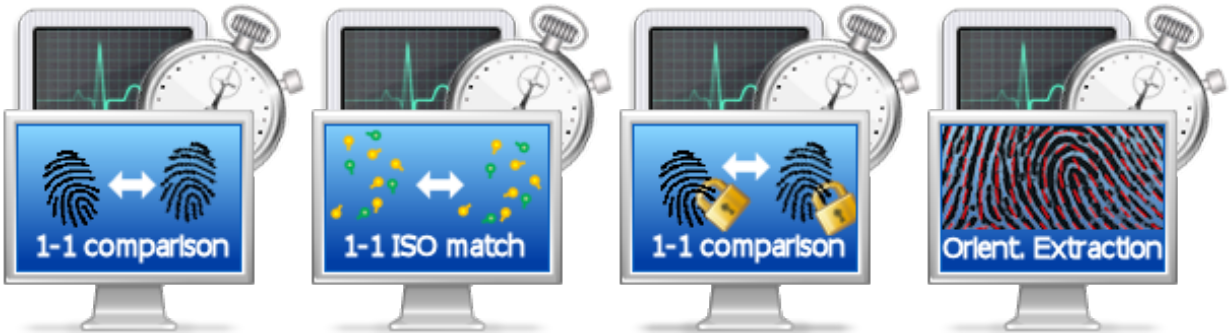

Figure 6.2: FVC-onGoing Benchmark Areas

high-quality optical scanners.

3. **FV-HARD-1.0**. Contains a relevant number of difficult cases (noisy images, distorted impressions, etc.) that makes fingerprint verification more challenging.

- **FMISO**: this benchmark area contains fingerprint matching benchmarks using a standard minutiae-based template format [ISO/IEC 19794-2 (2005)]. Algorithms submitted to these benchmarks are required to compare ISO fingerprint templates to determine whether they are impressions of the same finger or not (one-to-one comparisons). No fingerprint enrollment (feature extraction) is required, only the minutiae matching algorithms are evaluated by these benchmarks.

  1. **FMISO-TEST**. A simple dataset useful to test algorithm compliancy with the evaluation protocol.
  2. **FMISO-STD-1.0**. ISO templates created from fingerprint images acquired in operational conditions using high-quality optical scanners.
  3. **FMISO-HARD-1.0**. Contains a relevant number of difficult cases (noisy images, distorted impressions, etc.).

- **STFV**: this benchmark area contains fingerprint verification benchmarks for algorithms relying on protected templates to enhance privacy. Algorithms submitted to these benchmarks are required to enroll a given fingerprint into a protected template (that is, a template from which the fingerprint features cannot be extracted) and to compare it against a given fingerprint image.

1. **STFV-TEST**. A simple dataset useful to test algorithm compliancy with the evaluation protocol.
2. **STFV-STD-1.0**. Contains fingerprint images acquired in operational conditions using high-quality optical scanners. Results should reflect the expected accuracy in large-scale fingerprint-based applications.
3. **STFV-HARD-1.0**. Contains a relevant number of difficult cases (noisy images, distorted impressions, etc.) that makes fingerprint verification more challenging. Results do not necessarily reflect the expected accuracy in real applications but allow to better discriminate the performance of various fingerprint recognition algorithms.

6.3 The New Orientation Extraction Benchmark

The estimation of local fingerprint orientations is a fundamental step in fingerprint analysis and recognition (e.g., it is a prerequisite for image enhancement). The Fingerprint Orientation Extraction (FOE) benchmark area has been added to the FVC-onGoing in order to assess the accuracy of fingerprint orientation extraction algorithms.

Algorithms submitted to this area are required to extract local orientations from fingerprint images and to save them into a specific format. The extracted orientations are compared to the ground-truth in order to assess the algorithm accuracy. The ground-truth has been manually marked using an ad-hoc software tool (see the next section for more details).

This new area contains two benchmarks:

- **FOE-TEST**. A small benchmark useful to test algorithm compliancy with the testing protocol (results obtained on this benchmark are only visible in the participant private area and cannot be published). Fingerprints have been acquired using optical scanners.
- **FOE-STD-1.0**. Fingerprint orientation extraction benchmark on fingerprints acquired using optical scanners.

The FOE-TEST benchmark is publicly available and allows participants to test algorithm compliancy with the protocol and to adjust algorithm parameters. The FOE-STD-1.0 benchmark is sequestered and can be used to assess the performance of a fingerprint

Benchmark	Scanner Type	Resolution	Min Image Size	Max Image Size
FOE-TEST	Optical	500 dpi	328x364	448x560
FOE-STD-1.0	Optical	500 dpi	328x364	448x560

Table 6.1: Main characteristics of each benchmark.

Benchmark	Good Quality Dataset		Bad Quality Dataset	
	Or. Estimations	Fingerprints	Or. Estimations	Fingerprints
FOE-TEST	18946	10	75812	50
FOE-STD-1.0	19260	10	89562	50

Table 6.2: Number of orientation to estimate in each benchmark.

orientation extraction algorithm.

Each of them can contains two new datasets of identical size (60 fingerprints) and can be divided into

- Good Quality Dataset: 10 fingerprints of good quality acquired using optical scanners (see figure 6.4 for some examples) with the corresponding orientation ground-truth.
- Bad Quality Dataset: 50 fingerprints of low and very-low quality acquired using optical scanners (see figure 6.5 for some examples) with the corresponding orientation ground-truth.

With the term "low-quality images" we mean fingerprint impressions where the normal ridge-lines flow is corrupted by bad skin conditions (i.e., cuts, scars, bruises), sensor noise and incorrect finger pressure. All these distortions significantly affect the orientation extraction step. In spite of the large noise, a human expert can detect with good precision the ridge-line flow in the fingerprints of figure 6.5; this is not true for existing automatic orientation extraction algorithms. For the creation of the datasets, the fingerprint quality has been assessed by visual inspection and taking into account the NFIQ quality index [117].

Why providing two datasets (Good and Bad) in order to evaluate orientation extraction algorithms? A good orientation extraction algorithm should be able to deal with very low-quality images, without losing accuracy on good quality ones. Hence, a large Good Quality Dataset is not needed, since its only purpose is to ensure that algorithms do not over-smooth the orientations. On the other hand, a large database of bad quality

images would be welcome. Even if the tool described in section 6.4 greatly simplifies ground truth markup, performing this activity with the due care and precision remains critical and time consuming.

It is worth noting that, even if each set (FOE-TEST and FOE-STD-1.0) currently contains just 50 bad quality images and 10 good quality images, the total number of orientation estimations is 94,758 for FOE-TEST and 108,822 for FOE-STD-1.0. The main characteristics of each benchmark are summarized in Table 6.1 and Table 6.2.

6.4 Ground Truth Markup

For each image of both datasets, the ground-truth has been marked by a human expert by using the software tool introduced in section 4.3. This tool allows a semi-automatic markup of the local orientations through a few simple steps:

- the user selects the positions where he wants to manually set the orientation: for each position the tool proposes a local orientation which the user can adjust to visually match the true ridge orientation (Figure 6.3 top);
- the system automatically interpolates all the other local orientations through a Delaunay triangulation (see Figure 6.3 bottom).

6.5 Performance Evaluation of Orientation Extraction Algorithms

The FOE benchmarks use the *Average Root Mean Square Deviation* (see Equation 4.4) to evaluate the difference between an extracted orientation image and the ground-truth. This statistic equally weights extraction errors across the whole foreground; this choice is well suited in most of the feature extraction tasks where orientations are needed (e.g. minutiae detection). Other metrics may be more appropriate for specific tasks, such as singularity detection, where errors close to singularities should have higher weights.

Other secondary performance indicators are also reported:

- Average orientation extraction time.
- Maximum amount of memory allocated.

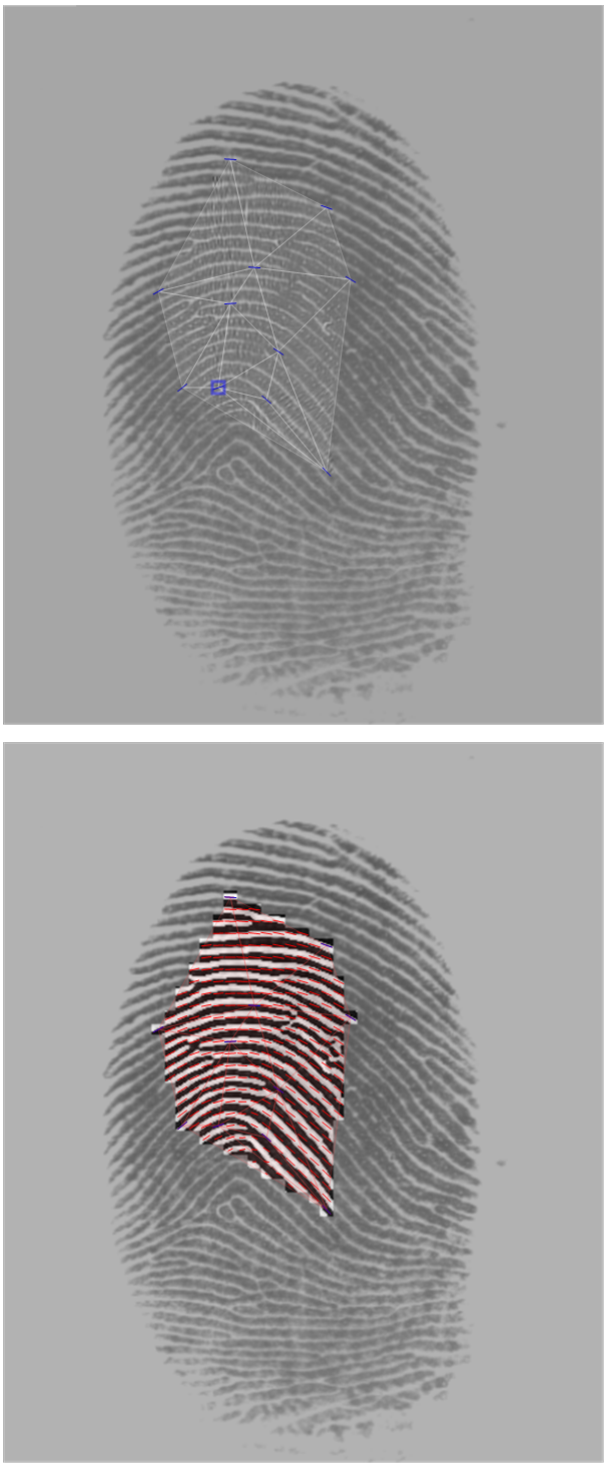

Figure 6.3: FOE Ground-truth markup. Example of ground-truth markup of a fingerprint that belongs to the FOE benchmark. Some local orientations are marked up by the user (vertices of triangles on the top image); others are interpolated by the software (bottom image).

Figure 6.4: Examples of Good Images.

- Orientation deviation distribution for both datasets (Histogram of the distribution of individual orientation extraction errors).

- Average error distribution for both datasets (Histogram of the distribution of average errors over the various fingerprints).

Figure 6.5: Examples of Bad Images.

6.6 FOE Benchmark Protocol

Algorithms submitted to the FOE Benchmark must be able to extract the orientation image from a fingerprint.

Each participant is required to submit, for each algorithm, one executable named `Extractor.exe` in the form of Win32 console application. The executable will take the input from command-line arguments and will save the output to file into a specific

format. The command-line syntax is:

`Extractor.exe <indexfile> <outputfolder>`

where:

- `<indexfile>` is a test file containing the file path of each fingerprint to be processed. The first line of the file contains the number of fingerprints; each of the following lines has the format:
  `<imagepath> <step> <border>`
  where:
  - `<imagepath>` is the file path of the fingerprint (bitmap file format);
  - `<step>` is the step to be used to calculate the orientation image;
  - `<border>` is the distance from the image border in pixels: this parameter determines the position of the top-left element.

  The parameter `<step>` and the number of sampling points are selected in a way that do not allow any sampling point to be closer to any of the borders than `<border>` pixels. This enables an algorithm to center, at each sampling point, a filter that extends up to `<border>` pixels in each direction. The participant can assume that the border is not smaller than 14 pixels. Figure 6.6 shows an example of such sampling.

- `<outputfolder>` is the path of the folder where the output files have to be saved.

For each input fingerprint, a further file with the same path and extension `.fg` (instead of `.bmp`) is provided. This file defines which elements of the orientation image belong to the fingerprint foreground. The algorithm is required to compute the orientation of those elements only: the remaining elements of the orientation image can be left to zero. The foreground file is a text file where the first line contains the number of rows and columns of the orientation image and the remaining lines denote foreground ('1') and background elements ('0'). Source code to read this file format is available for download in the FVC-onGoing website [3].

The algorithm is required to extract the orientation image from each input fingerprint and save it in the output folder to a file with the same name of the fingerprint but extension `.dirmap` (instead of `.bmp`). The output must be saved as a binary file

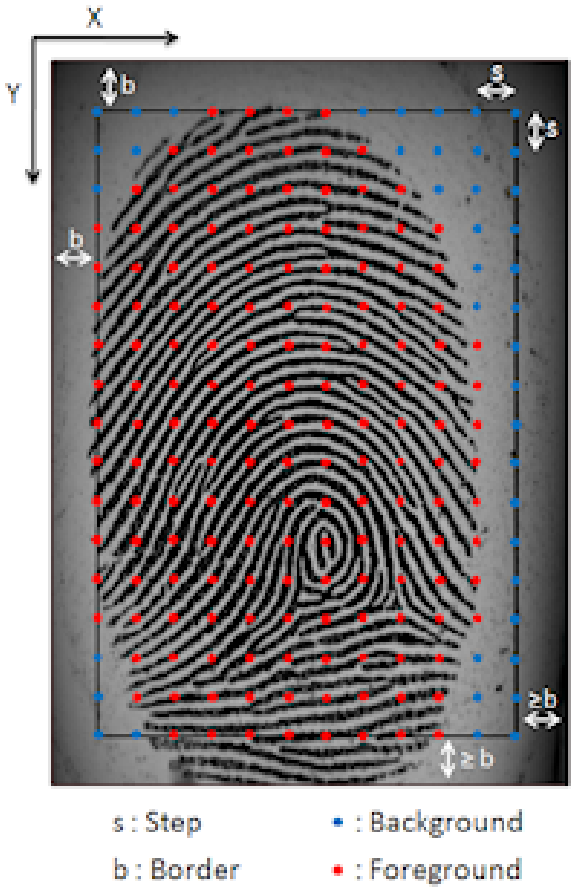

Figure 6.6: FOE Algorithm Parameters. The parameter "Step" and the number of sampling points are selected in a way that do not allow any sampling point to be closer to any of the borders than "Border" pixels.

Benchmark	**Max fingerprint proc. time**	**Max AvgError on Good Images**
FOE-TEST	10 seconds	7 degrees
FV-STD-1.0	10 seconds	7 degrees

Table 6.3: Execution constraints.

with a specific format: source code to save the file is provided in the download page. In the output file, each orientation element must be stored in one byte in units of 0.703125 (180/256) degrees; for example, a byte orientation value of 128 represents 90 degrees and a byte orientation value of 32 represents 22.5 degrees (note that a byte orientation

Benchmark	Minimum break
FOE-TEST	2 hour(s)
FOE-STD-1.0	1 day(s)

Table 6.4: Time-breaks constraints.

value of 255 is 179,296875 degrees and not 180 degrees). Each orientation angle shall be measured increasing counter-clockwise starting from the horizontal axis to the right.

The algorithm is also required to write the file name of each processed fingerprint to a named pipe, in order to inform the caller about its progress status.

C and C# language skeletons for `Extractor.exe` are available for download [3] to reduce the participants implementation efforts. These source files perform all the necessary I/O (including loading image and foreground, saving the orientation image and writing to the named pipe).

During test execution the constraints shown in Table 6.3 will be enforced. Each algorithm that violates one of the these constraints results in an execution failure and no performance indicators are provided. The time-breaks constraints shown in Table 6.4 are enforced between two consecutive submissions to the same benchmark by the same participant.

Chapter 7

FVC-onGoing Results

Performance evaluation of biometric systems is fundamental to stimulate the scientific community on challenging research topics and to monitor the advance of the state-of-the-art in the field.

In this chapter we present the results of two fingerprint recognition competitions organized by the Biometric System Laboratory of the University of Bologna [2] in conjunction with the International Joint Conference on Biometrics IJCB 2011 [1] held in Washington DC (USA) and the International Conference on Biometrics ICB 2012 [4] held in New Delhi (India).

Considering the benchmarks difficulty, some of the algorithms submitted achieved very good accuracies; from the results and the participant self-description of the algorithms it was possible to identify the most effective and promising approaches to the various fingerprint recognition sub-problems (e.g., enhancement, alignment, etc.).

7.1 Fingerprint Verification Competition at IJCB2011

FVC-onGoing@IJCB11 is a fingerprint verification competition organized by the Biometric System Laboratory of the University of Bologna [2] in conjunction with the International Joint Conference on Biometrics IJCB 2011 [1]. Previous testing initiatives for fingerprint recognition systems include the former FVC competitions [87] [88] [89] [25], and several evaluations conducted by NIST [58].

The competition was based on the FVC-onGoing framework and benchmarks [3] and open to companies, academic research groups and independent developers. A complete

description of the FVC-onGoing framework and benchmarks can be found in chapter 6.

7.1.1 Competition Benchmarks

The following benchmarks (whose details can be found in chapter 6) were included in the FVC-onGoing@IJCB11 competition:

- **FV-STD-1.0**: Contains fingerprint images acquired in operational conditions using high-quality optical scanners.
- **FV-HARD-1.0**: Contains a relevant number of difficult cases (noisy images, distorted impressions, etc.) that makes fingerprint verification more challenging.
- **FMISO-STD-1.0**: Contains ISO templates created from fingerprint images acquired in operational conditions using high-quality optical scanners.
- **FMISO-HARD-1.0**: Contains a relevant number of difficult cases (noisy images, distorted impressions, etc.) that makes fingerprint verification more challenging.

7.1.2 Algorithm submission and publication

Thanks to the FVC-onGoing framework, the main steps of the competition were easily automated:

- participant registration;
- algorithm submission;
- performance evaluation;
- reporting of the results.

In order to participate in FVC-onGoing@IJCB11, an algorithm had to be submitted to one of the benchmarks described in section 7.1.1, and be published, before May 15th, 2011, in the public section of the web site.

Figure 7.1 shows the number of submitted and published algorithms by month. It is well evident how the IJCB11 competition (announced in late January 2011) raised the interest of the scientific community (both from academia and industry) in FVC-onGoing. Before the organization of the FVC-onGoing@IJCB11, 672 algorithms had

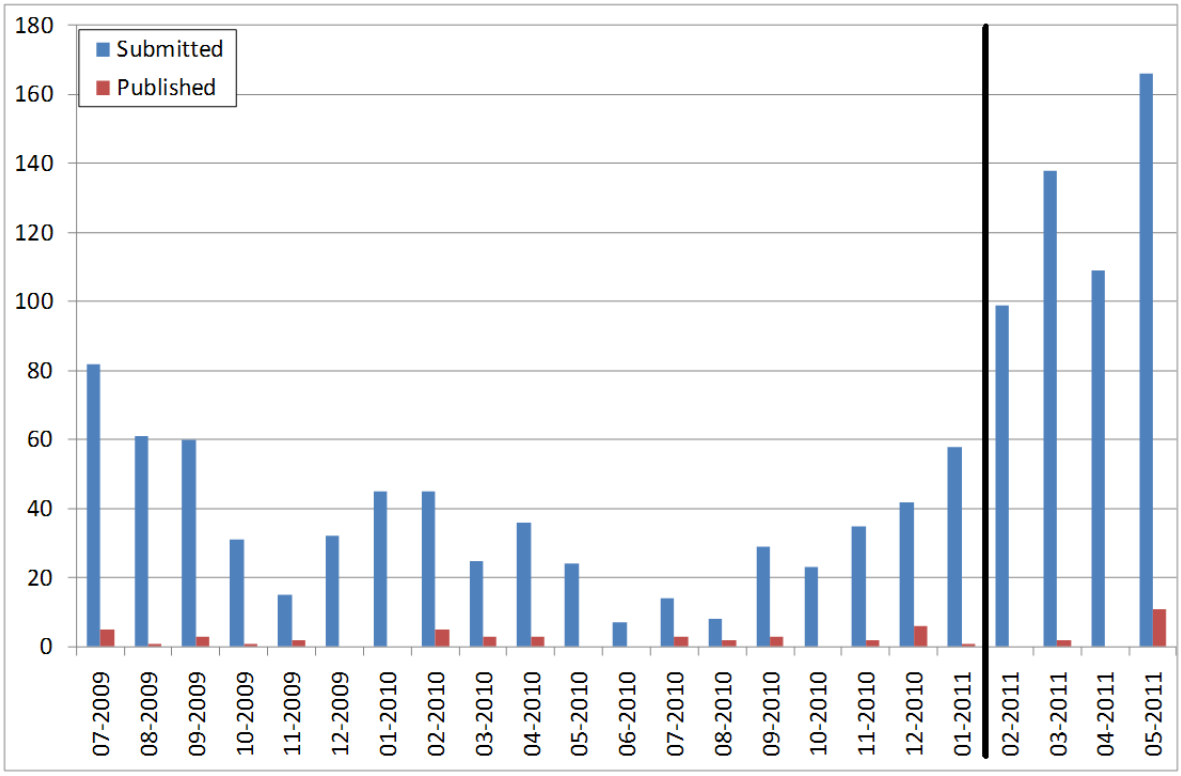

Figure 7.1: Double bar chart with the number of submitted and published algorithms by month. The separator between 01-2011 and 02-2011 denotes the FVC-onGoing@IJCB11 announcement.

been submitted and 40 of them had been published in 19 months (about 35.4 submissions and 2.9 publications per month). During the four months of the IJCB competition, 512 algorithms have been submitted and 13 of them have been published (about 128.0 submissions and 6.5 publications per month).

7.2 Results of FVC-onGoing@IJCB11

To compare algorithm performances, the following indicators were measured:

- Equal Error Rate (EER);
- FMR1000: the lowest FNMR for FMR.0.1;
- FMR10000: the lowest FNMR for FMR.0.01;

Date	Participant	Type	Algorithm	Version	EER	FMR_{1000}	FMR_{10000}
15/05/11	AA Tech. Ltd.	Company	EMB9200	2.3	0.176	0.188	0.303
15/05/11	UnionCommunity	Company	Triple_M	1.1	0.418	0.859	1.977
14/05/11	IACAS[1]	Academic	MntModel	1.0	0.293	0.512	1.209
14/05/11	YZ+BFL[2]	Independent	MiraFinger	2.2	6.701	67.475	84.488
14/09/10	Green Bit S.p.A	Company	GBFRSW	1.3.2.0	0.118	0.155	0.519
25/08/10	Robert Vanak	Independent	SourceAFIS	1.1	3.649	7.266	10.905
20/07/09	Neurotechnology	Company	MM_FV	3.0	0.281	0.386	0.581
15/07/09	Secuest Inc.	Company	STAR	1.0	1.265	2.504	4.026
24/06/09	jFinger Co. Ltd.	Company	JF_FV	V1.21a	1.618	2.872	4.545

Table 7.1: Published results on FV-STD-1.0 benchmark (percentage values) sorted by publication date.

- Detection-Error Tradeoff (DET) curve: a plot of FMR and FNMR that reports system performance at any possible operating point (matching threshold).

A description of such indicators can be found in 2.8.

Tables 7.1, 7.2, 7.3 and 7.4 report EER, FMR1000 and FMR10000 indicators of the best version of all the algorithms published on the four considered benchmarks.
For each benchmark, the best result on each indicator is highlighted in bold. Figures 7.4, 7.5, 7.6 and 7.7 show DET curves of all the algorithms listed in Tables 7.1, 7.2, 7.3 and 7.4, respectively.

Figures 7.2 and 7.3 tries to categorize the algorithms based on the features they exploit and processing stages they implement. This information is extracted from the web-based questionnaires that participants have to fill when they submit an algorithm.

7.2.1 Results over the FV Benchmarks

From DET curves in Figures 7.4 and 7.5 it is evident that best competitors on benchmark FV-STD-1.0 and FV-HARD-1.0 are EMB9200-v2.3 and GBFRSW-v1.3.2.0.

By looking at the entries in Table 7.2 (and the extra data reported in [3]) for EMB9200-v2.3 and GBFRSW-v1.3.2.0 we can conclude that for the most effective algorithms:

[1]Institute of Automation - Chinese Academy of Sciences
[2]Yanbing Zhang & Bao Feng Lan
[3]Biometric System Laboratory - University of Bologna

Date	Participant	Type	Algorithm	Version	EER	FMR_{1000}	FMR_{10000}
15/05/11	AA Tech. Ltd.	Company	EMB9200	2.3	0.700	1.247	1.817
15/05/11	UnionCommunity	Company	Triple_M	1.1	2.021	4.420	8.447
14/05/11	IACAS[1]	Academic	MntModel	1.0	1.257	2.795	4.436
14/09/10	Green Bit S.p.A	Company	GBFRSW	1.3.2.0	0.735	1.444	2.355
26/08/10	Robert Vanak	Independent	SourceAFIS	1.1	6.769	13.954	16.310
20/07/09	Neurotechnology	Company	MM_FV	3.0	1.528	3.043	4.079

Table 7.2: Published results on FV-HARD-1.0 benchmark (percentage values) sorted by publication date.

- enhancement/binarization is based on contextual filtering relying on the computation of local ridge orientation and frequency;
- fingerprint alignment mainly relies on minutiae. Using ridge geometry for alignment in conjunction with minutiae (see [61] [65] [84] for example) seems to help GBFRSW-v1.3.2.0 to match good/medium quality fingerprints (FV-STD-1.0) but not difficult cases (FV-HARD-1.0); as a side effect using ridge geometry leads to higher matching time and larger template size;
- fingerprint matching exploits multiple features; beside minutiae, ridge count (or local frequency) and local orientations are extensively used (see [90] for more details);
- minutiae alignment/matching is based on a two stage technique where an initial local matching is followed by a global consolidation (see [70] [121] [40] [31]).

7.2.2 Results over the FMISO Benchmarks

From DET curves in Figures 7.6 and 7.7 it is evident that the best algorithms on benchmarks FMISO-STD-1.0 and FMISO-HARD-1.0 are EMB9200-v2.41 and Triple_M_ISO-v1.2. By looking at the entries in Figure 7.3 (and the extra data reported in [90]) for EMB9200-v2.41 and Triple_M_ISO-v1.2 we can conclude that for the most effective algorithms:

- the performance of 'minutiae-only' algorithms is very good and not far from proprietary template algorithms;

Date	Participant	Type	Algorithm	Version	EER	FMR_{1000}	FMR_{10000}
15/05/11	AA Tech. Ltd.	Company	EMB9200	2.41	0.234	0.292	0.444
14/05/11	IACAS[1]	Academic	MntModel	1.0	0.380	0.505	0.819
24/03/11	UnionCommunity	Company	Triple_M_ISO	1.2	0.234	0.361	0.620
15/12/10	Suprema, Inc.	Company	SFCore	1.0	0.258	0.346	0.639
30/11/10	Communik8 Ltd.	Company	Authentik8	1.0	1.017	2.475	10.473
15/09/10	Robert Vanak	Independent	SourceAFIS	1.3	1.334	2.002	2.900
22/07/10	BioLab[3]	Academic	MCC	1.1	0.570	0.884	1.331
02/04/10	id3 Semiconductors	Company	FM ISO	1.0	0.559	0.783	1.147
12/10/09	Tiger IT Bangladesh	Company	Tiger ISO	0.1	0.317	0.447	0.866
26/09/09	APRO TECH. LTD.	Company	APF_FMISO	1.1	0.582	0.801	1.057
20/07/09	Neurotechnology	Company	MM_FMISO	3.0	0.598	0.801	1.234

Table 7.3: Published results on FMISO-STD-1.0 benchmark (percentage values) sorted by publication date.

Date	Participant	Type	Algorithm	Version	EER	FMR_{1000}	FMR_{10000}
15/05/11	AA Tech. Ltd.	Company	EMB9200	2.41	1.113	2.076	3.282
14/05/11	IACAS[1]	Academic	MntModel	1.0	1.588	2.821	3.965
24/03/11	UnionCommunity	Company	Triple_M_ISO	1.2	1.103	3.157	7.878
15/12/10	Suprema, Inc.	Company	SFCore	1.0	1.407	2.697	4.570
22/07/10	BioLab[3]	Academic	MCC	1.1	2.315	4.876	6.206
09/03/10	id3 Semiconductors	Company	FM ISO	1.0	2.400	4.260	6.605
26/09/09	APRO TECH. LTD.	Company	APF_FMISO	1.1	2.552	4.581	5.963
20/07/09	Neurotechnology	Company	MM_FMISO	3.0	2.430	4.607	6.139

Table 7.4: Published results on FMISO-HARD-1.0 benchmark (percentage values) sorted by publication date.

- all the minutiae information, including the minutia type (i.e., bifurcation, ridge ending or other) and the minutia quality are exploited;
- minutiae alignment/matching is based on a two stage technique where an initial local matching is followed by a global consolidation(see [70] [121] [40] [31]).

	Algorithm			EMB9200 2.3	Triple_M 1.1	MntModel 1.0	MiraFinger 2.2	GBFRSW 1.3.2.0	SourceAFIS 1.1	MM_FV 3.0	STAR 1.0	JF_FV 1.21a
Preprocessing	Segmentation			X	X	X		X	X	X	X	X
	Enhancement			X	X	X			X	X	X	X
	Binarization			X	X	X		X	X	X	X	X
Feature Used	Minutiae			X	X	X	X	X	X	X	X	X
	Singular Points									X	X	X
	Ridge Shape							X				
	Ridge Counts			X						X		
	Orientation Field			X	X	X		X		X	X	X
	Local Ridge Frequency				X			X		X	X	
	Texture						X				X	
Matching	Matching Strategy	Minutiae-Based	Local	X	X	X	X	X	X	X	X	X
			Global	X	X	X		X	X	X	X	X
		Based on Geometry Ridge Features						X				X
	Alignment Model	Displacement		X	X	X	X	X	X	X	X	X
		Rotation		X	X	X	X	X	X	X	X	X
		Scale					X				X	X
		Non-linear Distortion		X	X		X	X		X	X	

Figure 7.2: Characteristics of the algorithms published in FV benchmark area.

	Algorithm		EMB9200 2.41	MntModel 1.0	Triple_M_ISO 1.2	SFCore 1.0	Authentik8 1.0	SourceAFIS 1.3	MCC 1.1	Fingerprint Matcher ISO 1.0	Tiger ISO 0.1	APF_FMISO 1.1	MM_FMISO 3.0
Minutiae Feature Used	Position		X	X	X	X	X	X	X	X	X	X	X
	Direction		X	X	X	X	X	X	X	X	X	X	X
	Type		X		X	X		X			X	X	X
	Quality		X		X						X		
Matching	Matching Strategy	Local	X	X	X	X	X		X	X	X	X	X
		Global	X	X	X	X		X	X	X		X	X
	Alignment Model	Displacement	X	X	X	X	X	X	X	X	X	X	X
		Rotation	X	X	X	X	X	X	X	X	X	X	
		Scale			X								
		Non-linear Distortion			X						X	X	X

Figure 7.3: Characteristics of the algorithms published in FMISO benchmark area.

7.3 Fingerprint Orientation Extraction Competition at ICB2012

FOE@ICB12 is a fingerprint orientation extraction competition organized by the Biometric System Laboratory of the University of Bologna [2] in conjunction with the International Conference on Biometrics ICB 2012 [4].

This is the first online competition for orientation extraction algorithms. It is based on the FVC-onGoing framework and benchmarks [3] and open to companies, academic re-

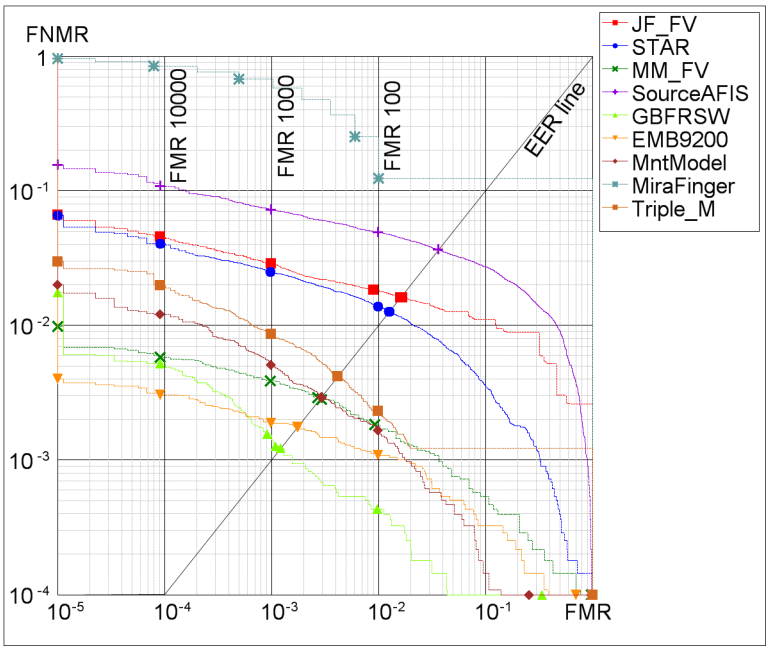

Figure 7.4: DET graph of the published algorithms on FV-STD-1.0 benchmark.

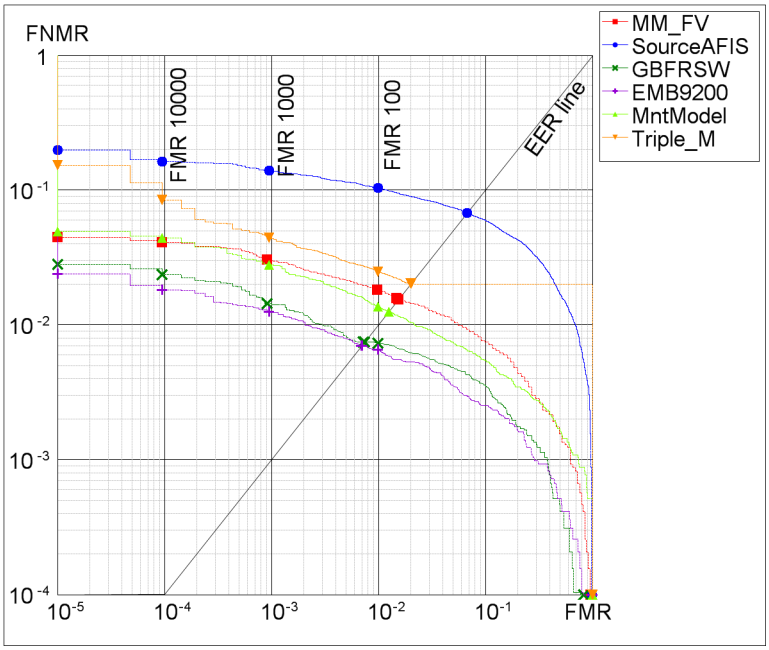

Figure 7.5: DET graph of the published algorithms on FV-HARD-1.0 benchmark.

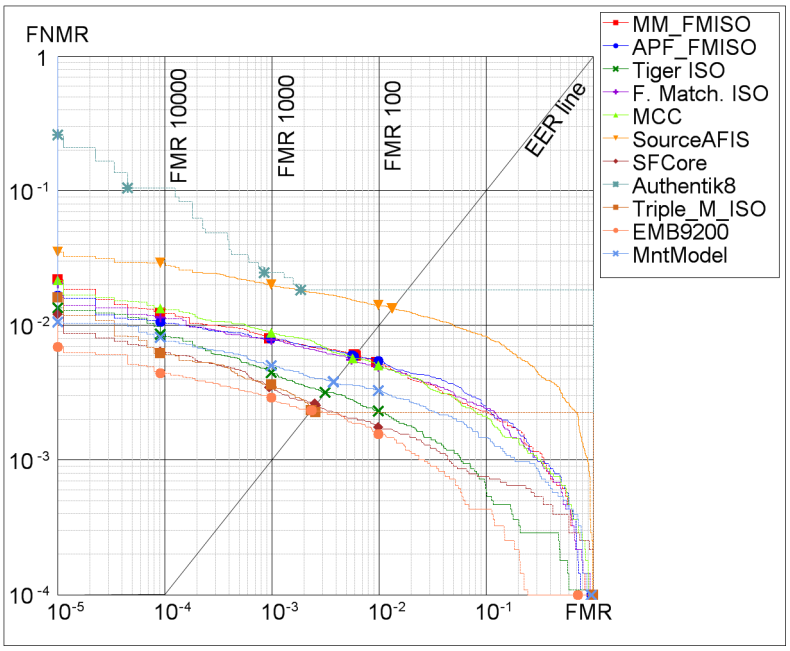

Figure 7.6: DET graph of the published algorithms on FMISO-STD-1.0 benchmark.

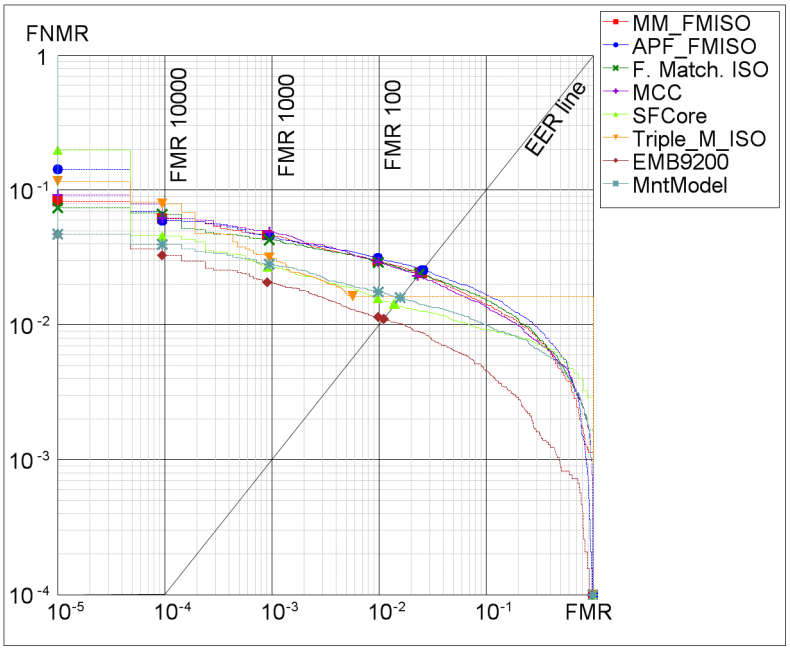

Figure 7.7: DET graph of the published algorithms on FMISO-HARD-1.0 benchmark.

search groups and independent developers. A complete description of the FVC-onGoing framework and benchmarks can be found in chapter 6.

7.3.1 Competition Benchmarks

The following benchmark (whose details can be found in chapter 6) was included in the FOE@ICB12 competition:

- **FOE-STD-1.0**: Fingerprint orientation extraction benchmark on fingerprints acquired using optical scanners.

The benchmark contains 60 fingerprints of good and bad quality with the corresponding manually marked orientation ground-truth. Even if the benchmark contains just 60 fingerprints, the total number of orientation estimates is 108,822.

7.3.2 Algorithm submission and publication

The submission and publication of algorithms is easily automated thanks to the FVC-onGoing framework. In order to participate to the competition the participant, after the registration, had submit his algorithms according to the FOE protocol before November 21st, 2011, in the public section of the website.

7.4 Results of FOE@ICB12

To compare the algorithm performances, the *AvgError* indicator was measured. Such indicator is described in Equation 4.4.

Table 7.5 reports the *AvgError* indicator of all algorithms published on the FOE-STD-1.0 benchmark. By looking the table we can see that the participants to this competition are mostly academic and independent developers. Companies in general are more interested in matching competitions.

The best result on this benchmark has been achieved by the MXR algorithm. Unfortunately we do not have access to the method details, but from the form filled by the participant before the submission we can just see that it is based on local-gradient estimations and a parametric global model. The first version of the algorithm (1.0.1)

Date	Participant	Type	Algorithm	Version	GoodRMSD	BadRMSD
22/11/11	Antheus Tech. Inc.	Company	AntheusOriEx	1.1.4	5.46°	17.06°
18/11/11	Zengbo Xu	Independent	MXR	1.0.5	5.59°	11.36°
08/11/11	BioLab[4]	Academic	Adaptive-3 (Baseline)	v0.2	5.93°	13.27°
30/10/11	Zengbo Xu	Independent	MXR	1.0.1	6.15°	13.00°
23/08/11	IACAS[5]	Academic	ROF	1.0	5.39°	12.30°
22/11/10	UNSW@ADFA[6]	Academic	FOMFE	1.0	6.70°	21.44°
19/07/10	BioLab[4]	Academic	Gradient (Baseline)	1.0	5.86°	21.83°

Table 7.5: Published results on FOE-STD-1.0 benchmark sorted by publication date.

obtains an *AvgError* of 13.00° on the bad quality dataset. With the adoption of a regularization approach based on scar detection (version 1.0.5) the performance is further improved. In the competition our algorithm Adaptive-3 has been published as baseline algorithm with the same parameters used in chapter 5 and a slight modification in the regularization parameter μ.

The FVC-onGoing framework provides, for each algorithm published in the FOE benchmark area, some useful distributions:

- orientation deviation distribution (Bad Quality);
- orientation deviation distribution (Good Quality);
- average error distribution (Bad Quality);
- average error distribution (Good Quality).

For each dataset (Good quality or Bad Quality):

- the *orientation deviation distribution* graph plots, for each specific deviation interval (expressed in degrees), the number of orientation elements that deviate from the true orientation. This distribution is computed over the whole set of orientations to estimate and should be sharply peaked around zero degrees for an algorithm that estimates correctly most of the orientations;

[5]Institute of Automation - Chinese Academy of Sciences
[4]Biometric System Laboratory - University of Bologna
[6]School of Engineering and Information Technology, UNSW@ADFA

- the *average error distribution* graph plots the number of fingerprints in the dataset with a specific average orientation error (expressed in degrees). In this graph, just the interval [0-10] should be filled is the algorithm estimates correctly the orientations in all the provided fingerprints. This performance can be easily achieved for good quality fingerprints, while it is a very difficult for bad quality fingerprints.

Figure 7.8 and 7.9 show the four aforementioned distributions for the Adaptive-3 and MXR algorithms.

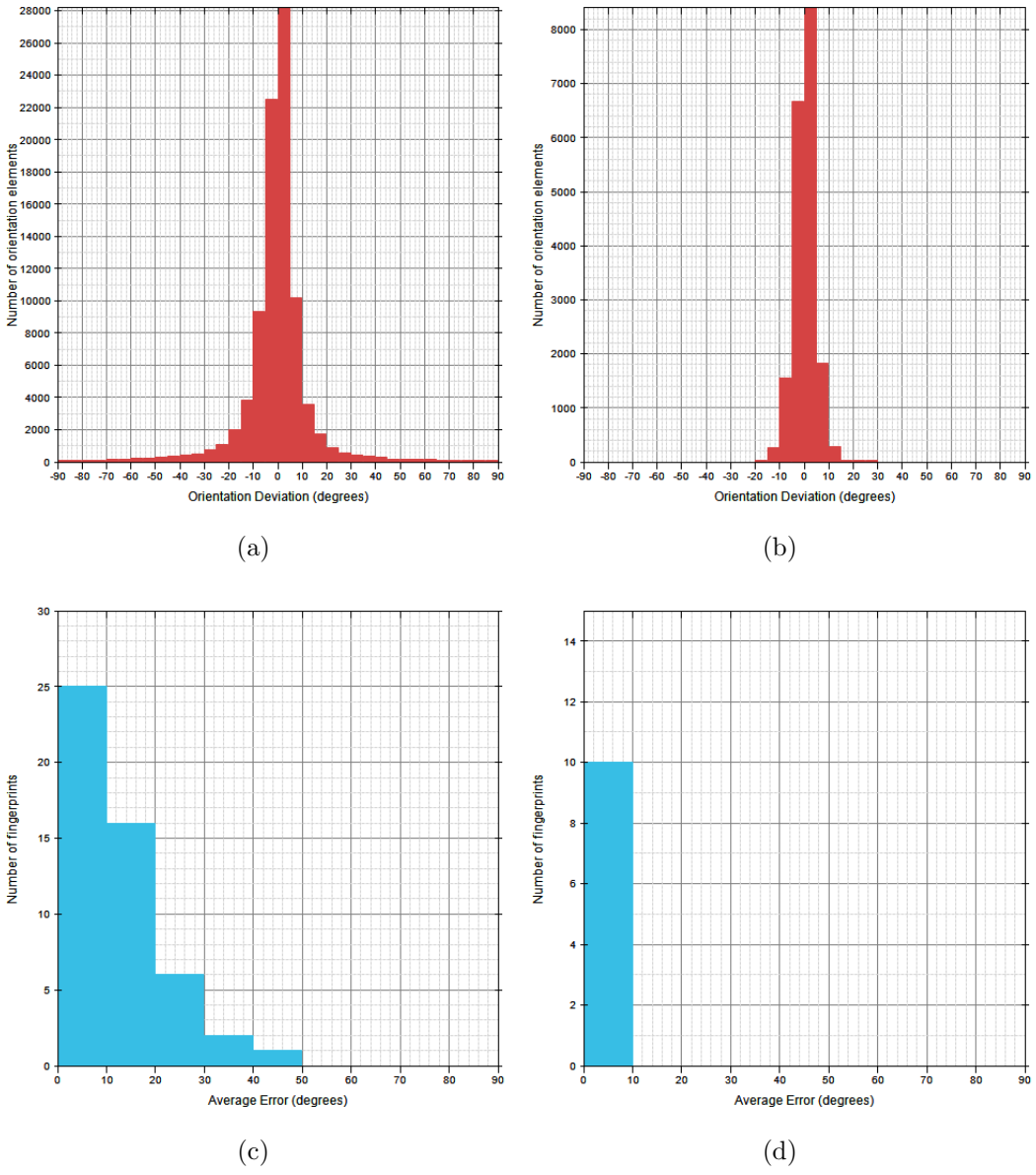

Figure 7.8: Distributions for the Adaptive-3 algorithm. Graphs (a) and (b) plot the orientation deviation distribution for the bad and good datasets respectively. Graphs (c) and (d) plot the average error distribution for the bad and good datasets respectively.

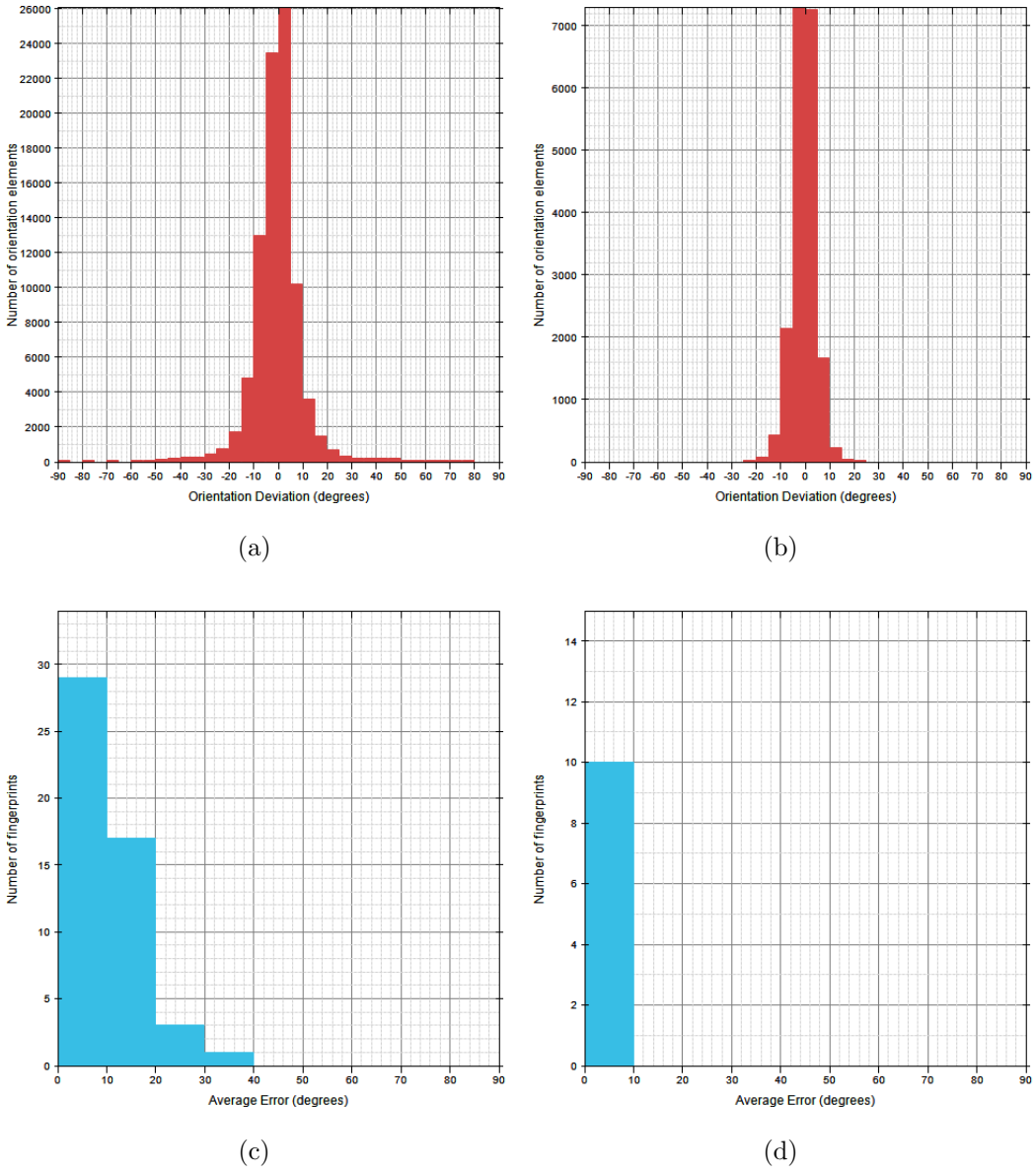

Figure 7.9: Distributions for the MXR algorithm. Graphs (a) and (b) plot the orientation deviation distribution for the bad and good datasets respectively. Graphs (c) and (d) plot the average error distribution for the bad and good datasets respectively.

Chapter 8

Concluding Remarks and Future Work

8.1 Conclusions

This Thesis has considered the problem of improving a fingerprint recognition system; it is divided in three main parts covering three important aspects: the fingerprint enhancement, the orientation extraction and the automatic evaluation of fingerprint algorithms.

After a summary of the state-of-the-art in fingerprint recognition methods (chapters 1 and 2), a new fingerprint enhancement method, which is both iterative and contextual, has been proposed in chapter 3. This approach detects automatically high-quality regions in fingerprints, and selectively applies contextual filtering starting from automatically-detected high-quality regions and then iteratively expanding like wildfire to low-quality ones. The proposed algorithm does not require any prior information like local orientations or frequencies. The improvements given by this algorithm have been assessed over both real and synthetic fingerprints with a state-of-the-art matcher (MCC).

The fingerprint local orientation has been shown to be a critical feature for most of fingerprint recognition systems. Its extraction is very difficult especially for noisy fingerprints. The orientation extraction problem has been introduced and reviewed in chapter 4. The introduction of a new taxonomy, which includes learning-based approaches, has been motivated by several experimental results on a new specifically-designed preliminary benchmark. The same benchmark has been further extended in chapter 6.

The fingerprint orientation extraction has been improved in chapter 5 following two

directions. First, several variants of state-of-the-art orientation extraction methods (local and global) have been implemented and, pointing out the role of pre- and post- processing, we have improved baseline methods. Second, the introduction of a new hybrid orientation extraction method, which follows an adaptive scheme, allowed us to improve significantly the orientation extraction in noisy fingerprints. The proposed method is called adaptive because it uses both the local information and the experience, represented by the knowledge of plausible fingerprint orientation structures, to compute the best orientation in a given point. Results of an extensive testing phase are also reported.

The lack of a publicly available framework to compare fingerprint orientation extraction algorithms, has motivated (chapter 6) the creation of a new benchmark area in the FVC-onGoing framework called FOE along with fingerprint matching benchmarks. It is constituted of fingerprint images, orientation ground-truth and a metric. The success of such online framework for the automatic evaluation of fingerprint algorithms, has been discussed in chapter 7 by providing statistics on the large number of participants: more than 1500 submitted algorithms and two international competitions.

8.2 Future Work

The work carried out in this Thesis encourages the following research directions.

- **Latent Fingerprints Enhancement**. Latent fingerprints (or latents) are an important source of evidence in crime scene investigation to identify and convict the suspects. The automatic feature extraction in latent fingerprints is a challenging problem due to their poor quality in terms of the clarity of the ridge information as well as the overlap of the region of interest with structured noise in the background (text, lines, stains, speckles). While a rolled fingerprint contains a large number of minutiae, in latents this number is considerably reduced. A latent identification algorithm should avoid the human intervention and rely on a robust feature extraction. An example of bad quality latent fingerprint with the corresponding rolled impression is shown in figure 8.1.

- **Orientation Extraction with Deep Learning Models**. Learning-based models represent a promising methodology for the fingerprint orientation extraction problem. Among various learning paradigms, we believe that good results may be achieved exploiting the deep learning paradigm [10]. Deep learning methods

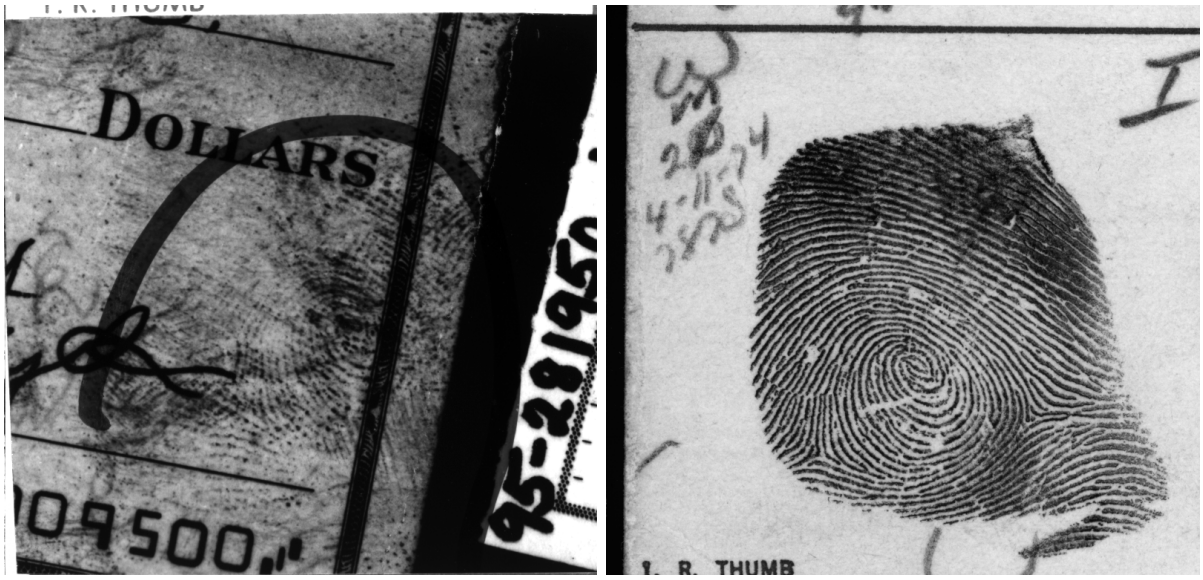

Figure 8.1: A latent fingerprint (left) and the corresponding rolled fingerprint (right).

Figure 8.2: Fingerprint overlapping (left) with the individual components (center, right).

aim at learning hierarchical structures of features where the features at high levels are based on a combination of low-level features. This learning paradigm can be defined biologically-inspired because of analogies with the architectural depth of human brain. The learning algorithm greedily trains one level at time, exploiting an unsupervised learning algorithm for each layer. Typical deep learning architectures are the Restricted Boltzman Machine (RBM), Deep Belief Networks (DBN), Auto-encoders and Denoising Autoencoders [49] [10]. We have conducted some preliminary learning experiments with Denoising Autoencoders in order to build a hierarchical structure of orientation features in fingerprints. The features are learnt

from the coarse orientation field of a fingerprint and its orientation ground-truth. After the learning step, the global orientation is represented by high-level features while local orientations represents low-level features.

- **FVC-onGoing**. The FVC-onGoing architecture can be improved in many ways: i) new benchmarks, in existing benchmark areas, can be added; ii) new fingerprint benchmark areas for other problems can be added (i.e. indexing, classification); iii) the whole system can be extended to other biometrics like palmprints or iris.

- **Separating Overlapped Fingerprints**. Fingerprint overlapping is a problem that mainly occurs in latent fingerprints lifted from crime scenes or in live-scan fingerprint images when the scanner surface contains residue of preceding fingerprints. It is desiderable to develop a method that automatically separates overlapped fingerprints in their individual fingerprints such that the matching is improved. The separation of overlapped fingerprints is a new problem and just few works have been published on this topic [28][27]. Current methods produce results that with noisy fingerprints are still unsatisfactory. Figure 8.2 shows an overlapping (on the left) and the individual fingerprints (center, right) that we want to isolate.

Appendix A

List of scientific publications

The author contributed to the following scientific publications during the timeframe of his PhD:

- Raffaele Cappelli, Davide Maltoni, Francesco Turroni, "Benchmarking Local Orientation Extraction in Fingerprint Recognition", ICPR, pp.1144-1147, 2010 20th International Conference on Pattern Recognition, August 2010, Istanbul (Turkey).
  Abstract. *The computation of local orientations is a fundamental step in fingerprint recognition. Although a large number of approaches have been proposed in the literature, no systematic quantitative evaluations have been done yet, mainly due to the lack of proper datasets with associated ground truth information. In this paper we propose a new benchmark (which includes two datasets and an accuracy metric) and report preliminary results obtained by testing four well-known local orientation extraction algorithms.*

- Turroni, F.; Maltoni, D.; Cappelli, R.; Maio, D.; , "Improving Fingerprint Orientation Extraction," IEEE Transactions on Information Forensics and Security, vol.6, no.3, pp.1002-1013, Sept. 2011.
  Abstract. *Computation of local orientations is a primary step in fingerprint recognition. A large number of approaches have been proposed in the literature, but no systematic quantitative evaluations have been done yet. We implemented and tested several well know methods and a plethora of their variants over a novel, specifically designed, benchmark, made available in the FVC-onGoing framework. We proved that parameter optimizations, pre- and post-processing stages can markedly improve*

accuracy of the baseline methods on bad quality fingerprints. Finally, in this paper we propose a novel adaptive method which selectively exploits accuracy of local-based analysis and learning-based global methods, thus achieving the overall best performance on a challenging dataset.

- Raffaele Cappelli, Matteo Ferrara, Davide Maltoni and Francesco Turroni, "Fingerprint Verification Competition at IJCB2011", IJCB11, International Joint Conference on Biometrics, October 2011, Washington USA.
  Abstract. *This paper summarizes the results of the fingerprint verification competition organized in conjunction with IJCB 2011. The competition focused on benchmarks covering both proprietary encoding and ISO template format. Considering the benchmarks difficulty, some of the algorithms submitted achieved very good accuracy: a 0.7% EER and a 1.1% EER were obtained on two challenging benchmarks, using proprietary and ISO template formats, respectively. Based on the participant self-description of the best performing algorithms we tried to figure out the most promising building-block technologies.*

- Francesco Turroni, Raffaele Cappelli and Davide Maltoni, "Fingerprint Enhancement using Contextual Iterative Filtering", ICB12, International Conference on Biometrics, March 2012, new Delhi, India.
  Abstract. *The performance of Automatic Fingerprint Identification Systems (AFIS) relies on the quality of the input fingerprints, so the enhancement of noisy images is a critical step. We propose a new fingerprint enhancement algorithm that selectively applies contextual filtering starting from automatically-detected high-quality regions and then iteratively expanding to low-quality ones. The proposed algorithm does not require any prior information like local orientations or frequencies. Experimental results over both real (FVC2004 and FVC2006) and synthetic (generated by the SFinGe software) fingerprints demonstrate the effectiveness of the proposed method.*

List of Figures

List of Tables

References

[1] IJCB 2011: International Joint Conference on Biometrics, October 2011. http://www.cse.nd.edu/IJCB_11/.

[2] Biometric Systems Laboratory - University of Bologna, January 2012. http://biolab.csr.unibo.it.

[3] FVC-onGoing Web site, January 2012. http://biolab.csr.unibo.it/FVCOnGoing.

[4] ICB 2012: International Conference on Biometrics, March 2012. http://icb12.iiitd.ac.in/.

[5] Andres Almansa and Tony Lindeberg. Fingerprint enhancement by shape adaptation of scale-space operators with automatic scale selection. *IEEE Transactions on Image Processing*, pages 2027–2042, 2000.

[6] ANSI/NIST. Data Format for the Interchange of Fingerprint Facial, and Other Biometric Information (revision of ANSI/NIST-ITL 1-2000). NIST Special Public Report, 2007.

[7] W.J. Babler. Embryologic development of epidermal ridges and their configuration. *Birth Defects Original Article Series*, 27(2), 1991.

[8] A. M. Bazen, G. T. B. Verwaaijen, S. H. Gerez, L. P. J. Veelenturf, and B. J. van der Zwaag. A correlation-based fingerprint verification system. In *11th Annual Workshop on Circuits Systems and Signal Processing (ProRISC), Veldhoven, the Netherlands*, pages 205–213, Netherlands, November 2000. Technology Foundation STW.

[9] Asker M. Bazen and Sabih H. Gerez. Systematic methods for the computation of the directional fields and singular points of fingerprints. *IEEE Trans. Pattern Anal. Mach. Intell.*, 24(7):905–919, 2002.

[10] Yoshua Bengio. Learning deep architectures for ai. *Found. Trends Mach. Learn.*, 2(1):1–127, January 2009.

[11] J. Bigün and G. H. Granlund. Optimal orientation detection of linear symmetry. In *Proceedings of the IEEE First International Conference on Computer Vision*, pages 433–438, London, Great Britain, June 1987.

[12] Josef Bigün, Gösta H. Granlund, and Johan Wiklund. Multidimensional orientation estimation with applications to texture analysis and optical flow. *IEEE Trans. Pattern Anal. Mach. Intell.*, 13(8):775–790, August 1991.

[13] Christopher M. Bishop. *Neural Networks for Pattern Recognition*. Oxford University Press, 1 edition, January 1996.

[14] Christopher M. Bishop. *Pattern Recognition and Machine Learning (Information Science and Statistics)*. Springer, 1 edition, October 2007.

[15] R.M. Bolle, N.K. Ratha, and S. Pankanti. An evaluation of error confidence interval estimation methods. In *Pattern Recognition, 2004. ICPR 2004. Proceedings of the 17th International Conference on*, volume 3, pages 103 – 106, August 2004.

[16] Xiang Can and You Lin. An adaptive algorithm for smoothing fingerprint orientation fields. In *Computational Intelligence and Natural Computing, 2009. CINC '09. International Conference on*, volume 1, pages 70 –72, june 2009.

[17] R. Cappelli, M. Ferrara, and D. Maltoni. Minutia cylinder-code: A new representation and matching technique for fingerprint recognition. *Pattern Analysis and Machine Intelligence, IEEE Transactions on*, 32(12):2128 –2141, December 2010.

[18] R. Cappelli, M. Ferrara, D. Maltoni, and M. Tistarelli. Mcc: A baseline algorithm for fingerprint verification in fvc-ongoing. In *Control Automation Robotics Vision (ICARCV), 2010 11th International Conference on*, pages 19 –23, December 2010.

[19] R. Cappelli, M. Ferrara, D. Maltoni, and F. Turroni. Fingerprint verification competition at ijcb2012. In *Proceedings of International Joint Conference on Biometrics (IJCB11)*, Washington DC, USA, 2011.

[20] R. Cappelli, A. Lumini, D. Maio, and D. Maltoni. Fingerprint classification by directional image partitioning. *Pattern Analysis and Machine Intelligence, IEEE Transactions on*, 21(5):402 –421, May 1999.

[21] R. Cappelli, D. Maio, and D. Maltoni. Semi-automatic enhancement of very low quality fingerprints. In *Image and Signal Processing and Analysis, ISPA2009*, pages 678–683, September 2009.

[22] R. Cappelli, D. Maio, D. Maltoni, and A. Erol. Synthetic fingerprint-image generation. *Pattern Recognition, International Conference on*, 3:3475, 2000.

[23] R. Cappelli, D. Maltoni, and F. Turroni. Benchmarking local orientation extraction in fingerprint recognition. In *Proceedings of 20th International Conference on Pattern Recognition (ICPR'10)*, pages 1144–1147, Istanbul, Turkey, 2010.

[24] R. Cappelli, F. Turroni, and Maltoni. Fingerprint enhancement using contextual iterative filtering. In *Proceedings of International Conference on Biometrics (ICB12)*, New Delhi, India, 2012.

[25] Raffaele Cappelli, Matteo Ferrara, Annalisa Franco, and Davide Maltoni. Fingerprint Verification Competition 2006. *Biometric Technology Today*, 15(7-8):7–9, August 2007.

[26] Raffaele Cappelli, Dario Maio, Davide Maltoni, James L. Wayman, and Anil K. Jain. Performance Evaluation of Fingerprint Verification Systems. *IEEE Trans. Pattern Anal. Mach. Intell.*, 28(1):3–18, 2006.

[27] Fanglin Chen, Jianjiang Feng, A.K. Jain, Jie Zhou, and Jin Zhang. Separating overlapped fingerprints. *Information Forensics and Security, IEEE Transactions on*, 6(2):346 –359, June 2011.

[28] Fanglin Chen, Jianjiang Feng, and Jie Zhou. On separating overlapped fingerprints. In *Biometrics: Theory Applications and Systems (BTAS), 2010 Fourth IEEE International Conference on*, pages 1 –6, September 2010.

[29] Jiangang Cheng and Jie Tian. Fingerprint enhancement with dyadic scale-space. *Pattern Recogn. Lett.*, 25(11):1273–1284, August 2004.

[30] Kuang chih Lee and S. Prabhakar. Probabilistic orientation field estimation for fingerprint enhancement and verification. In *Biometrics Symposium, 2008. BSYM '08*, pages 41–46, September 2008.

[31] Sharat Chikkerur, Alexander Cartwright, and Venu Govindaraju. K-plet and coupled bfs: A graph based fingerprint representation and matching algorithm. In David Zhang and Anil Jain, editors, *Advances in Biometrics*, volume 3832 of *Lecture Notes in Computer Science*, pages 309–315. Springer Berlin / Heidelberg, 2005.

[32] Sharat Chikkerur, Alexander N. Cartwright, and Venu Govindaraju. Fingerprint enhancement using stft analysis. *Pattern Recognition*, 40(1):198–211, January 2007.

[33] Louis Coetzee and Elizabeth C. Botha. Fingerprint recognition in low quality images. *Pattern Recognition*, pages 1441–1460, 1993.

[34] T. F. Cootes, C. J. Taylor, D. H. Cooper, and J. Graham. Active shape models—their training and application. *Comput. Vis. Image Underst.*, 61(1):38–59, 1995.

[35] Sarat C. Dass. Markov random field models for directional field and singularity extraction in fingerprint images. *IEEE Transactions on Image Processing*, 13(10):1358–1367, 2004.

[36] J. Daugman. How iris recognition works. *Circuits and Systems for Video Technology, IEEE Transactions on*, 14(1):21–30, Jan. 2004.

[37] M. J. Donahue and S. I. Rokhlin. On the use of level curves in image analysis. *CVGIP: Image Underst.*, 57(2):185–203, 1993.

[38] Richard O. Duda, Peter E. Hart, and David G. Stork. *Pattern Classification (2nd Edition)*. Wiley-Interscience, 2 edition, November 2000.

[39] Henry E. *Classification And Uses Of Finger Prints*. Routledge, London, 1900.

[40] Yansong Feng, Jufu Feng, Xiaoguang Chen, and Zhen Song. A novel fingerprint matching scheme based on local structure compatibility. In *Pattern Recognition, 2006. ICPR 2006. 18th International Conference on*, volume 4, pages 374–377, 2006.

[41] Julian Fiérrez-Aguilar, Daniel Garcia-Romero, Javier Ortega-Garcia, and Joaquin Gonzalez-Rodriguez. Bayesian adaptation for user-dependent multimodal biometric authentication. *Pattern Recognition*, 38(8):1317–1319, 2005.

[42] Julian Fiérrez-Aguilar, Javier Ortega-Garcia, Joaquin Gonzalez-Rodriguez, and Josef Bigün. Discriminative multimodal biometric authentication based on quality measures. *Pattern Recognition*, 38(5):777–779, 2005.

[43] H. Fronthaler, K. Kollreider, and J. Bigun. Pyramid-based image enhancement of fingerprints. In *Automatic Identification Advanced Technologies, 2007 IEEE Workshop on*, pages 45 –50, june 2007.

[44] H. Fronthaler, K. Kollreider, and J. Bigun. Local features for enhancement and minutiae extraction in fingerprints. *Image Processing, IEEE Transactions on*, 17(3):354 –363, March 2008.

[45] Francis Galton. *Finger Prints*. Macmillan, London, 1892.

[46] M.D. Garris and R.M. McCabe. NIST Special Database 27, fingerprint minutiae from latent and matching tenprint images, Fingerprint Database, 2000. http://www.nist.gov/srd/nistsd27.cfm.

[47] Rafael C. Gonzalez and Richard E. Woods. *Digital Image Processing (3rd Edition)*. Prentice-Hall, Inc., Upper Saddle River, NJ, USA, 2006.

[48] C. Gottschlich, P. Mihailescu, and A. Munk. Robust orientation field estimation and extrapolation using semilocal line sensors. *Information Forensics and Security, IEEE Transactions on*, 4(4):802 –811, December 2009.

[49] Geoffrey E. Hinton, Simon Osindero, and Yee-Whye Teh. A fast learning algorithm for deep belief nets. *Neural Comput.*, 18(7):1527–1554, July 2006.

[50] Lin Hong and Anil Jain. Integrating faces and fingerprints for personal identification. *IEEE transactions on pattern analysis and machine intelligence*, 20:1295–1307, 1998.

[51] Lin Hong, Anil Jain, Sharathcha Pankanti, and Ruud Bolle. Fingerprint enhancement. In *Workshop on Applications of Computer Vision*, pages 202–207, 1996.

[52] Lin Hong, Anil K. Jain, and Sharath Pankanti. Can multibiometrics improve performance. Technical Report MSU-CSE-99-39, Department of Computer Science, Michigan State University, December 1999.

[53] Lin Hong, Yifei Wan, and Anil Jain. Fingerprint image enhancement: Algorithm and performance evaluation. *IEEE Transactions on Pattern Analysis and Machine Intelligence*, 20:777–789, 1998.

[54] Ching-Tang Hsieh, Eugene Lai, and You-Chuang Wang. An effective algorithm for fingerprint image enhancement based on wavelet transform. *Pattern Recognition*, 36(2):303 – 312, 2003.

[55] Ching-Tang Hsieh, Eugene Lai, and You-Chuang Wang. An effective algorithm for fingerprint image enhancement based on wavelet transform. *Pattern Recognition*, 36(2):303–312, 2003.

[56] Shih hsu Chang, T' Fang hsuan Cheng, Wen hsing Hsu T, and Guo zua Wu T. Fast algorithm for point pattern matching: Invariant to translations rotations and scale changes. *Pattern Recognition*, 30:311–320, 1997.

[57] Stephan Huckemann, Thomas Hotz, and Axel Munk. Global models for the orientation field of fingerprints: An approach based on quadratic differentials. *IEEE Trans. Pattern Anal. Mach. Intell.*, 30(9):1507–1519, 2008.

[58] NIST Image Group Fingerprint Overview Testing, August 2012. http://www.nist.gov/itl/iad/ig/fingerprint.cfm.

[59] K. Ito, A. Morita, T. Aoki, T. Higuchi, H. Nakajima, and K. Kobayashi. A fingerprint recognition algorithm using phase-based image matching for low-quality fingerprints. In *Image Processing, 2005. ICIP 2005. IEEE International Conference on*, volume 2, pages 33–36, September 2005.

[60] Koichi Ito, Ayumi Morita, Takafumi Aoki, Hiroshi Nakajima, Koji Kobayashi, and Tatsuo Higuchi. A fingerprint recognition algorithm combining phase-based image matching and feature-based matching. In *ICB*, pages 316–325, 2006.

[61] A. Jain, Lin Hong, and R. Bolle. On-line fingerprint verification. *Pattern Analysis and Machine Intelligence, IEEE Transactions on*, 19(4):302 –314, April 1997.

[62] A. Jain, A. Ross, and S. Pankanti. A prototype hand geometry-based verification system. In *2nd International Conference on Audio- and Video-based Biometric Person Authentication, Washington D.C.*, 1999.

[63] A.K. Jain, L. Hong, and Y. Kulkarni. F2id: A personal identification system using faces and fingerprints. In *ICPR98*, volume 2, pages 1373–1375, 1998.

[64] A.K. Jain, L. Hong, and Y. Kulkarni. A multimodal biometric system using fingerprint, face and speech. In *AVBPA99*, pages 182–187, 1999.

[65] A.K. Jain, Lin Hong, S. Pankanti, and R. Bolle. An identity-authentication system using fingerprints. *Proceedings of the IEEE*, 85(9):1365 –1388, September 1997.

[66] A.K. Jain, S. Prabhakar, L. Hong, and S. Pankanti. Filterbank-based fingerprint matching. *Image Processing, IEEE Transactions on*, 9(5):846 –859, may 2000.

[67] Anil Jain, Arun Ross, and Salil Prabhakar. Fingerprint matching using minutiae and texture features. In *In International Conference on Image Processing*, pages 282–285, 2001.

[68] Anil K. Jain, Arun Ross, and Salil Prabhakar. An introduction to biometric recognition. *IEEE Trans. on Circuits and Systems for Video Technology*, 14:4–20, 2004.

[69] Xudong Jiang. Extracting image orientation feature by using integration operator. *Pattern Recognition*, 40(2):705–717, February 2007.

[70] Xudong Jiang and Wei-Yun Yau. Fingerprint minutiae matching based on the local and global structures. In *Pattern Recognition, 2000. Proceedings. 15th International Conference on*, volume 2, pages 1038–1041, 2000.

[71] Suksan Jirachaweng and Vutipong Areekul. Fingerprint enhancement based on discrete cosine transform. In Seong-Whan Lee and Stan Li, editors, *Advances in*

Biometrics, volume 4642 of *Lecture Notes in Computer Science*, pages 96–105. Springer Berlin / Heidelberg, 2007.

[72] Suksan Jirachaweng, Zujun Hou, Wei-Yun Yau, and Vutipong Areekul. Residual orientation modeling for fingerprint enhancement and singular point detection. *Pattern Recognition*, 44(2):431–442, February 2011.

[73] Biometric Database Julian, Julian Fierrez-Aguilar, Javier Ortega-garcia, Doroteo Torre-toledano, and Joaquin Gonzalez-rodriguez. Biosec baseline corpus: A multimodal. *Pattern Recognition*, 40(4):1389–1392, 2007.

[74] Li Jun and Yau Wei Yun. Prediction of fingerprint orientation. *Pattern Recognition, International Conference on*, 4:436–439, 2004.

[75] Michael Kass and Andrew Witkin. Analyzing oriented patterns. *Comput. Vision Graph. Image Process.*, 37(3):362–385, March 1987.

[76] Byung-Gyu Kim and Dong-Jo Park. Adaptive image normalisation based on block processing for enhancement of fingerprint image. *Electronics Letters*, 38(14):696–698, 2002.

[77] Michael Kücken and Alan C. Newell. Fingerprint formation. *Journal of Theoretical Biology*, 235(1):71 – 83, 2005.

[78] H.C. Lee and R.E. Gaensslen. *Advances in fingerprint technology*. CRC series in forensic and police science. CRC Press, 2001.

[79] Jun Li, Wei-Yun Yau, and Han Wang. Constrained nonlinear models of fingerprint orientations with prediction. *Pattern Recognition*, 39(1):102–114, 2006.

[80] Jun Li, Wei-Yun Yau, and Han Wang. Combining singular points and orientation image information for fingerprint classification. *Pattern Recognition*, 41(1):353–366, 2008.

[81] Stan Z. Li and Anil K. Jain, editors. *Encyclopedia of Biometrics*. Springer US, 2009.

[82] William A. Light. Some optimality conditions for chebyshev expansions. *Journal of Approximation Theory*, 27(2):113 – 126, 1979.

[83] David G. Luenberger and Yinyu Ye. *Linear and nonlinear programming*. Springer, 2008.

[84] Xiping Luo, Jie Tian, and Yan Wu. A minutiae matching algorithm in fingerprint verification. In *Pattern Recognition, 2000. Proceedings. 15th International Conference on*, volume 4, pages 833–836, 2000.

[85] D. Maio and D. Maltoni. Ridge-line density estimation in digital images. In *Pattern Recognition, 1998. Proceedings. Fourteenth International Conference on*, volume 1, pages 534 – 538, August 1998.

[86] Dario Maio and Davide Maltoni. Direct gray-scale minutiae detection in fingerprints. *IEEE Trans. Pattern Anal. Mach. Intell.*, pages 27–40, 1997.

[87] Dario Maio, Davide Maltoni, Raffaele Cappelli, James L. Wayman, and Anil K. Jain. FVC2000: Fingerprint Verification Competition. *IEEE Trans. Pattern Anal. Mach. Intell.*, 24(3):402–412, 2002.

[88] Dario Maio, Davide Maltoni, Raffaele Cappelli, James L. Wayman, and Anil K. Jain. FVC2002: Second Fingerprint Verification Competition. In *ICPR (3)*, pages 811–814, 2002.

[89] Dario Maio, Davide Maltoni, Raffaele Cappelli, James L. Wayman, and Anil K. Jain. FVC2004: Third Fingerprint Verification Competition. In *ICBA*, pages 1–7, 2004.

[90] Davide Maltoni, Dario Maio, Anil K. Jain, and Salil Prabhakar. *Handbook of Fingerprint Recognition*. Springer Publishing Company, Incorporated, 2009.

[91] John C. Mason and David Handscomb. *Chebyshev Polynomials*. Chapman & Hall/CRC, 2003.

[92] E. McCabe. *Automatic Fingerprint Recognition Systems*, chapter 21, Fingerprint Interoperability Standards, pages 433–451. Springer New York, 2004.

[93] Bijan Moayer and King-Sun Fu. A tree system approach for fingerprint pattern recognition. *Computers, IEEE Transactions on*, C-25(3):262 –274, March 1976.

[94] Andre A. Moenssens. *Fingerprint techniques [by] Andre A. Moenssens*. Chilton Book Co. Philadelphia,, [1st ed.] edition, 1971.

[95] L. O'Gorman and J.V. Nickerson. Matched filter design for fingerprint image enhancement. In *Proc. Int. Conf. on Acustic Speech and Signal Processing*, pages 916–919, 1988.

[96] L. O'Gorman and J.V. Nickerson. An approach to fingerprint filter design. *Pattern Recognition*, 22(1):29–38, 1989.

[97] M. A. Oliveira and N. J. Leite. A multiscale directional operator and morphological tools for reconnecting broken ridges in fingerprint images. *Pattern Recogn.*, 41(1):367–377, 2008.

[98] Surinder Ram, Horst Bischof, and Josef Birchbauer. Active fingerprint ridge orientation models. In *ICB '09: Proceedings of the Third International Conference on Advances in Biometrics*, pages 534–543, Berlin, Heidelberg, 2009. Springer-Verlag.

[99] Surinder Ram, Horst Bischof, and Josef Birchbauer. Modelling fingerprint ridge orientation using legendre polynomials. *Pattern Recogn.*, 43(1):342–357, 2010.

[100] N. Ratha, S. Chen, and A. Jain. Adaptive flow orientation based feature extraction in fingerprint images. *Pattern Recognition*, (28):1657–1672, November 1995.

[101] Nalini K. Ratha, Kalle Karu, Shaoyun Chen, and Anil K. Jain. A real-time matching system for large fingerprint databases. *IEEE Transactions on Pattern Analysis and Machine Intelligence*, 18:799–813, 1996.

[102] Arun Ross and Anil Jain. Information fusion in biometrics. *Pattern Recognition Letters*, 24:2115–2125, 2003.

[103] Arun Ross, Anil Jain, and Jian-Zhong Qian. Information fusion in biometrics. In *Proc. of 3rd International Conference on audio- and Video- based Person Authentication (AVBPA)*, volume 2091, pages 354–359, June 2001.

[104] Arun Ross, Anil Jain, and James Reisman. A hybrid fingerprint matcher. *Pattern Recognition*, 36(7):1661 – 1673, 2003.

[105] Arun Ross, James Reisman, and Anil K. Jain. Fingerprint matching using feature space correlation. In *In: Proc. BIOAW, Springer LNCS-2359*, pages 48–57. Springer, 2002.

[106] Arun A. Ross, Karthik Nandakumar, and Anil K. Jain. *Handbook of Multibiometrics (International Series on Biometrics)*. Springer-Verlag New York, Inc., Secaucus, NJ, USA, 2006.

[107] Barry G. Sherlock and Donald M. Monro. A model for interpreting fingerprint topology. *Pattern Recognition*, 26(7):1047–1055, 1993.

[108] B.G. Sherlock, D.M. Monro, and K. Millard. Algorithm for enhancing fingerprint images. *Electronic Letters*, 28(18):17–20, 1992.

[109] B.G. Sherlock, D.M. Monro, and K. Millard. Fingerprint enhancement by directional fourier filtering. In *IEE Procedings Vision Image and Signal Processing*, volume 141, pages 87–94, 1994.

[110] B.G. Sherlock, D.M. Monro, and K. Millard. Fingerprint enhancement by directional fourier filtering. *Vision, Image and Signal Processing, IEE Proceedings -*, 141(2):87–94, April 1994.

[111] Zhixin Shi and Venu Govindaraju. Fingerprint image enhancement based on skin profile approximation. In *ICPR (3)*, pages 714–717, 2006.

[112] Xin Shuai, Chao Zhang, and Pengwei Hao. The optimal ros-based symmetric phase-only filter for fingerprint verification. In *ICIP (2)'07*, pages 381–384, 2007.

[113] United States. *Electronic Fingerprint Transmission Specification [electronic resource]*. U.S. Dept. of Justice, Federal Bureau of Investigation, Criminal Justice Information Services Division, [Washington, D.C.] :, 1999.

[114] R.M. Stock and C.W. Swonger. Development and evalutation of a reader of fingerprint minutiae. Technical report, Cornell Aeronautical Laboratory, 1969.

[115] P.K. Suetin. *Orthogonal polynomials in two variables*. Analytical methods and special functions. Gordon and Breach Science Publishers, 1999.

[116] P. Sutthiwichaiporn, V. Areekul, and S. Jirachaweng. Iterative fingerprint enhancement with matched filtering and quality diffusion in spatial-frequency domain. In *Pattern Recognition (ICPR), 2010 20th International Conference on*, pages 1257 –1260, August 2010.

[117] Elham Tabassi, Charles L. Wilson, and Craig I. Watson. Fingerprint image quality: Nistir 7151. Technical report, NIST, 2004.

[118] Xunqiang Tao, Xin Yang, Kai Cao, Ruifang Wang, Peng Li, and Jie Tian. Estimation of fingerprint orientation field by weighted 2d fourier expansion model. In *Proceedings of the 2010 20th International Conference on Pattern Recognition*, ICPR '10, pages 1253–1256, Washington, DC, USA, 2010. IEEE Computer Society.

[119] Ashkan Tashk, Mohammad Sadegh Helfroush, and Mohammad Javad Dehghani. A conditional selection of orthogonal legendre/chebyshev polynomials as a novel fingerprint orientation estimation smoothing method. In *Proceedings of the 2009 Second International Conference on Machine Vision*, ICMV '09, pages 59–63, Washington, DC, USA, 2009. IEEE Computer Society.

[120] Sergios Theodoridis and Konstantinos Koutroumbas. *Pattern Recognition, Fourth Edition*. Academic Press, 4th edition, 2008.

[121] Xifeng Tong, Jianhua Huang, Xianglong Tang, and Daming Shi. Fingerprint minutiae matching using the adjacent feature vector. *Pattern Recognition Letters*, 26(9):1337–1345, 2005.

[122] F. Turroni, D. Maltoni, R. Cappelli, and D. Maio. Improving fingerprint orientation extraction. *Information Forensics and Security, IEEE Transactions on*, 6(3):1002 –1013, September 2011.

[123] B.V.K. Vijaya Kumar, M. Savvides, C. Xie, K. Venkataramani, J. Thornton, and A. Mahalanobis. Biometric verification with correlation filters. *Appl Opt.*, 43(2):391–402, 2004.

[124] Pedro R. Vizcaya and Lester A. Gerhardt. A nonlinear orientation model for global description of fingerprints. *Pattern Recognition*, 29(7):1221–1231, 1996.

[125] Yi Wang, Jiankun Hu, and Fengling Han. Enhanced gradient-based algorithm for the estimation of fingerprint orientation fields. *Applied Mathematics and Computation*, 185(2):823–833, 2007.

[126] Yi Wang, Jiankun Hu, and Damien Phillips. A fingerprint orientation model based on 2d fourier expansion (fomfe) and its application to singular-point detection and fingerprint indexing. *IEEE Trans. Pattern Anal. Mach. Intell.*, 29(4):573–585, 2007.

[127] Yi Wang, Jiankun Hu, and Heiko Schroder. A gradient based weighted averaging method for estimation of fingerprint orientation fields. *Digital Image Computing: Techniques and Applications*, 0:29, 2005.

[128] C.I. Watson. NIST Special Database 10, supplemental fingerprint card data (sfcd) for nist special database 9, Fingerprint Database, 1993. http://www.nist.gov/srd/nistsd10.cfm.

[129] C.I. Watson. NIST Special Database 14, Fingerprint Database, September 1993. http://www.nist.gov/srd/nistsd14.cfm.

[130] C.I. Watson and C.L. Wilson. NIST Special Database 4, Fingerprint Database, 1992. http://www.nist.gov/srd/nistsd4.cfm.

[131] C.I. Watson and C.L. Wilson. NIST Special Database 9, Fingerprint Database, 1992. http://www.nist.gov/srd/nistsd9.cfm.

[132] C.I. Watson and C.L. Wilson. NIST Special Database 24, digital video of live-scan fingerprint data, Fingerprint Database, 1998. http://www.nist.gov/srd/nistsd24.cfm.

[133] James L. Wayman, Anil K. Jain, Davide Maltoni, and Dario Maio. *Biometric Systems: Technology, Design and Performance Evaluation*. Springer-Verlag New York, Inc., Secaucus, NJ, USA, 2004.

[134] Harry Wechsler. *Reliable Face Recognition Methods: System Design, Implementation and Evaluation (International Series on Biometrics)*. Springer-Verlag New York, Inc., Secaucus, NJ, USA, 2006.

[135] C. L. Wilson, C. I. Watson, and E. G. Paek. Combined optical and neural network fingerprint matching. In *Proc. of SPIE (Optical Pattern Recognition VIII)*, volume 3073, pages 373–382, 1997.

[136] Jie Zhou and Jinwei Gu. A model-based method for the computation of fingerprints' orientation field. *IEEE Transactions on Image Processing*, 13(6):821–835, 2004.

[137] Jie Zhou and Jinwei Gu. Modeling orientation fields of fingerprints with rational complex functions. *Pattern Recognition*, 37(2):389–391, 2004.

[138] Guocai Zhu and Chao Zhang. A top-down fingerprint image enhancement method based on fourier analysis. In Stan Li, Jianhuang Lai, Tieniu Tan, Guocan Feng, and Yunhong Wang, editors, *Advances in Biometric Person Authentication*, volume 3338 of *Lecture Notes in Computer Science*, pages 343–394. Springer Berlin / Heidelberg, 2005.